Investigating the effects of cisplatin on long non-coding RNAs ANRIL and PANDA in oesophageal squamous cell carcinoma (OSCC) cell lines.

by

Lebogang Moshupya

(1131005)

Dissertation

Submitted in fulfilment of the requirements for the degree

Master of Science

in

Molecular and Cell Biology

in the Faculty of Science, University of the Witwatersrand, Johannesburg, South Africa

Supervisor: Prof. Demetra Mavri-Damelin

Co-supervisor: Dr Rupal Jivan

August, 2022

Declaration

I, **Lebogang Nkone Moshupya** (1131005) am a student registered for the Master of Science degree at the University of the Witwatersrand in the academic year 2022

I hereby declare the following:

- I am aware that plagiarism (the use of someone else's work without their permission and/or without acknowledging their original source) is wrong.
- I confirm that the work submitted for assessment for the above degree is my own unaided work except where explicitly indicated otherwise.
- I have not submitted this work before for any other degree or examination at this or any other University.
- I have followed the required conventions in referencing the thoughts and ideas of others.
- I understand that the University of the Witwatersrand may take disciplinary action against me if there is a belief that this may not be my own unaided work or that I have failed to acknowledge the source of ideas or words in my writing.

Signature:  Date: 29 August 2022

Dedication

To my parents, Lesibana Robert Moshupya and Dingaan Christina Moshupya.

Abstract

Oesophageal cancer is the 8th most common cancer type and the 6th most death causing cancer type worldwide. One of its subtypes, oesophageal squamous cell carcinoma (OSCC) is prevalent in Eastern to Central Asia and along the Rift Valley in East Africa and into South Africa. The prognosis of OSCC remains poor, detected at the advanced stage with low survival rates. There are various treatment options for OSCC and cisplatin is the first line chemotherapeutic drug used in South Africa and other developing countries as it is readily available and affordable. However, it is associated with poor efficacy, chemoresistance and chemotoxicity.

This study investigated the expression of ANRIL and PANDA long non-coding RNAs (lncRNAs) in response to cisplatin and immediately after cisplatin withdrawal, aiming to provide potential lncRNA-targeted strategies for overcoming cisplatin resistance in cancer therapy, especially OSCC. Cisplatin cytotoxicity and EC_{50} concentrations in OSCC (WHCO1 and WHCO5) and HEK293 cell lines were determined by an MTT assay. Cisplatin cytotoxic effects were exerted in all cell lines, with the HEK293 control being more sensitive to cisplatin compared to the cancerous OSCC cell lines. Western blot was used to observe DNA double stranded break (DSB) formation in the presence of cisplatin and in the first hour after cisplatin withdrawal in HEK293, WHCO1 and WHCO5 cell lines by measuring gammaH2AX (γH2AX), a DSB marker. The western blot results showed an increase in γH2AX levels post cisplatin treatment in all three cell lines. This showed cisplatin treatment induced DNA DSBs and activated the DNA damage response (DDR) in HEK293 control as well as WHCO1 and WHCO5. RT-PCR measured ANRIL and PANDA expression during cisplatin treatment and DDR, where PANDA expression appeared upregulated and ANRIL fluctuated during DDR in OSCC cell lines.

In conclusion, cisplatin activates DDR, upregulates PANDA but causes fluctuating ANRIL expression in OSCC cell lines. This study indicates roles for PANDA and ANRIL lncRNAs during cisplatin chemotherapy that warrant further investigation in OSCC.

Acknowledgement

First and foremost, I would like to sincerely acknowledge and thank my supervisors Professor Demetra Mavri-Damelin and Doctor Rupal Jivan for their invaluable advice, guidance and support throughout the course of this project. I have acquired a lot of skills, both as an individual and an aspiring scientist. This project was one of the most challenging stages of my life and I feel blessed to have walked this journey with you.

I would also like to thank Aalia Patel and all my colleagues from the Functional Genetics research laboratory Kayleen Jegels, Thokozile Makhanya, Tebogo Marutha and Jemma Falkov, for the great three years spent together and for the beautiful friendship. Thank you all for the laughs and sweet moments shared. You have all made the journey less hectic.

I owe a deep sense of gratitude to my parents for always being there for me and for their continuous support since day one. Thank you for not only believing in my dreams and goals but for also being there for me each and every step of the way. Your endless love and prayers will always be appreciated. To all my siblings, thank you for making me believe it is possible and for holding my hand throughout.

To my friends, who have carried me almost every day, thank you for always checking upon me and cheering me. The past two years were the most challenging, but with the endless support from my family and friends, I managed to get through it. I love you all, ALWAYS.

I would also like to thank the Nedbank Eyethu Community Trust and the University of the Witwatersrand for funding me through the Postgraduate DHET Gap Grant fund. Thank you so much for the financial support. Lastly, I would like to thank the University of the Witwatersrand for allowing me to fulfil my dreams at such a prestigious institution.

"The sun will rise and so will we" Jennae Cecelia

Table of Contents

List of Abbreviations

AC	-	Adenocarcinoma
ASOs	-	Antisense oligonucleotides
ADHB1	-	Alcohol dehydrogenase 1B
AJCC	-	American Joint Committee on Cancer
ALDH2	-	Aldehyde dehydrogenase 2 family members
ANRIL	-	Antisense non-coding RNA in the INK4 locus
APS	-	Ammonium persulfate
ATM	-	Ataxia telangiectasia mutated protein
ATR	-	Ataxia telangiectasia mutated RAD3-related protein
B-actin	-	Beta-actin
BACE1-AS	-	Beta-secretase APP cleaving enzyme 1
BER	-	Base excision repair
BSA	-	Bovine serum albumin
CANSA	-	Cancer association of South Africa
CHK1	-	Checkpoint kinase 1
CHK2	-	Checkpoint kinase 2
CDK	-	Cyclin dependent kinase
CDKN1A	-	Cyclin-dependent kinase inhibitor 1A
CDKN2A/B	-	Cyclin-dependent kinase inhibitor 2A/B
COLDAIR	-	Cold-assisted intronic non-coding RNA
CRISPR	-	Clustered Regularly Interspersed Short Palindromic Repeats
CT	-	Computed tomography
CTR1	-	Copper transporter 1
DDR	-	DNA damage response
DMEM	-	Dulbecco’s Modified Eagle Medium

DMSO	-	Dimethyl sulfoxide
DNA PKCs	-	DNA-dependent catalytic subunits
DSBs	-	Double stranded breaks
EDTA	-	Ethylenediamine tetraacetic acid
EERC1	-	Excision repair complementing 1
EMT	-	Epithelial-mesenchymal transition
ENCODE	-	Encyclopedia of DNA elements
EUS	-	Endoscopic ultrasound
5-FU	-	5-Fluorouracil
FBS	-	Fetal Bovine Serum
GENCODE	-	Generalised coding
GSH	-	Glutathione
GST	-	Glutathione-S-transferase
H3K4me	-	Histone H3 lysine 4 methylation
HCC	-	Hepatocellular carcinoma
HOTAIR	-	HOX antisense intergenic RNA
HOTTIP	-	HOXA transcript at the distal tip
HR	-	Homologous recombination
HRP	-	Horse radish peroxidase
IARC	-	International Agency for Research on Cancer
ICLs	-	Inter-strand crosslinks
LincRNA	-	Long intergenic non-coding RNA
LncRNA	-	Long non-coding RNA
LINE	-	Long interspersed retrotransposable elements
MAPK	-	Mitogen activated protein kinase
MDC1	-	Mediator of DNA damage checkpoint protein 1
MDM2	-	Mouse double minute 2 homolog
MiRNA	-	MicroRNA

MMR	-	DNA mismatch repair
MRI	-	Magnetic resonance imaging
MRN	-	Mre11-Rad50-Nbs1
MT	-	Metallothionine
MTAP	-	S-methyl-5'-thioadenosine phosphorylase
MTT	-	3-(4,5-dimethylthiazol-2-yl)-2,5-diphenyltatrazolium bromide
NATs	-	Natural antisense transcripts
NCR	-	National cancer research
NcRNA	-	Non-coding RNA
NF-YA	-	Nuclear transcription factor Y subunit
NHEJ	-	Non homologous end joining
NER	-	Nucleotide excision repair
NSCLC	-	Non-small cell lung cancer
NTC	-	Non template control
ORF	-	Open reading frame
OSCC	-	Oesophageal squamous cell carcinoma
PAH	-	Polycyclic aromatic hydrocarbons
PANDA	-	p21 associated ncRNA DNA damage activated
PBS	-	Phosphate-buffered saline
PcG	-	Polycomb group proteins
PET	-	Positron emission tomography
PIKKs	-	Phosphatidylinositol 3-kinase-related kinases
piRNA	-	Piwi-RNA
PMSF	-	Phenylmethylsulfonylfluoride
Poly (A)	-	Polyadenylation
PRC-1	-	Polycomb repressive complex 1
PRC-2	-	Polycomb repressive complex 1
pTNM	-	Pathological stage grouping

RB	-	Retinoblastoma
RBP	-	RNA binding protein
RIPA	-	Radioimmunoprecipitation
RNA pol II	-	RNA polymerase II
rRNA	-	Ribosomal RNA
RT-PCR	-	Reverse-transcriptase PCR
SAFA	-	Scaffold attachment factor A
SDS	-	Sodium dodecyl sulphate
SDS-PAGE	-	Sodium dodecyl sulphate polyacrylamide gel electrophoresis
SINE3	-	Short interspersed transposable elements
SiRNA	-	Small interfering RNA
SnRNA	-	Small nuclear RNA
SnoRNA	-	Small nucleolar RNA
SNPs	-	Single nucleotide polymorphisms
TAD	-	Topologically associated domain
TCA	-	Trichloro acetic acid
TEMED	-	Tetramethylethylenediamine
TF	-	Transcription factor
tRNA	-	Transfer RNA
TLS	-	Translesion synthesis
TSS	-	Transcription start site
3′ UTR	-	3′ untranslated region
Uchl1	-	Ubiquitin C-terminal hydrolase L1
WDR5	-	WD repeat-containing protein 5
WHO	-	World Health Organisation

List of Figures

List of Tables

1. Introduction

Cancer is a disease that results when genes responsible for controlling our cell functions such as growth and division experience certain changes. These cancer-causing genes can be inherited as a form of germline mutations thus increasing an individual's risks for cancer. Some genetic changes can be acquired as a result of errors during cell division or through exposure to carcinogenic substances that cause DNA damage. Genotoxic stress cause DNA structural changes by disrupting covalent bonds between nucleotides thus preventing the correct replication of the genome. Failure of the DNA damage machinery to correct the induced lesions leads to defects in the genes resulting in mutations which accumulate, eventually resulting in a cancer phenotype (Broustas and Lieberman, 2014). Errors in the epigenetic process also cause cancer by altering the gene expressions. Epigenetic mechanisms that affect gene regulation include histone modification, DNA methylation and non-coding RNA (ncRNA) (Peschansky and Wahlestedt, 2014).

Cancer is one of the leading causes of death globally. According to the World Health Organisation (WHO), cancer was the second leading death causing disease globally in 2018 with 9.6 million deaths and 18.1 million new cancer cases (WHO, 2018). Global studies show that 1 in 6 deaths are caused by cancer and about 70% of deaths are due to cancer in low- and middle-income countries. It is projected that by the year 2040, there will be 29.5 million new cancer cases and 16.4 million cancer related deaths (Ernst *et al.*, 2007).

Oesophageal cancer is a cancer type that occurs in the tube running from the throat to the stomach, known as oesophagus. It occurs when oesophageal cells develop errors, such as mutations in their DNA, which causes them to continuously grow and divide thus resulting in tumours. Oesophageal cancer can be classified into two major subtypes and this classification depends on the type of cells affected: oesophageal squamous cell carcinoma (OSCC) and adenocarcinoma (AC). OSCC differs from AC in that it affects the epithelial cells in the upper 2/3 lining of the oesophagus whereas AC affects the lower part of the oesophagus closer to the stomach. The geographical distribution for these cancers differs considerably with AC being more prevalent in many developed countries and OSCC predominating East Asia and Africa (Rustgi and El-Serag, 2014; Arnold*et al.*, 2015).

1.1. OSCC

OSCC is considered a major malignancy with respect to mortality rate and prognosis (Pennathur *et al*., 2013). Individuals diagnosed with OSCC have a poor survival rate as patients usually present when the cancer is already at an advanced stage; the 5-year survival rate of OSCC is 15-25% at its advanced stage (Rustgi and El-Serag, 2014). It predominantly affects more elderly people with ages ranging from 60 to 70 years and is seen more commonly in males (Daly *et al*., 2000). OSCC is caused by genetic predisposition, alcohol consumption, excessive smoking, nutritional deficiencies and history of thoracic radiation, however, these causes have shown todiffer based on ethnicity and geographical regions (Yang *et al*., 2005; Morita *et al*.,2010).

Studies have shown that alcohol consumption and tobacco use have synergistic effects thus increasing the relative risk (Morita *et al*., 2010; Engel *et al*., 2003). Studies have shown that individuals with high alcohol consumption acquire mutations in alcohol metabolising enzymes including aldehyde dehydrogenase 2 family member (ALDH2) and alcohol dehydrogenase 1B (ADH1B1), which means that alcohol has DNA mutagenic potential (Brown e*t al*., 1994; IARC, 2012). Cigarette smoke contains carcinogens such as N-nitrosamine compounds and polycyclic aromatic hydrocarbons (PAHs), which react with DNA to form DNA adducts thus affecting the DNA helical structure leading to defective DNA synthesis (Abnet *et al*., 2018). Some of the tobacco-specific nitrosamines include 4-(metylnitrosamino)-1-(3-pyridyl)-1-butanone (NNK) and N-nitrosonornicotine (NNN). N-nitrosamine compounds have also been found in some dietary products including salted fish, pickled vegetables and cured meat (Griesenberg *et al*., 2009; Miller *et al*., 1989). High N-nitrosamine concentration found in tobacco and food is considered a risk factor for OSCC development (Abnet *et al*., 2018). These N-nitrosamine compounds require metabolic activation to exert their toxicological properties, for example the activation of N-nitrosamine by cytochrome P450 results in DNA adducts formation such as O^6-methylguanine, 7-methylguanine and 3-methylguanine (Autrup *et al.*, 1984). However, only the O^6-methylguanine which causes AT-GC transition mutation is accountable for the mutagenicity of N-nitrosamines (Jagerstad and Skog, 2005). OSCC is not only caused by lifestyle factors but rather by multiple factors that may cause or promote the disease

progression (Ribeiro *et al*., 1996). Therefore, it is important to refrain from alcohol consumption and smoking to help reduce or prevent the incidence of OSCC (Chung *et al.,* 2010). The symptoms of OSCC include coughing, weight loss, chest pains, difficulty in swallowing and hoarseness of the voice.

According to GLOBOCAN data, in 2022, oesophageal cancer had the 8th highest incidence and the 6th highest number of cancer-related deaths worldwide (Figure 1.1). Oesophageal cancer rates have been increasing in the past years. The International Agency for Research on Cancer (IARC) showed that worldwide oesophageal cancer cases were about 572 034 in 2018, with the age-standardised incidence rates of 11.1 per 100 000 and 5 per 100 000 in men and women respectively (Bray *et al*., 2018). The latest GLOBOCAN results from 2020 showed an increase compared to the 2018 results with oesophageal cancer incidence of 604 100 cases and age-standardised incidence rates of 9.3 per 100 000 and 3.6 per 100 000 in men and women respectively (Morgan *et al*., 2022).

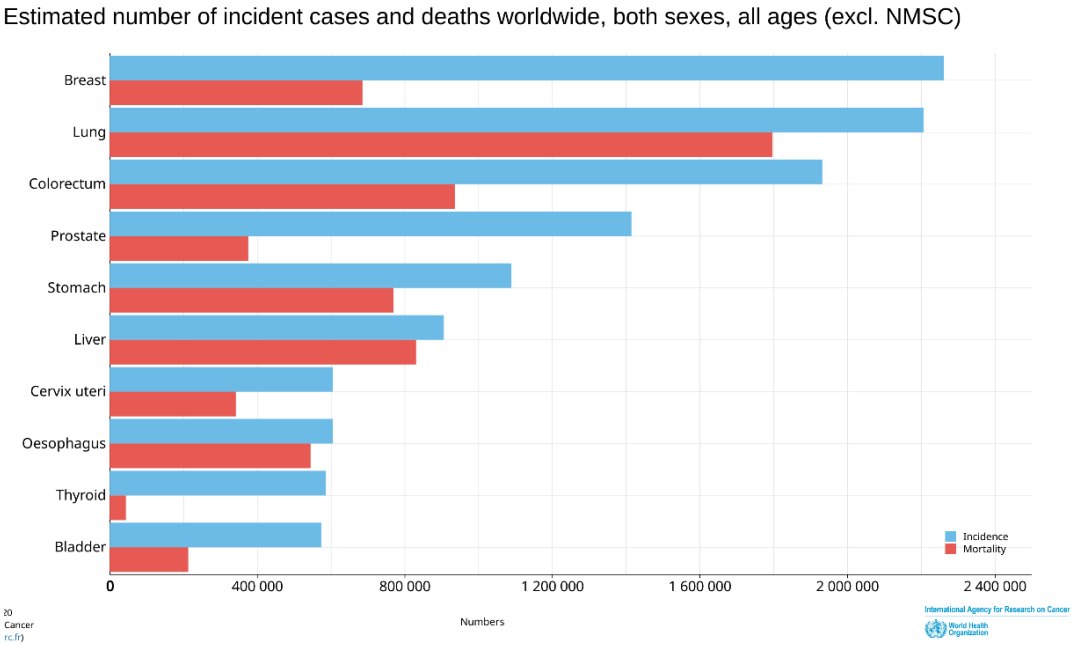

Figure 1.1: Top ten predominant cancers worldwide. According to GLOBOCAN 2022 data, oesophageal cancer ranks as the 8th most diagnosed cancer type with an incidence rate of 604 100 cases and the 6th in number of deaths with 544 076 cases worldwide (Morgan et al., 2022).

Incidence of oesophageal cancer differs across regions and populations. In 2018, eastern Asia, eastern and southern Africa had the highest number of oesophageal

cancer cases with lowest cases observed in Central America regions (Morgan *et al.*, 2022). Although these data include both OSCC and AC, it is estimated that 87% of all oesophageal cancers are OSCC and 11% are AC (Arnold *et al*., 2015). Moreover, considerable differences in OSCC exist based on ethnicity, age and gender, which may be due to differences in exposure to risk factors. In South Africa, black individuals above the age of 30 have the highest number of OSCC cases compared to other population groups (CANSA, 2017).

OSCC is a major threat to health in developing countries such as South Africa and is an increasing health concern that is expected to rise by 140% in 2025 (Lambert and Hainaut, 2007). It is one of the top ten prevalent cancers in South Africa with a high death rate. The South African Cancer Registry showed that the prevalence of oesophageal cancer among the black population is higher in comparison to other population groups due to genetic predisposition (National Health Laboratory Service (NHLS), 2008). Cancer reports conducted by Cancer Associationof South Africa (CANSA) and the National Cancer Registry (NCR) of South Africa showed that although the incidence rates for both sexes increases with age, men are at a 2 to 8 times at higher risk than women in developing OSCC (Siewert and Ott, 2007; Bray *et al*., 2018; NCR, NHLS, 2011).

1.1.1. OSCC diagnosis, screening and prevention

The diagnosis for OSCC involves various aspects such as symptoms, imaging results as well as physical examination and pathological findings. Barium oesophagography is one of the major examinations applied in the diagnosis of oesophageal cancer whereas oesophagogastroduodenoscopy is used for biopsy to confirm the diagnosis of OSCC (Levine *et al*., 1997). This approach allows physicians to see the proximal extent of the tumour and its relation to the cricopharyngeus in patients with OSCC. Once the diagnosis is made, correct staging must be done prior to treatment as this helps predict the spread of the cancer and which treatments are most appropriate (Krasna *et al*., 2001).

After the diagnosis, it is important to examine if the cancer has metastasised and this process is called staging. Oesophageal cancer staging was characterised using the American Joint Committee on Cancer (AJCC) TNM system, which considers

three main categories such as the primary tumour extent (T), the spread to the lymph node (N) and distant sites metastasis (M) (Figure 1.2) (Greene *et al*., 2002). Pathological stage grouping (pTNM) is essential for early-stage cancers and it is also important for serving as survival reference point (Rice *et al*., 2017).

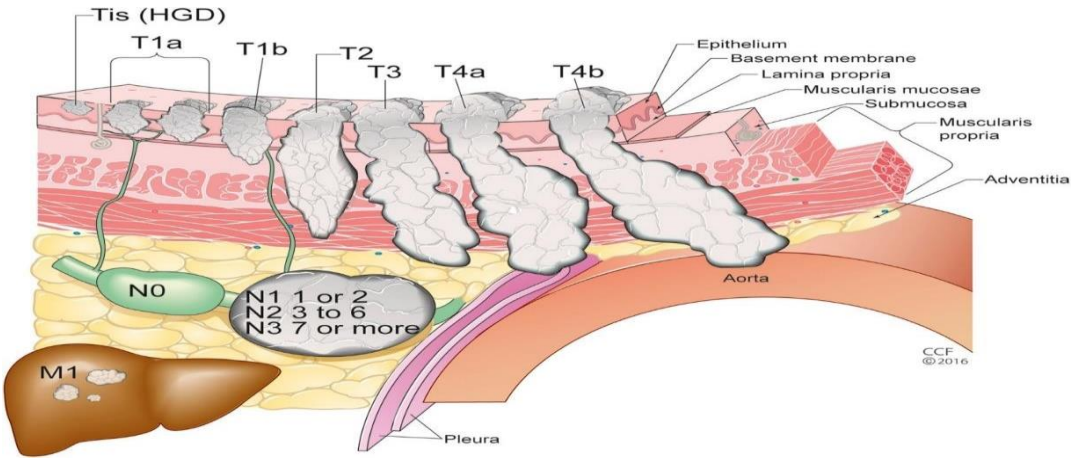

Figure 1.2: Oesophageal cancer TNM staging system. The T stage is categorised as high-grade dysplasia and is subdivided into subtypes based on the level of invasion. N is categorised into 4 subtypes based on the cancer spread to the lymph node. N0 showing no regional lymph node metastasis, N1, 2 and 3 are associated with regional lymph node metastasis of 1 or 2, 3 to 6 and 7 or more nodes. M1 shows distal metastasis (Rice *et al*., 2017).

Staging may be assessed radiologically and pathologically. The clinical stage of oesophageal carcinoma can be determined by multiple diagnostic imaging procedures such as computed tomography (CT), positron emission tomography (PET), endoscopic ultrasound (EUS) and magnetic resonance imaging (MRI) scan (Chandawarkar *et al*., 1996). However, the abovementioned scans cannot distinguish tumour depth and have poor lymph node sensitivity, which fails to detect minor metastasis. The EUS, which has now become the popular oesophageal cancer diagnosis technique, provides correct information in terms of depth of infiltration (He *et al*., 2014). A study comparing CT scan to EUS in oesophageal cancer staging showed that CT scan can identify lymph-node involvement in 23% of patients whereas EUS identified 83% (Subasinghe and Samarasekera, 2010).

Therapeutic strategies are decided based on the grade of malignancy and the patient's general condition. Current treatments for OSCC include radiotherapy,

chemotherapy and surgery. Surgical resection is the traditional OSCC treatment. There is also an increased use of chemotherapy, combination therapy (the use of multimodal therapies such as chemoradiotherapy and combination of chemotherapy with surgery to treat a disease) as well as radiotherapy before surgery. However, these have little effects on OSCC as the patients are displaying chemoresistance to the drugs and the patients' 5 years survival rate is less than 25% (Then *et al*., 2020).

The proposed study aims to mainly focus on response to chemotherapy, which is a drug treatment that employs powerful chemicals for killing rapidly growing cancerous cells in the body. The chemotherapeutic drugs can either be used alone, combined with other drugs or with radiotherapy for the treatment of different cancer types. The advantage of using chemotherapy as the primary treatment for OSCC is because it also targets micro-metastasis and reduces the risk of distant metastasis in addition to slowing cancer growth and shrinking tumour enough for surgery (Le Bras *et al*., 2016). Some of the chemotherapeutic drugs used for the treatment of OSCC are cisplatin, 5-fluorouracil (5-FU) and paclitaxel (Gu *et al*., 2012). According to the WHO guidelines, systemic chemotherapy must be used for the treatment of advanced OSCC. Cisplatin and 5-FU are two drugs commonly used in South Africa and whilst readily available and relatively inexpensive they have been associated with poor efficacy, chemoresistance and chemo-toxicity (Levard *et al*., 1998; Ando *et al*., 2012). Due to late presentation and poor response to therapy, OSCC prognosis remains poor, thus, understanding causes of chemoresistance and developing alternative treatments for OSCC is highly desirable.

1.1.2. Treatment

Cisplatin is a platinum containing drug displaying clinical activity against multiple solid tumours, including lung, testicular, bladder, ovarian as well as head and neck cancer (Rosenberg *et al*., 1969). Cisplatin is a potent apoptosis inducer in cancer cells (Ormerod *et al.*, 1996). Together with its analogues carboplatin and oxaliplatin, they have shown efficacy in cancer treatment with palliative and curative intent (Muggia *et al*., 2015). Since its discovery, cisplatin has shown high degree of activity against tumour growth in various cancer types. Despite its major clinical success, it is associated with chemoresistance in cancer cells. It is estimated that 50% of cancer patients will be treated with cisplatin in their anticancer therapy (Ghosh, 2019). It is therefore important to improve clinical utility of cisplatin.

1.1.2.1. Cisplatin mechanism of action and DDR

The cisplatin drug is composed of one platinum atom linked to two chlorides and two amides. It enters cells through the plasma membrane by passive diffusion or by active transport using copper transport 1 (CTR1) protein (Ishida *et al*., 2002). Once inside the cells, cisplatin becomes activated by undergoing an aquation process where its chloride ions get replaced with water molecule. This aquation process makes cisplatin highly reactive, allowing it to readily bind to various biomolecules inside the cell such as reduced glutathione (GSH), metallothionine (MT), methionine and other cysteine rich proteins (El-Khateeb *et al*., 1999). The aquated form of cisplatin covalently binds to DNA bases to form DNA adducts. It particularly reacts with N7 position of purine bases, adenine and guanine resulting in DNA crosslinks. These crosslinks can be on the same strand (intra-strand) or different strands (inter-strand) crosslinks (ICLs) (Eastman *et al*., 1987). The cisplatin-induced DNA adducts disturbs transcription and DNA replication thus inducing replication stress and DNA damage response (DDR) eventually resulting in the arrest of the cell cycle and apoptosis.

Responding to genotoxic stress, the DDR network induces a signal transduction cascade including the activation of pathways responsible for genome protection such as cell cycle control, DNA repair, apoptosis, chromatin remodelling and transcription. The DDR pathways involved in removing cisplatin-induced DNA damages are the homologous recombination (HR), non-homologous end joining (NHEJ), DNA mismatch repair (MMR) and nucleotide excision repair (NER) (Bernstein *et al*., 2002). However, cisplatin has shown to exert its cytotoxic effects through intra and ICLs. The ICLs are considered the most toxic since they covalently bind two strands of the DNA helix preventing strand separation (Deans and West, 2011). Initial repair of ICLs include single strand break repair pathways, MMR and NER. In thecase of excessive cisplatin-induced adducts, this leads to the formation of DSBs (Vare *et al*., 2012). This is because the ICL adducts are adjacent to a nick and whenthe strand adjacent to a nick is incised, more DNA DSBs form. DDR mechanisms responsible for repairing DSBs, NHEJ and HR repair may be activated (Figure 1.3). DNA DSBs are considered the most hazardous type of DNA damage.

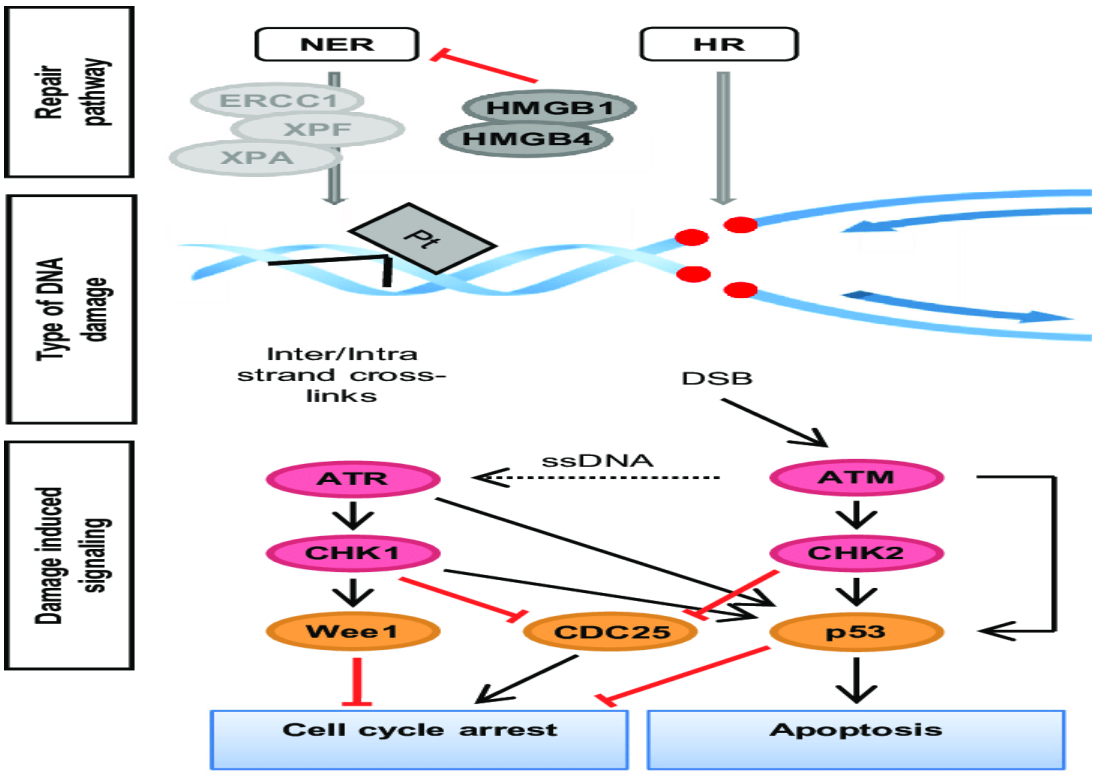

Figure 1.3: Overview of cisplatin-induced DNA damage and repair. Cisplatin induces DNA intra and inter-strand crosslinks. These crosslinks are repaired by NER or HR repair pathways. The presence of DSBs activates ATM, which in turn activates a signal cascade for p53 phosphorylation induction, resulting in the inhibition of apoptosis and cell cycle arrest (de Vries *et al*., 2020).

The DNA DSBs results in the activation a set of responses in eukaryotic cells such as cell cycle arrest and apoptosis. When cells fail to arrest cellular functions and induce apoptosis, high genomic instability results, which is linked to high probability of oncogenic transformation (Zhivotovsky and Kroemer, 2004). In the event of DSBs, DDR machinery is activated to respond to DSBs. Cisplatin-induced DNA DSBs are formed as a result of the inhibition of the HR pathway (Rocha *et al*., 2018). In response to DSBs, the DDR machinery recruits the ataxia telangiectasia mutated (ATM) protein kinase to the DSBs site by the MRE11-RAD50-NSB1 (MRN) complex and activates the ATM signalling pathway (Bassing and Alt, 2004) (Figure 1.3). The ATM kinase is a DSBs sensor and causes G1 cell cycle arrest by phosphorylating the p53 protein thus activating the p53-dependent transcriptional program leading to cell cycle arrest and apoptosis (Figure 1.3).

The stability and transcriptional activation of p53 is regulated by two kinases, namely the ATM and ataxia telangiectasia RAD3-related protein (ATR) (Zhao *et al*., 2001). Cisplatin-activated ATR phosphorylates p53 on serine-15 and activates it leading to increased signalling through the death receptor pathway and thus cell death. The ATR and ATM proteins also activate downstream targets, namely checkpoint kinase 1 (CHK1) and checkpoint kinase 2 (CHK2) (Figure 1.3). ATR-activated CHK1 phosphorylates p53 on serine-20 (Shieh *et al*., 2000). The activation of p53 by cisplatin also causes the transactivation of genes associated with cell cycle arrest, apoptosis and DNA repair such as *p21* and Bcl-2-associated X (*Bax*). The *p21* transactivation by p53 is believed to activate the cell cycle checkpoints and induce S-phase cycle arrest (Bai and Zhu, 2006).

The phosphatidylinositol 3-kinase-related kinases (PIKKs) namely the ATR, ATM and DNA-dependent catalytic subunits (DNA-PKCs) phosphorylate histone H2AX variant in response to DSBs (Burma *et al*., 2001; Mannironi *et al*., 1989). These kinases each have a distinct role in histone H2AX phosphorylation and activation of repair proteins. The histone H2AX variant accounts for about 2 to 25% of the total histone H2A in human cells and also participates in the DDR (Mannironi *et al*., 1989). In the presence of DSBs formed either during exposure to ionising radiation or induced by chemotherapeutic agents, the ATM or DNA-PKCs phosphorylates histone H2AX variant at serine 139 (Rogakou *et al*., 1998). This phosphorylated form of histone H2AX is commonly known as the gammaH2AX (γH2AX), a biomarker of DSBs (Kuo and Yang, 2008).

This phosphorylation process forming γH2AX occurs a few seconds after DNA damage recognition. This results in the spread of γH2AX along the chromosome forming discrete γH2AX foci. Studies have reported that γH2AX foci formation reaches a peak 30 minutes to an hour after phosphorylation. These foci then attract other repair factors resulting in high concentration of repair proteins in the DSBs sites (Vandersickel, 2010). The most common repair proteins that interacts with γH2AX is the mediator of DNA damage checkpoint protein 1 (MDC1) and MRN. MDC1 is responsible for orchestrating the assembly of all important repair proteins to the site of the DNA damage (Stucki and Jackson,2006). Besides its role in recruitment and accumulating DNA repair proteins, γH2AX also interact with cohesins to maintain chromatid cohesion during DNA repair. The loss of γH2AX

at the DSBs is associated with DDR. This decrease usually takes place 24 hours after γH2AX induction (Van der Kogel and Joiner, 2009; Marriotti *et al*., 2013).

1.1.2.2. Mechanisms of cisplatin of resistance

Resistance to chemotherapy is the major limitation of the effectiveness of chemotherapeutic drugs used in cancer treatment. Drug resistance can be intrinsic with tumours resistant to chemotherapy before treatment or acquired throughout treatment by tumours that were initially sensitive to chemotherapy (Longley and Johnston, 2005). This resistance can happen at various levels including increased or decreased drug efflux, apoptosis evasion, drug activation and changes in drug target (Longley and Johnston, 2005). Various cancer types have shown resistance to cisplatin and these include gastric, lung, NSCLC, ovarian, bladder etc.

Mechanisms of cisplatin resistance are multifactorial and differ in different cancer types. These mechanisms include (1) low intracellular cisplatin accumulation, (2) high inactivation of cisplatin by thiol containing molecules such as GSH and MT, (3) changes in DNA damage repair, (4) DNA damage tolerance changes and (5) changes in apoptotic cell pathways (Figure 1.4) (Rabik and Dolan, 2007; Kartalou and Essigmann, 2001).

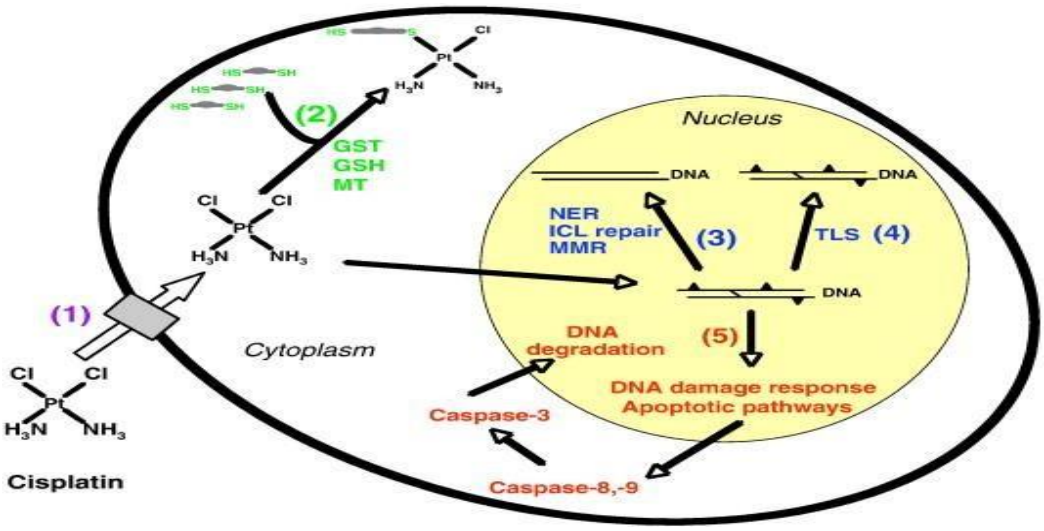

Figure 1.4: Mechanisms of cisplatin resistance. Cisplatin resistance can be due to five different mechanisms: cellular drug accumulation, inactivation by thiol proteins, DNA damage changes, DNA damage tolerance changes and apoptotic induction (Köberle *et al*., 2010).

Most tumour cell lines with acquired cisplatin resistance displayed low cisplatin accumulation compared to the parental cell line, suggesting that changes in drug transport is responsible for the decreased drug uptake mechanism of resistance (Loh *et al*., 1992). A plasma membrane transporter CTR1, has been shown to be responsible for cellular cisplatin uptake (Ishida *et al*., 2002). It has been reported that cisplatin results in rapid degradation of CTR1, causing diminished cisplatin influx and thus resistance (Holzer *et al*., 2006). Cells with high CTR1 levels have shown increased cisplatin accumulation and sensitivity. Low CTR1 levels have been reported in cisplatin resistant lung cancer (Song *et al*., 2001) whereas in oral squamous cell carcinoma, same CTR1 levels were observed in resistant and sensitive cell line (Yoshizawa *et al*., 2007). Therefore, this suggests that CTR1 relevance in cisplatin resistance is cancer type specific.

Conjugates forming between thiol-containing molecules, such as GSH, and platinum-containing drugs such as cisplatin, play a crucial role in cisplatin inactivation (Figure 1.4). GSH is a powerful antioxidant responsible for the inhibition of oxidative stress which is responsible for DNA damage. The conjugation process between GSH and cisplatin is catalysed by glutathione-S-transferase (GST) and this conjugation prevents cisplatin from binding the DNA

(Köberle *et al*., 2010). It has been reported that tumour cells with high GSH levels are resistant to platinum containing drugs (Kelland, 1993). These increased GSH levels were observed in bladder, ovarian, lung, cervical, and embryonal cell lines displaying cisplatin resistance (Jansen e*t al*., 2002; Mellish *et al*., 1993; Meijer *et al*., 1992), as well as the OSCC cell lines used in this study (Damelin *et al*., 2014).

To respond to DNA damage, the DDR is activated to repair cells or induce apoptosis. NER mechanism is responsible for the removal of cisplatin-induced DNA damage (Reardon *et al*., 1999). Defects in the NER pathway is linked to cisplatin hypersensitivity and its restoration reduces this sensitivity to normal levels (Furuta *et al*., 2002). Numerous proteins are involved in the NER pathway, however only an upregulation of the rate limiting factors such as the excision repair complementing 1 (EERC1) protein increase the cell's capacity for NER (Hassan *et al*., 2014). EERC1 plays a major role in the determination of cisplatin sensitivity. Studies proved that elevated EECR1 expression is responsible for cisplatin resistance (Youn *et al*., 2004; Melton *et al*., 1998). High EERC1 levels ingastric, NSCLC and ovarian cancer have been reported to correspond with poor cisplatin response (Lord *et al*., 2002; Dabholkar *et al*., 1994).

Cisplatin-induced lesions cause DNA distortions thus interfering with DNA replication and arresting DNA polymerases (Siddik *et al*., 2003). To avoid the collapse of the arrested replication fork, DNA damage can be tolerated by translesion DNA synthesis (TLS) (Figure 1.4) (Sale, 2012). TLS is mediated by DNA polymerases, which can replicate across damaged sites on the DNA template. TLS cells rescue from the collapse of the replication fork is believed to contribute to cisplatin resistance (Mamenta *et al*., 1994).

The main goal of cytotoxic chemotherapies is inducing apoptosis in cancer cells. Cisplatin induced apoptosis can be activated by the intrinsic mitochondrial or extrinsic death receptor pathways. There are multiple proteins associated with the abovementioned pathways and these include p53, Bcl-2 pro and anti-apoptotic proteins such as Bad, Bax and Bak as well as Bcl-xl, Bcl-2 and Mcl-1 respectively (Hengartner, 2000). Cisplatin resistance can be caused by loss or reduced pro-apoptotic proteins or increased anti-apoptotic protein levels (Brozovik and Osmak, 2007). There are contradictory results regarding p53 expression in cisplatin induced apoptosis; some studies show that high p53 levels are responsible for cisplatin

resistance in certain cancer types (Branch *et al*., 2000) and others argue that the downregulation of p53 is associated with apoptotic cisplatin resistance (Xu *et al*., 2005; Spiering *et al.,* 2003).

1.1.2.3. Cisplatin treatment on OSCC

Cisplatin is the most used chemotherapeutic drug for OSCC treatment and is associated with poor efficacy and chemoresistance. So far, cisplatin studies on OSCC are those of combination therapy of cisplatin with other anticancer drugs such as 5-FU, Paclitaxel and docetaxel (Kies *et al*., 1987; Hara *et al*., 2013; Yamasaki *et al*., 2011). Colleagues from our laboratory also performed combination studies of cisplatin with metformin on OSCC (Damelin *et al*., 2014). The study showed that metformin results in an intracellular reductive state which protects OSCC cells from cisplatin.

Despite chemotherapy being a major therapeutic approach for OSCC, its clinical efficacy remains disappointing due to chemoresistance (Mao *et al*., 2021). Chemoresistance is associated with unsuccessful treatment outcome due to poor response rate of the patients. This is often multifactorial and complex depending on the cancer subtype. To overcome chemoresistance, new targets for therapy are under research and evaluation. For OSCC, this includes the use of combination therapy such as cisplatin-based and 5-FU-based therapy targeting different mechanisms (Yang *et al*., 2020). Targeted molecular therapy such as antibody monotherapies are a relatively new supplement for chemotherapy and have also been confirmed to play a crucial role in OSCC treatment, however, access to such therapies is limited in developing countries due to cost (Syrigos *et al*., 2008). Modern RNA research has revolutionised diagnosis and therapeutics of various diseases, for example RNA modulation has become a promising therapeutic approach with ncRNAs showing a great potential for the treatment of different cancer types, including OSCC (Sundaram and Veera Bramhachari, 2017; Deng *et al*., 2017). Genome-wide studies have shown that a type of ncRNA known as long non-coding RNAs (lncRNAs) may be involved in cancer progression. Their expression has been shown to be altered in various cancer types, often inactivating tumour suppressors and activating oncogenes. These lncRNAs also regulate DDR and repair through the modulation of various DDR signalling pathways (Su *et al*.,

2018). Recent studies have shown that the dysregulation of lncRNAs in cancer makes them novel biomarkers for diagnosis and prognosis of human cancers, and may be new therapeutic targets (Hung *et al*., 2011; Luo *et al*., 2016). However, further research is required to identify the involvement of lncRNA in drug response and chemoresistance.

1.2. Long-coding RNA

With the advent of advanced genome sequencing technologies such as the tiling resolution genomic microarrays, encyclopedia of DNA elements (ENCODE) and deep sequencing, our understanding of the human genome has been revolutionised. Studies have proved that whilst about 90% of the human genome is actively transcribed, only 2% encodes for proteins (Ponting *et al*., 2010). Within these non-protein coding sequences, ncRNAs are transcribed (Comings, 1972). NcRNAs have been shown to participate in many biological and developmental processes and certain diseases such as cancer (Pavet *et al*., 2011). There are two classifications of ncRNAs, these being the regulatory or housekeeping ncRNAs. Housekeeping ncRNAs are relatively expressed and act as regulatory molecules in various cellular processes. The housekeeping ncRNAs include ribosomal (rRNA), small nucleolar RNA (SnoRNA), transfer (tRNA) and small nuclear (snRNA) (Zhang *et al*., 2019). Regulatory ncRNAs are divided into two groups, namely the short ncRNAs and lncRNAs with less than 200 nucleotides and greater than 200 nucleotides respectively. The short ncRNAs include small interfering RNAs (siRNAs), microRNAs (miRNAs) and piwi-associated (piRNAs) whereas the lncRNAs are categorised based on their proximal adjacent protein coding genes.

According to the human generalised coding (GENCODE), the human genome has greater than 16 000 lncRNA genes but other studies argue that there are more than 100 000 lncRNA genes (Uszczynska-Ratajczak *et al*., 2018; Fang *et al*., 2018). These lncRNAs have regulated expression and differ in the way they regulate gene expression. However, not all these lncRNAs are functional; the number of functional lncRNAs is still under debate but most of them have proven to have significant cellular functions (Palazzo and Lee, 2015). Most lncRNAs are transcribed by RNA polymerase II (RNA pol II) and have structural features similar to that of mRNAs as they encompass a 5′ cap, polyadenylation (polyA) tail and a

promoter structure (Derrien *et al*., 2012). They also undergo post transcriptional processes like alternative splicing and carry single nucleotide polymorphisms (SNPs). In contrast to mRNAs, these lncRNAs have low expression levels, longer but fewer exons, are poorly evolutionarily conserved, lack an open reading frame (ORF) as well as a 3′ untranslated region (3′ UTR) (Yu *et al*., 2004; Hezroni *et al*., 2015).

1.2.1. Classifications of lncRNA based on genomic location

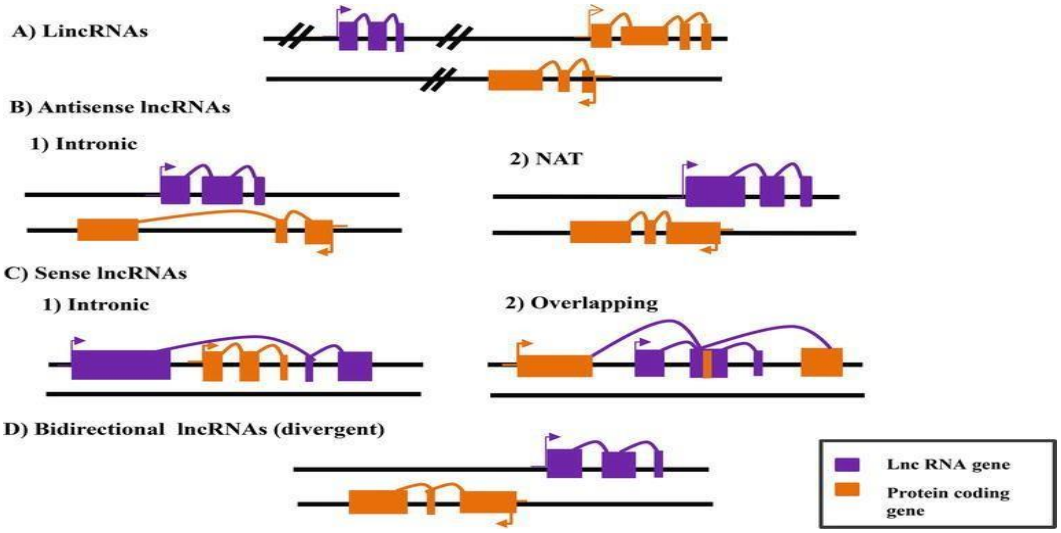

Figure 1.5: LncRNAs categorisation according to their position in relation to the protein coding genes. LncRNAs are categorised according to different positions in relation to the protein coding genes and direction of transcription. These classifications include lincRNAs, antisense, sense and bidirectional lncRNAs (Hrdlickova *et al*., 2014).

LncRNAs are categorized into four different classes based on their position in relation to protein coding genes which they may regulate (Figure 1.5) (Hrdlickova *et al*., 2014). These categories are: (1) long intergenic lncRNAs (lincRNAs) representing the largest group of lncRNAs and are transcribed adjacent to protein coding genes; (2) sense lncRNAs: sense overlapping or sense intronic, are positioned on one and transcribed in a similar direction as protein coding genes; (3) antisense lncRNAs are overlapping and are transcribed from an antisense strand. Based on the overlap, antisense lncRNAs are further divided into classes namely the intronic antisense and natural antisense transcripts (NATs), and (4) bidirectional lncRNAs are transcribed on the opposite strand within 1 kilobase (kb) from the

protein coding gene and have their transcription start site (TSS) next to that of the protein coding genes (Figure 1.5) ((Hrdlickova *et al*., 2014).

1.2.2. Classifications of lncRNA according to their mechanism of action

LncRNAs interact with RNA, DNA and proteins. These RNA-DNA, RNA-protein and RNA-RNA interactions depend on the site at which the lncRNA acts (Guttman and Rinn, 2012). The main function of lncRNAs is regulating gene expression via chromatin modification, transcriptional and post-transcriptional regulation (Whitehead *et al*., 2009; Bernstein and Allis, 2005). Studies proved that most lncRNAs are located in the nucleus and a large fraction are exported to the cytosol where they are assigned to specific organelles and associate with RNA binding proteins (RBP) (Carlevaro and Johnson, 2019). It was discovered that these lncRNAs can employ their functions acting in the nucleus, cytosol or both. Studies have also shown that some lncRNAs are linked to polysomes and ribosomes, acting as coding transcripts thus resulting in small peptides (Kung *et al*., 2013).

LncRNAs are divided into four broad groups based on their mechanism of action: signal, guide, decoy or scaffold (Wang and Chang, 2011). As signals, lncRNAs regulate transcription by responding to different stimuli thus serving as an indicator for transcriptional activity. Some examples of lncRNAs with signal archetype are hox transcript antisense RNA (HOTAIR) and p21 associated ncRNADNA damage activated (PANDA) involved in embryonic development, DNA damage and stress response respectively (Wang and Chang, 2011). Guide lncRNAsbind proteins and direct the localisation of chromatin modifying enzymes to specific targets either in *cis* or *trans.* They can interact with both transcriptional activators and repressors. Some of the lncRNAs employing this mechanism are X-inactive specific transcript (Xist), lincRNAp2 and HOTAIR (Gupta *et al*., 2010). Decoy lncRNAs bind and interfere with the RNA and protein functions. They bind to regulatory proteins such as transcription factor (TF) and miRNA and prevent them from binding to their targets. An example of this is PANDA binding to TF nuclear transcription factor Y subunit A (NF-YA) thus preventing the activation ofNF-YA induced pro-apoptotic targets (Hung *et al*., 2011). Scaffold lncRNAs play a structural role by acting as adaptors and allow the assembly of two or more proteins to form nucleoprotein complexes that affect histone modifications. Some of the examples of scaffold lncRNAs with scaffolding mechanism include antisense noncoding RNA in the

INK4 locus (ANRIL) and HOTAIR (Li *et al*., 2016).

1.2.3. Gene regulation by lncRNAs

LncRNAs regulate gene expression at different levels. They regulate gene expression by modulating chromatin remodeling, transcription and post-transcriptional processes of target genes.

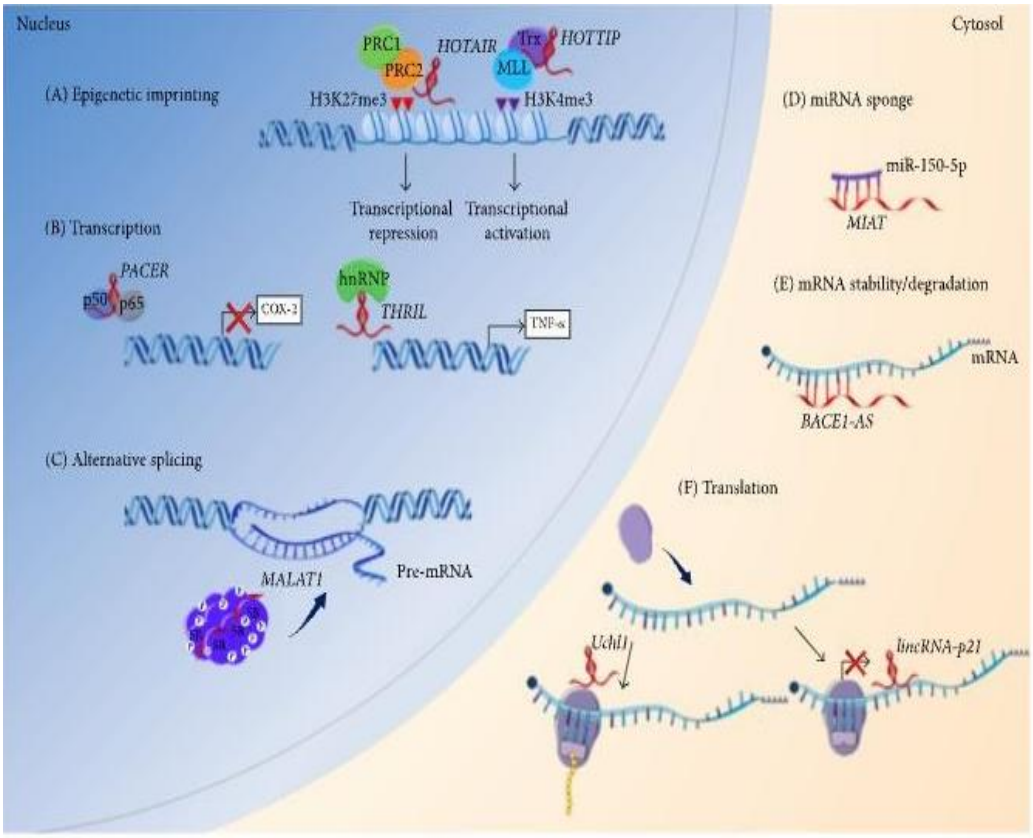

Figure 1.6: Mechanism of lncRNA gene regulation. LncRNAs regulate gene expression at multiple levels including transcription, epigenetic imprinting, alternative splicing, acting as miRNA sponge and translation. Different lncRNAs are involved in each process (Losko *et al*., 2016).

1.2.3.1. Epigenetic transcriptional regulation by lncRNAs

Epigenetic transcriptional regulation is the most dominant function explored in lncRNAs studies. This mechanism of gene regulation results in transcriptional repression or activation (Chu *et al*., 2011) (Figure 1.6). HOTAIR and ANRIL forms part of lncRNAs with repressive functions, whereas hox A distal transcript antisense RNA (HOTTIP) forms part of transcription activating lncRNAs. These lncRNAs use scaffolding mechanism by coupling with histone modifying or

chromatin remodelling complexes to exert transcriptional activation or repression (Kurokawa *et al*., 2009; Roberts *et al*., 2014). The polycomb group (PcG) proteins, namely the polycomb repressive complex-1 (PRC-1) and polycomb repressive complex-2 (PRC-2) are the common protein partners of lncRNAs with repressive or activating functions. These complexes facilitate chromatin compaction and heterochromatin formation thus repressing transcription (Figure 1.6). Although PRC-1 and PRC-2 are the most notable lncRNAs protein partners, there are various epigenetic complexes involved in ncRNA-mediated gene regulation.

1.2.3.2. Post-transcriptional regulation by lncRNAs

LncRNAs regulate mRNA processing at various steps including alternative splicing, stabilisation of mRNA and translation of proteins (Zhang *et al*, 2019) (Figure 1.6). Most lncRNAs involved in post-transcriptional regulation interact through sequence complementarity (Khochbin *et al*., 1992). However, antisense transcripts still affect alternative splicing of sense transcripts by using base complementarity to mask the splice sites. An example of alternative splicing modulation by non-sequence complementarity is the MALATI lncRNA which regulates pre-mRNA active serine/arginine splicing factors (Tripathi *et al.*, 2010) (Figure 1.6).

LncRNAs acting on post transcriptional regulation modulate the miRNA pathways (Figure 1.6). The primary function of miRNA is to anneal to the 3′ UTR or coding sequence of the complementary target mRNA and recruit translation impairment or transcript degradation protein factors thus decreasing protein levels. Various lncRNAs have miRNA binding sites, acting as sponges to sequester miRNA from their mRNA targets. These lncRNAs include linc-ROR and KRAP1. (Poliseno *et al*., 2010; Wang *et al*., 2013). For mRNA stability, lncRNAs compete with miRNAs for their mRNA target site. This is demonstrated by lncRNA beta-site amyloid precursor protein cleaving enzyme 1 (BACE1-AS) antisense transcript binding its sense BACE1 transcript lncRNA at miR-485 and impairing its function (Figure 1.6) (Faghihi *et al.*, 2010). The translational process is also facilitated or repressed by lncRNA-mRNA pairing. For translational activation, lncRNA ubiquitin carboxyterminal hydrolase L1 (Uchl1) recruits polysomes to short interspersed transposable element 3 (SINE3) repetitive domain and promote cap independent translation. For translational repression, lincRNA-p21 repress beta-catenin and

JunB mRNA by recruiting translation repressors (Figure 1.6) (Carrieri *et al*., 2012; Yoon *et al*., 2012).

1.2.4. ANRIL

ANRIL, is a lncRNA located at the genomic locus cyclin-dependent kinase inhibitor 2A/B (*CDKN2A/B*), a hotspot for heritable diseases at chromosome 9p21(Figure 1.7). This gene cluster that extends over 350 kb and housed in the topologically associated domain (TAD), has three protein coding genes and antisense to them is the ANRIL lncRNA (Rao *et al*., 2014). These protein coding genes include S-methyl-5′-thioadenosine phosphorylase (MTAP), *CDKN2A* encoding splice variants p14ARF and p16INK4A as well as *CDKN2B* encoding p15INK4B (Figure 1.7) (Holdt *et al*., 2011). The *CDKN2A* and *CDKN2B* encodedproteins are tumour suppressors playing a role in cell cycle arrest, affecting major cellular processes including apoptosis, proliferation, senescence and aging (Kong *et al*., 2018). The p16INK4A and p15INK4B proteins act as cyclin dependent kinase (CDK) inhibitors that inhibit retinoblastoma (RB) phosphorylation by CDK4/6 whereas p14ARF binds Mouse double minute 2 homolog (MDM2) and degrades it and it is also involved in p53 activation and cell cycle arrest.

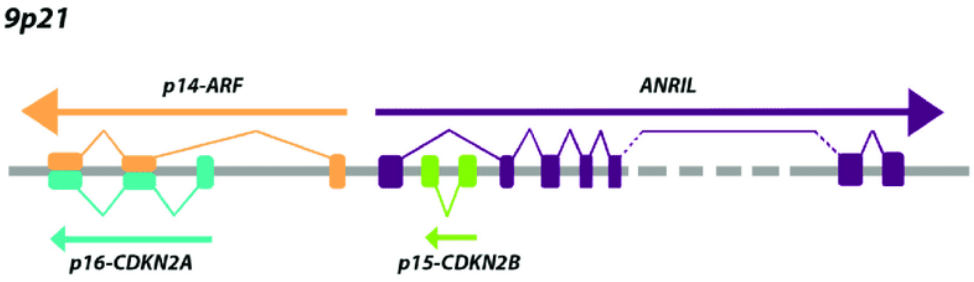

Figure 1.7: ANRIL-ARF bidirectional promoter. ANRIL and *p14-ARF* gene share a bidirectional promoter. ANRIL is transcribed from the opposite strand to the cluster. The *CDKN2A* encodes proteins p14-ARF and p16-CDKN2A, whereas *CDKN2B* encodes p15-CDKN2B (Drak Alsibai *et al*., 2019).

ANRIL was discovered in members of a French family showing a history of melanoma and neural system tumours with a 403 kb germ line deletion (Pasmant *et al*., 2007). It is transcribed by RNA pol II in the opposite direction from the *CDKN2A/B* cluster. Ithas 20 exons and the 5′ end of the first exon is located 300 bp upstream of the p14ARF TSS, suggesting that these two may share a bidirectional

promoter (Figure1.7). Most of these ANRIL exons consist of short interspersed retro-transposable elements (SINE), long interspersed retro-transposable elements (LINE) and Alu repetitive elements that can be spliced into multiple linear and circular isoforms (Jarinova *et al.*, 2009). Many of these isoforms exist in the same cell type and othersare tissue specific emphasising the complexity of their regulatory function.

1.2.4.1. Functions of ANRIL

ANRIL is predominantly localized in the nucleus (Kong *et al*., 2018). It is suggested that this lncRNA acts as a molecular scaffold of chromatin modifying complexes controlling gene expression through the modification of histone tails. Transcriptional activity of the *CDKN2A/B* gene cluster is controlled by the PcG and histone H3 lysine 27 trimethylation (H3K27me3), which represses the gene cluster; these PcG proteins were identified as two multiprotein complexes discovered in drosophila melanogaster and named PRC-1 and PRC-2 (Figure 1.8) (Yap *et al*., 2010). Both these complexes are involved in the polycomb inhibitory chromatin state, activating and deactivating genes at the right time in appropriate cells.

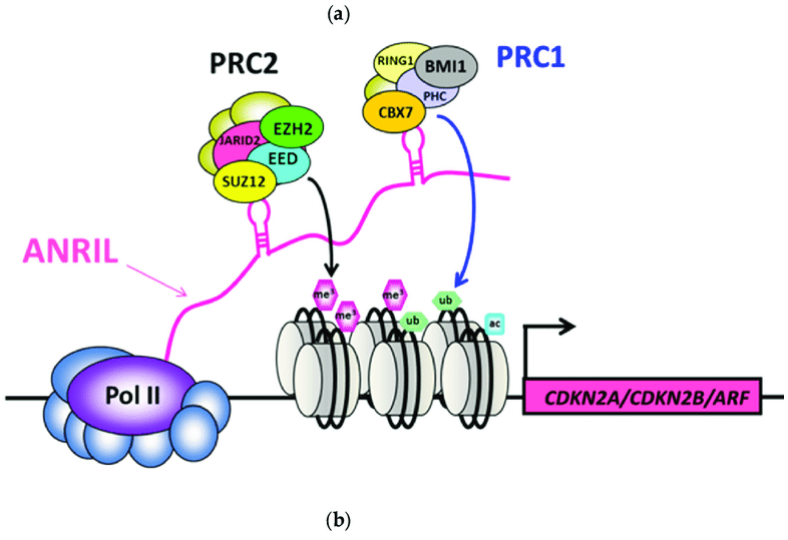

Figure 1.8: PRC1/2 complexes and ANRIL interaction at the CDKN2A/B locus. The interaction between ANRIL and the PcG proteins PRC-1 and PRC-2 complexes to epigenetically regulate gene expression (Drak Alsibai *et al*., 2019).

ANRIL acts in PRC1/2 dependent mechanisms to either mediate epigenetic transcriptional repression of neighboring genes *CDKN2A* and *CDKN2B* or to repress distant genes acting *in trans* (Holdt *et al*., 2013). The PRC-1 complex consists of multiple subunits such as CBX7, PHC etc. which catalyse mono-ubiquitination of H2A on K119 (H2AK19ub1) for maintaining chromatin inactivation (Figure 1.8). PRC-2 complex maintain chromatin repression by catalysing mono-, di- and trimethylation of histone H3 lysine 27 (H3K27me1, H3K27me2 and H3K27me3) (Figure 1.8). Acting in *cis,* ANRIL interacts with the CBX7 to recruit PRC-1 to p16INK4A and p14ARF loci thus silencing the *CDKN2A* by H3K27me3. This H3K27me3 of the *CDKN2A* and *CDKN2B* results in chromatin compaction. At *CDKN2B,* ANRIL recruits SUZ12, the PRC-2 subunitto p15INK4B. Unlike cis regulation, ANRIL *trans* regulation is dependent on Alu motifs found in ANRIL transcripts and promoters of ANRIL target genes (Figure 1.8) (Drak Alsibai *et al*., 2019).

1.2.4.2. ANRIL in cancer

The *CDKN2A/B* locus is linked to the risk of cancer, frailty, stroke, type 2 diabetes, atherosclerosis and Alzheimer's disease (Kong *et al*., 2016; Hannou *et al*., 2015). Studies have proven that the dysregulation of ANRIL expression in cancer changes the expression of genes involved in cell proliferation and apoptosis (Sato *et al*., 2010; Holdt *et al*., 2013). ANRIL was shown to have oncogenic properties and its overexpression promotes cell proliferation, invasion, migration, metastasis but inhibits apoptosis whereas its loss of function has opposite effects (Dong *et al*., 2017; Zhao *et al.,* 2018; Qiu *et al*., 2016). Studies show that ANRIL is implicated in multiple malignancies such as bladder, prostate, oesophagus, liver, cervix, ovary, lung and breast cancer etc (Kong *et al*., 2018; Zhang *et al*., 2018).

1.2.4.2.1. Molecular mechanism of ANRIL in cancer

ANRIL lncRNA overexpression promote cancer through various mechanisms (Lou *et al*., 2020). It can use the transcriptional mechanism acting *in cis* to suppress the *CDKN2A/B* tumour suppressor gene or through PRC-mediated *in trans* gene regulation. In cancer cells, ANRIL lncRNA redirects the PRC-1 and PRC-2 complexes to specific genomic loci causing the inhibition of gene expression thereby regulation cancer metastasis and invasion (Shen *et al*., 2016). Another mechanism of ANRIL in cancer is the miRNA regulation whereby ANRIL binds to

miRNA. An example of this includes the positive feedback loop between E2F TF and miRNA-449a in gastric cancer; E2F1 activates ANRIL, allowing it to bind the miRNA-99a/miRNA-449a promoter region and PRC-2. When the miRNA-449a is silenced, the E2F1 TF dissociates from the complex and promotes cancer cell proliferation (Zhang *et al*., 2014).

1.2.4.2.2. ANRIL in OSCC

ANRIL lncRNA promotes cell growth by inhibiting the TGFβ/Smad signalling pathway and was also found to be highly expressed in OSCC (Chen *et. al.*, 2014). However, the exact molecular mechanism between ANRIL and TGF-β1 is still unclear. According to another study by Cao *et al*., 2018, ANRILexpression was upregulated in OSCC tissues but lower in OSCC patients with early tumour stage, no lymph node and no metastasis. ANRIL showed a positive correlation with lymph nodes metastasis TNM stage and clinical stage (Cao *et al*. 2018). Moreover, a positive relationship was observed between ANRIL expressionlevel, tumour stage and lymph node metastasis. Upregulated ANRIL expression was associated with a shorter survival rate in OSCC patients. There is currently limited information on ANRIL expression in OSCC, although it has beenfound to be highly expressed in multiple cancer types.

1.2.5. LncRNA PANDA

PANDA is transcribed at cyclin-dependent kinase inhibitor 1A (*CDKN1A*) locus and located on the human chromosome 6p21.1. It is polyadenylated and 5′ capped but non-spliced (Shi *et al*., 2019). This lncRNA is located 5 kb upstream of the *CDKN1A* locus and transcribed in the opposite direction to *CDKN1A* (Figure 1.9). The genomic region for PANDA and *CDKN1A*is regulated by the p53 tumour suppressor which binds upstream of the *CDKN1A* TSS and has also been shown to induce expression of numerous lncRNAs including lincRNA-p21 and PANDA (Figure 1.9) (Huarte *et al*., 2010; Hung *et al*., 2011). The genomic DNA of PANDA is made up of one exon and transcribed in the opposite direction of *CDKN1A* with a 1.5 kb transcript product. In response to DNA damage, p53 activates the transcription of p21 CDK inhibitor,a product of *CDKN1A* and PANDA to induce G1 cell cycle arrest and promote cell survival respectively (Figure 1.9).

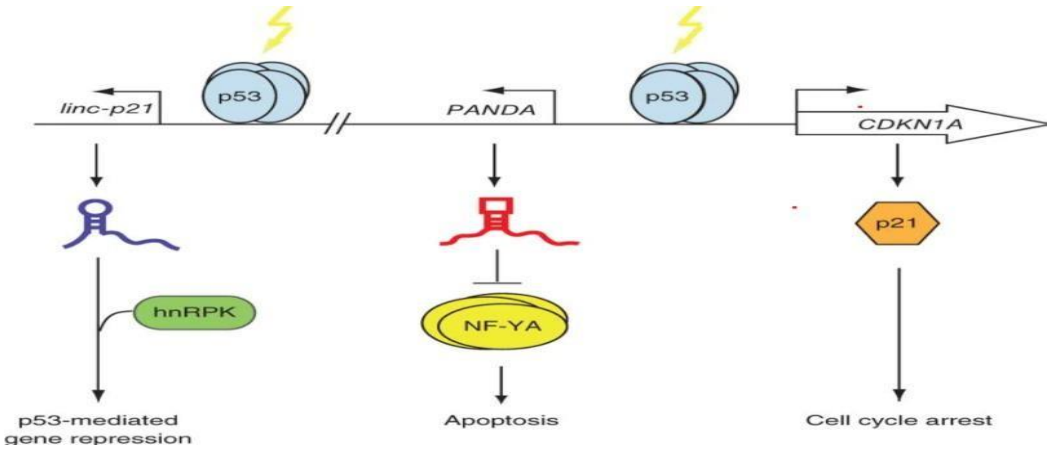

Figure 1.9: Tumour suppressor p53 induce the expression of PANDA, p21 and linc-p21 lncRNA. The genomic region of PANDA and *CDKN1A* is regulated by p53 protein which binds upstream the *CDKN1A* TSS (Hung *et al*., 2011).

PANDA is anti-apoptotic and functions in *trans*, whereas lincRNA-p21 is proapoptotic and functions in *cis* (Figure 1.9) (Chaudhary and Lal, 2017). Studies show that PANDA associates with subunit A of nuclear transcription factor Y (NY-F). NY-F is a heterotrimeric TF and is made up of three subunits namely NY-FA, NY-FB and NY-FC (Figure 1.9) (Mantovani, 1998). NF-Y binds and activates apoptotic gene FAS by binding to its promoter. PANDA blocks the NY-F from binding to the promoters of apoptotic activators namely B-cell/lymphoma 2-interacting killer (BIK), apoptotic peptidase activating factor 1 (APAF-1), LDD and FAS thus repressing their transcription.

PANDA can also coordinate scaffold attachment factor A (SAFA) to regulate cell proliferation and senescence (Figure 1.10) (Puvvula *et al*., 2014). SAFA is a nuclear protein with the ability to bind DNA, RNA and some lncRNA (Helbig and Fackelmayer, 2003). It is involved in numerous transcriptional and post-transcriptional processes and also associated with Xist and PRC-2 mediated H3K27me3 mark of the inactive X chromosome (Pullirsch *et al*., 2010). Puvvula *et al*., 2014 demonstrated that PANDA and SAFA interact with PRCs 1 and 2 and NF-YA to induce or suppress senescence. In proliferating cells, PANDA and SAFA interact with PRC-1 and PRC-2 subunits BMI1 and EZH2 respectively to repress the transcription of pro-senescence genes (Figure 1.10). In senescence cells, there is no interaction between SAFA, PANDA and PRC1/2. This allows PANDA to sequester NF-YA TF inhibiting it from interacting with E2F TF for the co-

activation of proliferating-promoting genes (Figure 1.10).

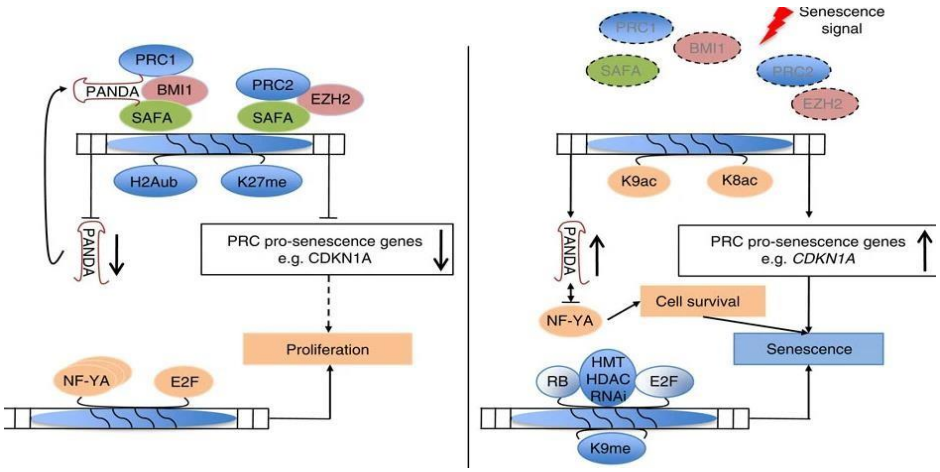

Figure 1.10: SAFA, PANDA and PRC1/2 mediated mechanism for cell proliferation and senescence. The interaction between SAFA, PANDA and PRC1/2 prevents PANDA from interacting with NY-FA and E2F2 to co-activate transcription thus promoting proliferation. Senescence cells lack SAFA, PANDA and PRC1/2 interaction allowing PANDA to sequester NF-YA to inhibit proliferation (Puvvula *et al*., 2014).

1.2.5.1. PANDA in cancer

Aberrant expression of PANDA affects cell proliferation, senescence and apoptosis and may be involved in tumourigenesis (Peng *et al*., 2017). The molecular mechanism of PANDA in cancer development is still under investigation. Lu*et al*. 2017 reported that PANDA underlies chromosomal instability and metastatic progression in many cancer types. The epithelial mesenchymal transition (EMT) is a crucial mechanism in cancer metastasis and PANDA may promote migration and invasion through EMT induction in colorectal cancer (Tam *et al*., 2020). PANDA induce EMT by upregulating the expression of mesenchymal markers namely vimentin, N-cadherin, β-catenin, Twist and Snail and decreasing E-cadherin levels, which promotes cell migration, invasion and metastasis, metabolism and chemoresistance in cancer cells.

The functions and expression levels of PANDA in cancer remains unclear as it has been shown to be upregulated and downregulated in some cancer types. The cancer types with high PANDA expression include gastric, colorectal, bladder, thyroid, osteosarcoma and breast cancer (Ma *et al*., 2016; Sang *et al*., 2016; Kotake *et al*., 2017). Moreover, Puvvula *et al*., 2014 showed that PANDA is down-regulated in hepatocellular carcinoma (HCC) whereas Peng and Fan, 2015 argued that the PANDA expression is overexpressed in HCC. This further complicates the role and expression of PANDA lncRNA in cancer.

1.2.5.2. PANDA expression in OSCC

Shi *et al*. 2019 reported that PANDA lncRNA is highly expressed in OSCC. This overexpression was caused by PANDA drifting from the NY-FA TF, allowing it to bind to E2F1 to co-regulate proliferation-promoting genes (as shown in Figure 1.10) and limit apoptosis. Similar to ANRIL, PANDA expression was upregulated in OSCC tissues with advanced clinical stages (Shi *et al*., 2019). More studies need to be conducted on PANDA expression in OSCC.

1.2.5.3. ANRIL and PANDA in DDR

Studies have shown that lncRNAs participate in the regulation of DDR through the modulation of DDR signalling pathways including the p53 as well as the ATM/ATR pathway (Zhang and Peng, 2015; Tehrani *et al*., 2018). These lncRNAs are not restricted to a specific role but are involved in various aspects of the DDR activation. In response to DNA damage, particularly DSBs, lncRNAs are involved in all DDR signalling stages such as DSB sensing, signal mediation as well as transducer and effector activity (Dutertre and Vagner, 2017; Tehrani *et al*., 2018). During the regulation of the DSBs repair system, lncRNAs exert their function epigenetically via chromatin modification complexes and post transcriptional control of their target genes.

LncRNAs participate in the DDR either directly through the binding of DNA repair proteins or indirectly via the regulation of translational proteins involved in DNA repair and genome stability. Examples of lncRNAs indirectly regulating DNA repair include ANRIL and PANDA (Thapar, 2018). ANRIL participates in the maintenance of the DDR by controlling cell cycle checkpoints, DNA repair and apoptosis. Upon DSBs damage, E2F1 TF induce ANRIL expression in an ATM

dependent manner (Zhang and Peng, 2015). This results in an increase in ANRIL expression thus suppressing the *CDKN2A/B* locus, inhibiting the transcription of p14 and p16 as well as p16 tumour suppressor proteins in *CDKN2A* and *CDKN2B* respectively. The tumour suppressor proteins p16 and p15 are CDK inhibitors and their inhibition due to increased ANRIL expression in the presence of DSBs hinders cell cycle checkpoints and enhance cell cycle progression in DDR (Kumari and Jat, 2021). DSBs activates the ATM signaling pathway to induce PANDA expression, inhibiting apoptosis and promoting cell survival by interfering with the apoptotic gene expression program described in 1.2.4. (Figure 1.9) (Mantovani, 1998).

1.3. LncRNA-based therapies

RNA based therapeutics were initially introduced in the 1990s and with fomivirsen, also known as vitravene, being the first FDA approved RNA-based drug in 1998 (Roehr, 1998). Recently, ncRNA-based therapies have attracted more attention since RNA modulation is becoming a promising therapeutic approach for the treatment of various diseases. It is believed that the tissue specific expression of lncRNA make them advantageous as biomarkers and therapeutic targets over protein coding genes (Ayers, 2013). Due to the diversity of their modes of action, lncRNAs can serve as therapeutic targets using multiple approaches (Fatima *et al*., 2015). These approaches include transcriptional inhibition by CRISPR/Cas 9, post-transcriptional lncRNA knockdown by antisense oligonucleotides (ASOs) andRNA interference (RNAi) mediated downregulation of lncRNAs.

RNAi mediated gene silencing provides a direct approach to selectively inhibit the target molecules in various diseases. This can be through siRNA, miRNA and shRNA approaches (Burnett *et al*. 2011; Dorsett *et al*., 2004). These RNAi based therapeutics have shown to effortlessly target lncRNAs in cells but will require delivery vehicles *in vivo*. ASOs are short single stranded DNA/RNA molecules 18-30 bps designed to inhibit the function of mRNA. They bind mRNA through base pairing, thus impairing translation and degrading mRNA by RNAse H (Agrawal, 1996). There are already two FDA approved ASO based drugs, formivirsen and mipomersen used for the treatment of cytomegalovirus retinis and hypercholesterolemia respectively (Grillone and Lans, 2001; Wong and Goldberg, 2014). ASOs targeting the antisense lncRNAs named AntagoNATs are being employed for the upregulation of specific mRNAs to silence the corresponding

antisense lncRNAs (Modarresi *et al*., 2012). AntagoNATs have an advantage over RNAi therapies due to their stability caused by 5′ and 3′ modifications in their terminiand backbone enhancing their cellular uptake whereas RNAi based therapies require vehicles for *in vivo* targets (Veedu and Wengel, 2010).

CRISPR/Cas is a useful system for targeting ncRNAs including miRNAs and lncRNAs. There are different versions of the CRISPR/Cas molecules namely CRISPR-Cas9, CRISPR interference (CRISPRi), CRISPR activation (CRISPRa) for the deletion, inhibition and activation for lncRNA-encoding genes as well as transcript degradation by CRISPR-Cas13 (Ran *et al*., 2013; Perez-Pinera *et al*., 2013). These technologies are associated with fast overexpression, knockdown and knockout of lncRNAs. Compared to RNAi, CRISPR/Cas9 approach has a greater target range as it does not compete with endogenous RNA machinery. Due to its ability to simultaneously repress transcription at DNA level and repress multiple genes, it is believed that CRISPR/Cas9 holds a great promise for the knockdown experiments with the aim of revealing roles of lncRNAs involved in different cancer types (Gilbert *et al*., 2013). However, due to their lack of a functional ORF, *in vivo* targeting of lncRNA using CRISPR/Cas is more difficult than targeting protein coding genes (Statello *et al*.,2021). This is because in the protein coding gene, wild type CRISPR/Cas9 can be used to generate DSBs in the ORF to generate frameshift mutations through the NHEJ repair pathway thus generating an effective knockout of the targeted coding gene (Cong *et al*., 2013). Whereas in lncRNA genes, the complex architecture of the genomic loci greatly limits the potential use of CRISPR/Cas9 to genetically manipulate the lncRNAs due to the possibility of disturbing the overlapping genes (Goyal *et al*., 2017). Although many lncRNA based therapeutic drugs are still in pre-clinical studies, their potential use as cancer therapeutics is promising.

1.4. Aim and objectives

Aim

Aberrant lncRNA expression is associated with tumourigenesis. PANDA and ANRIL lncRNAs show dysregulated expression in various cancer types and have previously been shown to be overexpressed in OSCC. This study explored the expressions of ANRIL and PANDA lncRNAs in response to cisplatin and immediately after cisplatin withdrawal, aiming to provide potential lncRNA-targeted strategies for overcoming cisplatin resistance in cancer therapy

Objectives:

1. Assess cisplatin cytotoxicity in OSCC cell lines and determine cisplatin EC_{50} by MTT assay.
2. To observe DNA double stranded break (DSB) formation in the presence of cisplatin and in the first hour after cisplatin withdrawal in HEK293, WHCO1 and WHCO5 cell lines.
3. To observe the expression profile of lncRNAs PANDA and ANRIL in the presence of cisplatin and during cisplatin withdrawal by RT-PCR in HEK293, WHCO1 and WHCO5 cell lines.

2. Methods and materials

2.1. Cell culture

This study utilised OSCC cell lines WHCO1 and WHCO5, with HEK293 cell line serving as the control. The HEK293 cell line is a non-OSCC cell line that was used as a point of reference. This cell line is easy to grow and maintain and produce highly consistent and reproducible results. They are frequently used as a control in studies testing the effects of treatments on cancer specific cell lines. The HEK293 cells, were a gift from Dr Clement Penny and the human OSCC cell lines WHCO1 and WHCO5, were a gift from Prof. Rob Veale. These cell lines were maintained in Dulbecco's Modified Eagle Medium/Hams F12 (DMEM/Hams F12) (ThermoFisher Scientific, Waltham, Massachusetts, USA) supplemented with 1% 100 U/ml penicillin/0.1 mg/ml streptomycin antibiotics and 10% fetal bovine serum (FBS) (ThermoFisher Scientific, Waltham, Massachusetts, USA). The cells were cultured in 100 mm culture dishes (NEST Biotechnology, Wixu, China) and maintained in an incubator with a humidified atmosphere of 37 ºC and 5% Carbon dioxide (CO_2).

Cells were routinely sub-cultured when they reached 75-90% confluency. This was done by first discarding the old medium and washing cells three times in 1X phosphate buffered saline (PBS) (ThermoFisher Scientific, Waltham, Massachusetts, USA). After the washes, cells were detached from the plates with 1 ml of 0.25% trypsin: ethylenediaminetetraacetic acid (EDTA) (1X) (ThermoFisher Scientific, Waltham, Massachusetts, USA) for WHCO1 and WHCO5 and 1:1 ratio of 500 µl Trypsin-EDTA and 500 µl 1XPBS by incubating for 5 minutes at 37 ºC. After incubation, 1 ml of the fresh DMEM/Hams F12 was added in the plate to inactivate Trypsin-EDTA. In a new culture plate, 200 µl of the cell suspension was further re-suspended in 8 ml of fresh DMEM/Hams F12 and the media was changed every other day until the cells wereconfluent for experimental use or further sub-culturing.

2.2. Cell count

For treatments, a constant cell number was required for each experiment and this was achieved by cell counting using trypan-blue stain. Trypan-Blue stain uses the dye exclusion test to establish the number of viable cells, appearing clear in comparison to non-viable cells stained blue (Strober, 2001). For the cell count, cells

were detached from the plates as previously stated and a 10 µl aliquot of the cell suspension was mixed with equal volumes of trypan-blue solution (Appendix A). The cell-trypan blue mixture was pipetted onto a Neubauer haemocytometer and viewed under the light microscope (Zeiss (Pty) Ltd, Jena, Germany). Counts were used to calculate cell concentration and total cells to seed per well.

2.3. MTT assay

The 3-(4,5-dimethylthiazol-2-yl)-2,5-diphenyltatrazolium bromide (MTT) assay was used for the assessment of cell viability and cytotoxicity of WHCO1 and WHCO5 OSCC cell lines as well as HEK293 cells upon the exposure to the cisplatin drug (Mosmann, 1983). The MTT assay is used to assess cell metabolic activity. MTT is a yellow tetrazole that gets reduced to purple formazan in viable cells. Viable cells have healthy mitochondria that have different enzymes, one of them being NADPH dependent oxidant reductase which converts the tetrazolium dye into a purple-coloured compound. The absorbance of the coloured solution is then quantified spectrophotometrically with the absorbance readings proportional to the number of viable cells (Gillies *et al*., 1986).

An equal number of 5000 cells/well (n=4) were seeded into a 96 well plate and left to grow for 48 hours at 37 ºC until they were about 75-80% confluent. After 48 hours, cells were treated with varying cisplatin concentrations ranging from 0-800 µM with a dilution factor of 2 (18-fold dilution) for 24 hours. For untreated controls, the culture medium was replaced with a fresh one. For the MTT assay, the culture medium was replaced with 100 µl of MTT solution and incubated at 37 ºC for 2.5 hours to allow live cells to reduce the MTT dye to formazan crystals. From each well, either 80 µl of the culture medium (untreated) and MTT solution were discarded, followed by the addition of 100 µl of dimethyl sulfoxide (DMSO) (Sigma-Aldrich, St Louis, Missouri, USA) for formazan crystal solubilization by incubating the plate for 5 minutes at 37 ºC. The plate was shaken on a shaker for 25 minutes in the dark at room temperature. The absorbance readings were measured at 570 nm using the Multiskan GO Microplate Spectrophotometer (ThermoFisher Scientific, Waltham, Massachusetts, USA). The analyses of these were expressed as absorbance vs log cisplatin concentration hill dose-response curves to calculate the EC_{50} using GraphPad Prism 8 software (n=4).

2.4. Western blot

All reagents used for western blotting were prepared according to Appendix A, unless stated otherwise.

Western blot, which is also known as protein blotting is a technique that allows for protein transfer from sodium dodecyl sulphate polyacrylamide gel (SDS-PAGE) to an adsorbent membrane (Towbin *et al*., 1979). It allows for the detection and characterization of different types of protein. In this study, western blot was used to detect the γH2AX protein in cisplatin treated and untreated OSCC and HEK293 cell lines.

2.4.1. Drug treatment

For cisplatin treatment, cells were evenly seeded in 100 mm culture dishes with 8 ml medium and left to grow for 72 hours at 37 ºC until they reached 70% confluency. After 72 hours the cells were treated for 8 hours with the EC_{50} cisplatin concentrations calculated from the MTT assay, differing per cell line. The 8 hours cisplatin treatment was selected because studies have shown that cisplatin treatment induce apoptosis 8 hours post treatment in different cell lines (Pabla *et al*., 2008; Kuashal *et al*., 2001; Lau, 1999). This was done by continuously monitoring changes in cell metabolism and morphology (Alborzinia *et al*., 2011). There were five culture plates per cell line with different cisplatin withdrawal times, namely: 0, 5, 30 and 60 minutes as well as the untreated plate. After 8 hours treatment, the cisplatin media mixture was discarded and replaced with fresh medium and each plate incubated at 37 ºC as per its withdrawal time. Once the withdrawal time was over, the medium was discarded and cells were rinsed three times with cold 1XPBS.

2.4.2. Cell preparation and lysis

After the washes with 1XPBS, 1 ml of cold 1X PBS was added to the plates and whole cell protein extraction was done by scraping cells and transferring the cell suspension into 1.5 ml micro-centrifuge tubes. This was followed by centrifugation at 4 ºC at 11 000 rpm for 10 minutes and the supernatant was discarded. The cells were then lysed with 1X radioimmunoprecipitation (RIPA) buffer. The volume of the 1XRIPA lysis buffer was dependent on the pellet sizes, ranging from 60-100 µl. During cell lysis, the samples were vortexed every 5 minutes for 45 minutes to thoroughly lyse the cells. After 45 minutes, the samples were centrifugedat 13 400 rpm for 10 minutes at 4 ºC to pellet the debris. The protein containing supernatant

was aliquoted into PCR tubes and stored at -70 ºC to preserve the protein.

2.4.3. Protein quantification (Bramhall assay)

Bramhall assay is a type of protein quantification assay used in the presence of detergents and reducing agents such as SDS which interferes with other protein assay techniques (Bramhall *et al*., 1969). To carry out the Bramhall assay, a grade 1 Whatman™ filter paper was cut in half and soaked in the following solutions: distilled water (dH_2O) for 20 minutes, 50 ml of 95% ethanol, 100% ethanol and 100% acetone for 5 minutes each with gentle shaking. The filter paper was dried in the extraction hood until completely dry. A standard curve was set using 1mg/ml of BSA stock solution with differing volumes of 1, 3, 6, 12, 16 and 20 µl along with 2 µl of unknown protein samples pipetted out on the sides of the dry filter paper and traced each spot by circling with a pencil. The proteins were allowed to dry and the filter paper was further soaked in 7.5% trichloroacetic acid (TCA) for 45 minutes with gentle shaking to fix the protein on the paper. The filter paper was then soaked in coomassie blue stain for 1 hour, followed by an hour in destain solution. The filter paper was allowed to dry and the protein samples as well as the BSA standards were cut out and placed individually in 2.5 ml of the elution buffer and incubated overnight in the dark. The following day the tubes were shaken and 160 µl from each tube was pipetted into a 96 well plate in triplicates. Absorbance readings were measured at 595 nm using a Multiskan GO microplate reader (ThermoFisher Scientific, Waltham, Massachusetts, USA). A standard curve of protein concentration (µg/ml) vs. absorbance was plotted using Microsoft Office Excel and the unknown protein concentrations in cell lysate were calculated using the standard curve derived equation.

2.4.4. SDS-PAGE

SDS-PAGE was employed for the separation of the extracted protein based on the molecular weight and size. A 15% separating gel with 7% stacking gel were prepared according to Appendix B. and each left for 30 minutes to polymerise. Equal amounts of protein (30 µg) samples to be loaded were prepared in a 3:1 ratio of protein to 4X protein loading buffer and denatured at 95 ℃ for 5 minutes in the water-bath. After the gel polymerised, it was then transferred to a running tank and filled with SDS-PAGE running buffer. The protein samples and the PageRuler™ prestained protein ladder (ThermoFisher Scientific, Waltham,

Massachusetts, USA) were loaded into the gel wells. The gel was electrophoresed at a constant voltage of 150 V for 1 hour after which,the region with the protein of interest was cut and prepared for immunoblotting. The remaining gel was stained in coomassie blue stain for 1 hour and destained overnight dye overnight to assess the quality of the electrophoresis.

2.4.5. Immunodetection

Following SDS-PAGE, proteins of interest were blotted onto nitrocellulose membrane. The sponges and four filter papers were soaked in the transfer buffer. The dimensions of the gel were measured and the nitrocellulose membrane was cut based on the size of the gel containing protein of interest and soaked in the transfer buffer. A transfer sandwich was then assembled by placing a sponge on the black side of the cassette; two filter papers, a gel, nitrocellulose membrane then two filter papers and a sponge. The sandwich was put in a transfer tank and filled with ice cold transfer buffer. The transfer was carried out at 4 ºC for 2 hours at a constant current of 300 mA with the ice was changed every 30 minutes and the buffer changed after an hour until the transfer was complete. Once the transfer was complete, the sandwich was disassembled and the gel was stained in coomassie blue dye overnight followed by an overnight destaining as previously described in 2.4.4. to assess the quality of the transfer. The membranes were incubated in the blocking buffer at room temperature for 1 hour with gentle shaking to prevent non-specific antibody binding. After an hour of blocking, the membraneswere washed once with cold 1XTBS/T for 10 minutes and incubated in primary antibody (1:1000) for γH2AX (mouse monoclonal IgG_1 p-Histone H2A.X (Ser 139) (SC-517348)) (Santa Cruz Biotechnology, Dallas, Texas, USA) and 1:2000 for β-actin (rabbit monoclonal (D6A8) #8457) (Cell Signaling Technology, Danvers, Massachusetts, USA), both diluted in 5% BSA in 1XTBS/T and incubated overnight at 4 ℃. The following day, the membranes were washed with cold 1XTBS/T five times for 5 minutes each to remove any unbound antibody and incubated for 1 hour with the corresponding HRP-bound secondary antibody in thedark at room temperature. For secondary antibody dilutions, 1:2000 and 1:3000 secondary antibodies dilutions were done for γH2AX, an anti-mouse m-Igk BP- HRP (SC-516102) (Santa Cruz Biotechnology, Dallas, Texas, USA) and β-actin anti-rabbit IgG, HRP-linked (#7074) (Cell Signaling Technology, Danvers, Massachusetts, USA) respectively,

diluted in 5% BSA in 1XTBS/T. The unbound secondary antibody was washed five times for 5 minutes each with cold 1XTBS/T.In the autoradiography room, antibody detection was measured using western Bright^{TM} ECL plus chemiluminescent reagents (Advansta Inc, San Jose, California, USA) and x-ray films used for band detection, followed by rinsing in the developer and fixer. Densitometry of captured images was performed using ImageStudio Lite software with the statistical significance calculated using a paired student's t-test using Excel 2019 with $p<0.05$ considered significant (n=3).

2.5. RT-PCR

Reverse-transcription polymerase chain reaction (RT-PCR) is a semi-quantitative technique combining reverse transcription of RNA to cDNA and amplification of specific DNA targets using PCR. RT-PCR was performed on HEK293, WHCO1 and WHCO5 cell lines to establish the presence/absence of lncRNAs PANDA and ANRIL in untreated and cisplatin treated cells. This was accomplished through multiple techniques including total RNA extraction using Tri-Reagent® (Sigma-Aldrich, St Louis, Missouri, USA) protocol, cDNA synthesis by Revert-Aid cDNA synthesis kit, cDNA amplification using PCR and visualisation using agarose gel electrophoresis.

2.5.1. RNA extraction

All reagents used for RNA extraction were purchased from Sigma-Aldrich (St Louis, Missouri, USA) unless stated otherwise.

For RNA extraction, untreated and cisplatin treated cells were lysed with 1 ml Tri-Reagent ®. The mixture was transferred into 1.5 ml microcentrifuge tube and allowed to stand for 5 minutes at room temperature. For phase separation, 200 µl of chloroform was added followed by vigorous shaking for 15 seconds and allowed to stand for 15 minutes at room temperature. The mixture was then centrifuged at 11 500 rpm for 15 minutes at 4 °C. Centrifugation separates the mixture into three phases including a red organic phase containing protein, an interphase containing DNA and a colourless upper aqueous phase containing RNA. The upper aqueous phase was transferred into a fresh tube and 500 µl of 2-propanol was added and samples were allowed to stand for 10 minutes at room temperature. After 10 minutes, the samples were centrifuged at 11 500 rpm for 10 minutes at 4 °C resulting in the RNA precipitation and pellet formation on the side bottom of the tube. The

supernatant was removed and the pellet was washed with 1 ml of pure ethyl alcohol and vortexed, followed by centrifugation at 13 400 rpm for 5 minutes at 4 °C. The supernatant was discarded allowing the RNA pellet to dry for 5 minutes by air drying. Appropriate volumes (20-30 µl, depending on the pellet size) of nuclease free water was added to the pellet, mixed and incubated at 60 ºC for 10 minutes. RNA was quantified at 260 nm using a Nanodrop (Nanodrop One, ThermoFisher Scientific, Waltham, Massachusetts, USA).

2.5.2. Agarose gel electrophoresis

The RNA quality and purity are important for the success of RT-PCR. The quality and integrity of the RNA was determined by RNA separation on a 1% agarose gel. To make 1% agarose gel, 0.5 g agarose powder was mixed with 50 ml 1XTAE buffer and dissolved by heating gradually in a microwave until it is bubbling and all powder has dissolved. The liquid agarose was allowed to cool and 5µl ethidium bromide (EtBr) was added to the agarose solution. Immediately after adding EtBr, the mixture was mixed by swirling and poured into the gel casting tray, combs inserted and allowed to set for about 30 minutes at room temperature. Once the gel had set, it was placed in the tank and 1XTAE buffer was poured into the tank until the gel was fully submerged. The comb was removed and GeneRuler™ 1 kb DNA ladder (ThermoFisher Scientific, Waltham, Massachusetts, USA) and the RNA samples mixed 6X DNA loading dye (BioLabs, Inqaba, SA) were loaded into the wells and separated at 100V for 45 minutes.After the gel was done running, the bands intensity was visualised under UV light using the Bio-Rad gel dock XR system and Image Lab 6.0 software (Bio-Rad, Berkeley, California, USA).

2.5.3. cDNA synthesis

After confirming the quality of RNA, the RevertAid™ First strand cDNA synthesis kit (ThermoFisher Scientific, Waltham, Massachusetts, USA) was used to synthesise cDNA as per the manufacturer's instructions. After thawing the reagents of the kit, they were addedto a sterile nuclease-free PCR tubes on ice. The first reagents added into the mixtureincludes 5 µg total RNA or 2 µg GAPDH control RNA serving as the positive control, 1µl oligodT_{18} primer, and nuclease-free water up to 12 µl. This reaction mixture was centrifuged for 1 minute at 11 500 rpm and incubated in the thermal cycler at 65 ºC for 5 minutes followed by cooling for a minute on ice andcentrifuging 1 minute at 11 500 rpm again. After centrifugation,

more reagents wereadded to the reaction mixture in the indicated order: 4 µl 5X reaction buffer, 1 µl Ribolock Rnase inhibitor (20 U/µl), 2 µl 10 mM dNTP mix and 1µl RevertAid M-MuLV RT (200 U/µl) making up to 20 µl of the total reaction mixture. The mixturewas mixed and centrifuged at 11 500 rpm for 1 minute and incubated in the thermalcycler with Table 2.1 cycling conditions.

Table 2.1: RevertAid^{TM} cDNA synthesis conditions

Step	Temperature (℃)	Time
Denaturation	65	60 minutes
Termination	70	5 minutes
Hold	4	∞

2.5.4. PCR

PCR was performed on the synthesised cDNA to determine the expression of lncRNAs PANDA and ANRIL with GAPDH as the positive control in HEK293, WHCO5 and WHCO1 cell lines. The KAPA Taq ReadyMix DNA Polymerase (KAPA Biosystems, Wilmington, Massachusetts, USA) was used for PCR as per manufacturer's instructions. According to RevertAid™ First strand cDNA Synthesis kit, the volume of the cDNAadded must not comprise more than 1/10 of the total PCR reaction. For a total of 20µl reaction mixture 2 µl was added for the cDNA, 12,5 µl 2X ReadyMix with Mg^{+}, 0.5 µM forward primer, 0.5 µM reverse primer and nuclease free water up to 20 µl. The samples were vortexed and centrifuged at 11 500 rpm for 1 minute,followed by incubation on the thermal cycler according to table 2.2.

Table 2.2: KapaTaq PCR cycling conditions.

Step	Temperature (℃)	Duration	Number of cycles
Initial denaturation	95	5 minutes	1
Denaturation	95	30 seconds	35
Annealing	T_m – 5	30 seconds	
Extension	72	1 minute	
Final extension	72	5 minutes	1
Hold	4	∞	1

A control PCR was first conducted with GAPDH primers (Table 2.3.) to confirm the successful synthesis of the cDNA. Thereafter, the lncRNAs PANDA and ANRIL primers (Table 2.3.) were tested by PCR on all cell lines. All PCR products were visualised on a 4% agarose gel in 1XTAE with the GeneRuler ultra low range DNA ladder (ThermoFisher Scientific, Waltham, Massachusetts, USA) and viewed under UV light as previously described in section 2.5.2. A 4% agarose gel was prepared by weighing 2 g of agarose powder and mixed with 50 ml 1XTAE buffer. The mixture was dissolved by heating gradually in a microwave until it is bubbling and all powder has dissolved. The liquid agarose was allowed to cool and 5 µl ethidium bromide (EtBr) was added to the agarose solution. The gel was left to cool and run as per 2.5.2. description.

Table 2.3: GAPDH, PANDA and ANRIL primer sequences and PCRconditions.

Region	Primer sequences	Annealing temperature (℃)	Amplicon size (bp)
GAPDH	Forward: 5′ GTCAGTGGTGGACCTGACCT 3′ Reverse: 5′ AGGGGAGATTCAGTGTGGTG 3′	49.9	396
PANDA	Forward: 5′ GAAGTCCTGATGCAGACCATAA 3′ Reverse: 5′GATAGCTGGAAAGCTGAGAGAG 3′	49	93
ANRIL	Forward: 5′ CTATCCGCCAATCAGGAGGC 3′ Reverse: 5′ TCGTGGCAAATAGTCCTAGTCC 3′	50	190

2.6. Statistical analysis

For MTT assay, statistical significance was determined by the unpaired Student's t-test using GraphPad Prism 8.0.2 software using four technical replicates (n=4). For western blot analysis, the experiments were performed in triplicate and expressed as mean ± standard deviation (n=3 ± SD) with statistical significance determined by paired Student t-test using Microsoft Excel. For both MTT and western blot, statistical significance determined was relative to untreated samples, and according to the following p-values:

P< 0.0001****;

P< 0.001***;

P< 0.01**;

P< 0.05*.

3. Results

3.1. Cisplatin exerts cytotoxic effects on HEK293 and OSCC cell lines.

Cisplatin has shown cytotoxic effects in various cancer cell lines, including OSCC cell lines (Siddik, 2003; Li *et al*., 2019). For this study, an MTT assay was conducted to determine the cisplatin EC_{50} concentrations in HEK293 control as well as WHCO1 and WHCO5 OSCC cell lines. The HEK293 cell line is a non-OSCC cell line that was used as a point of reference. This cell line is easy to grow and maintain and produce highly consistent and reproducible results. They are frequently used as a control in studies testing the effects of treatments on cancer specific cell lines. Cells were treated with different cisplatin concentrations ranging from 0-800 µM for 24 hours. Cisplatin cytotoxicity was demonstrated by the sigmoidal dose-response curve showing absorbance readings plotted against Log concentrations and the bar graph with absorbance readings plotted against actual cisplatin concentrations. The sigmoidal dose curves were used to determine the EC_{50} concentrations and the bar graphs were used to determine statistical significance per concentration in comparison to the untreated control. The right downward shift in the sigmoidal dose-response curves show increased cisplatin cytotoxicity whereas on the bar graphs, increased cytotoxicity was observed with a decrease in absorbance readings and an increase in cisplatin concentration.

In the HEK293 control cell line, the dose-response curve displayed a right downward shift in response to cisplatin treatment, indicating increased cell cytotoxicity (Figure 3.1A). The HEK293 cell line is a non-OSCC cell line that was used as a point of reference. The bar graph showed that desired response was achieved with cisplatin concentrations ranging from 12.5 to 800 µM, showing less absorbance readings in comparison to the untreated controls (Figure 3.1B). Maximal cisplatin cytotoxicity was observed with concentrations ranging from 200 to 800 µM (Figure 3.1B). The concentrations ranging from 0.2 to 1.56 µM as well as 6.25 µM and 50 µM showed no statistically significant difference between the untreated and cisplatin treated sample (Figure 3.1B). However, when HEK293 cells were treated with the following cisplatin concentrations: 3.13, 12.5, 25, 100, 200, 400 and 800 µM, statistically significant differences between the untreated and cisplatin treated samples were observed (Figure 3.1B).

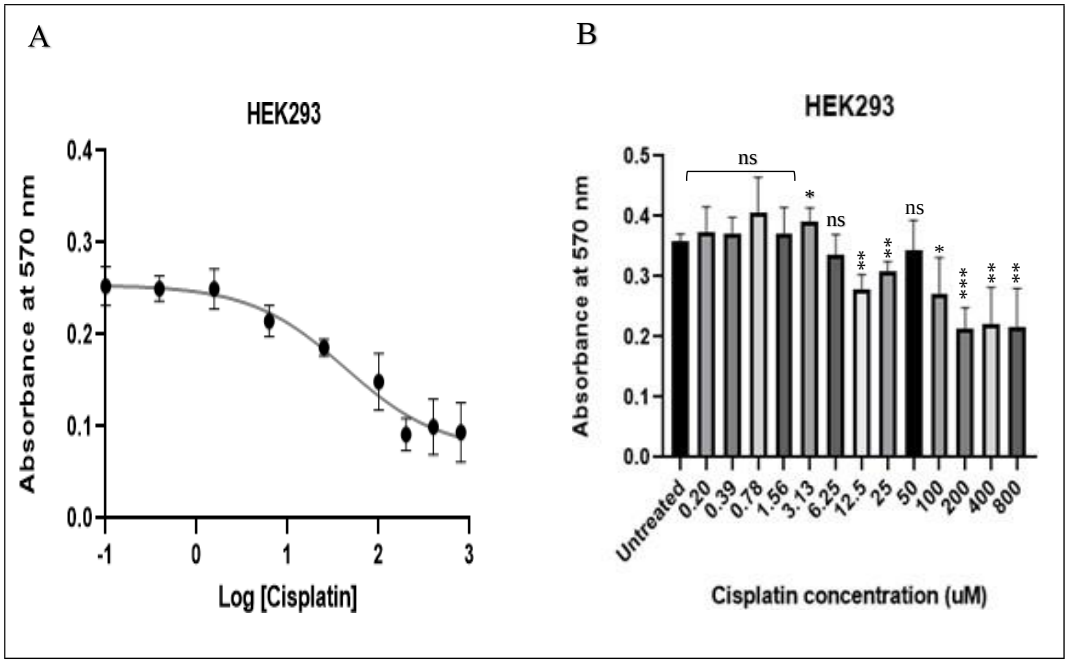

Figure 3.1: Cisplatin induces cytotoxicity in HEK293 cell line. HEK293 cell lines were exposed to cisplatin for 24 hours with concentration ranges of 0-800 µM. **(A)** Dose-response curves of HEK293 cells exposed to cisplatin as determined by cytotoxicity MTT assay. **B)** Bar graphs denoting MTT assay data fitted as absorbance vs cisplatin concentration in HEK293 control cell line for untreated control and cisplatin treated samples. The values are shown relative to the untreated controls (n=4 ± SD), ***P<0.001, **P<0.01 and *P<0.05.

The WHCO1 cell line showed cisplatin cytotoxicity as can be seen with the right downward shift of the sigmoidal dose-response curve (Figure 3.2.A). Maximal cisplatin cytotoxicity was observed with concentrations ranging from 100 to 800 µM (Figure 3.2B). No statistical significance was observed with cisplatin concentration ranges of 0.20 to 6.25 µM in comparison to the untreated controls. An increase in cisplatin concentrations from 12.5 to 800 µM resulted in cisplatin cytotoxicity and a statistically significant increase in comparison to the untreated WHCO1 cells (Figure 3.2B).

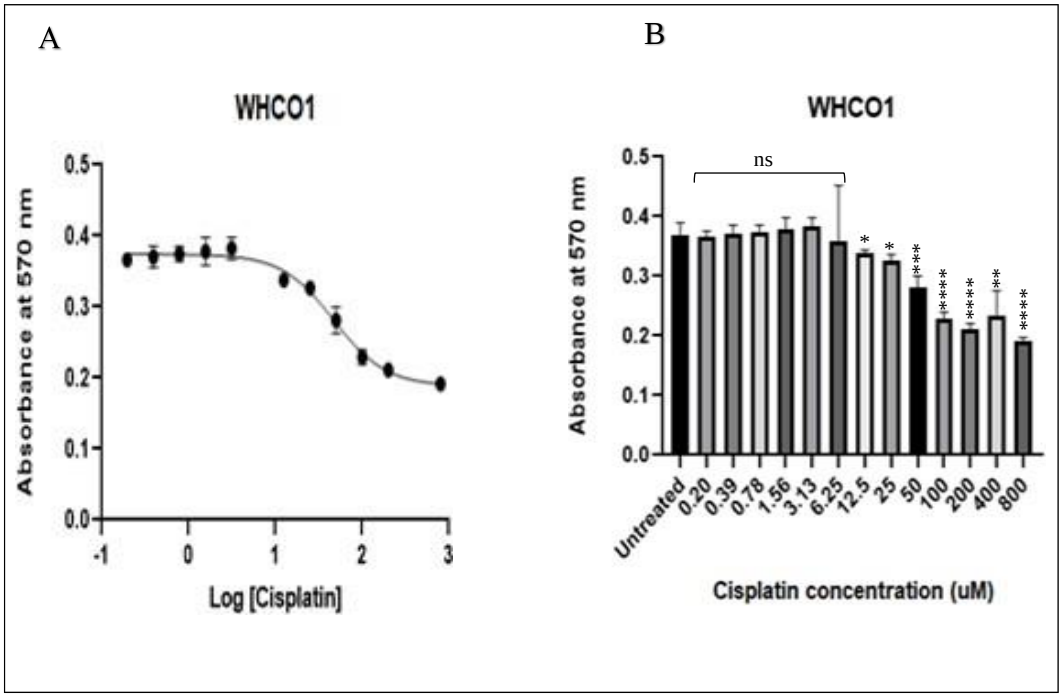

Figure 3.2: Cisplatin induces cytotoxicity in WHCO1 OSCC cell line. WHCO1 cell lines were exposed to cisplatin for 24 hours with concentration ranges of 0-800 µM. **A)** Dose-response curves of WHCO1 cells exposed to cisplatin as determined by cytotoxicity MTT assay. **B)** Bar graphs denoting MTT assay data fitted as absorbance vs cisplatin concentration for WHCO1 for untreated control and cisplatin treated samples. The values are shown relative to the untreated controls (n=4 ± SD), ****p<0.0001, ***P<0.001, **P<0.01 and *P<0.05.

WHCO5 cells showed cytotoxic effects to cisplatin after 24 hours post treatment. Increase in cisplatin concentrations showed a decrease in absorbance, indicating a decrease in cell viability. Same as the WHCO1, no statistical significance was observed with cisplatin concentration ranges of 0.20 to 6.25 µM in comparison to the untreated controls (Figure 3.3B). Differences in statistical significance were observed between cisplatin treated WHCO5 and untreated control with concentrations from 12.5 to 800 µM (Figure 3.3B). Maximum cisplatin cytotoxic effects were observed at 100 to 800 µM in comparison to other concentrations and the untreated control (Figure 3.3B).

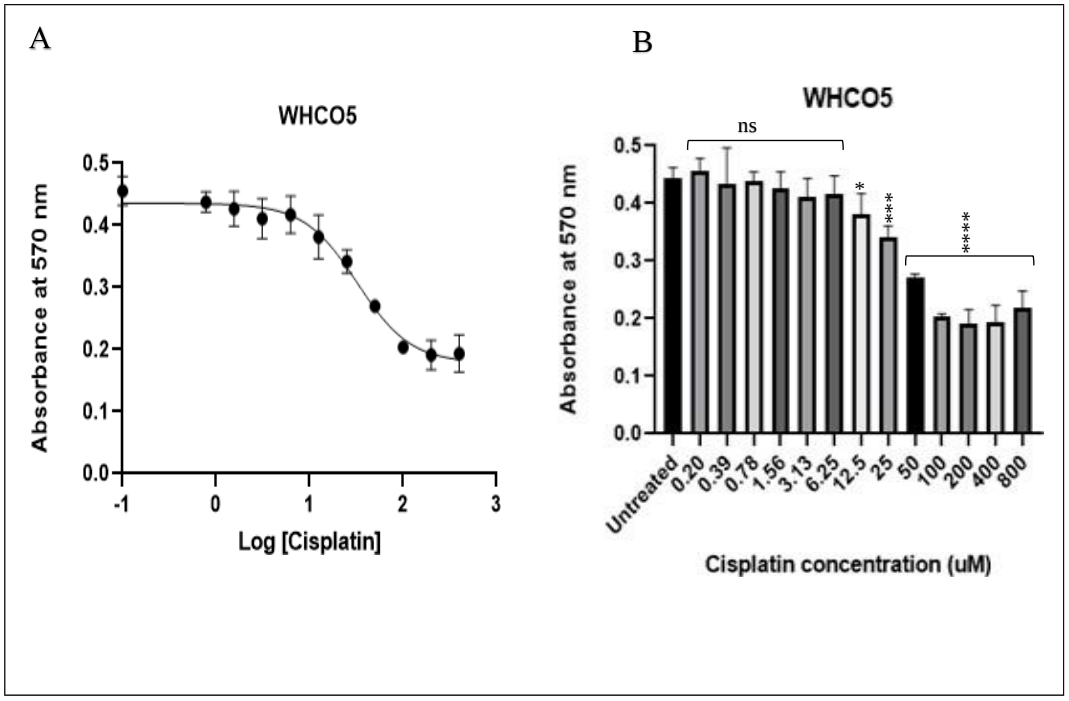

Figure 3.3: Cisplatin induces cytotoxicity in WHCO5 OSCC cell line. WHCO5 cell lines were exposed to cisplatin for 24 hours with concentration ranges of 0-800 µM. **A)** Dose-response curves of WHCO5 cells exposed to cisplatin as determined by cytotoxicity MTT assay. **B)** Bar graphs denoting MTT assay data fitted as absorbance vs cisplatin concentration for WHCO5 for untreated control and cisplatin treated samples. The values are shown relative to the untreated controls (n=4 ± SD), ****p<0.0001, ***P<0.001, **P<0.01 and *P<0.05.

The EC_{50} is the half maximal effective concentration at which there is 50% cell death. GraphPad Prism 8.0 software was used to calculate the EC_{50} concentrations, with the control as the baseline. After plotting the Hill dose-response curve, the software allows the automatic calculation of different parameters such as the EC_{50} concentrations. Statistical significance was determined using GraphPad 8.0 software and the unpaired Student's t-test was used to calculate the mean and standard deviation. HEK293 cells required a low cisplatin dose of 18.6 µM to produce half maximum response in comparison to OSCC cell lines, WHCO1 and WHCO5 which required 47.1 µM and 32.5 µM, respectively (Table 3.1). Although both are OSCC cell lines, this study has shown that cisplatin has a higher potency in WHCO5 in comparison to WHCO1 cell line with an EC_{50} concentration of 32.5 µM (Table 3.1).

Table 3.1: The EC_{50} values determined using MTT assay. The HEK293 control showed lower EC_{50} value in comparison to the WHCO1 and WHCO5 OSCC cell lines.

	EC_{50} (µM)		
	HEK293	**WHCO1**	**WHCO5**
Cisplatin	18.6	47.1	32.5

3.2. Cisplatin induces γH2AX expression in HEK293 and OSCC cell lines.

One of mechanism through which cisplatin induces DSBs in the DNA is via the inhibition of the HR repair pathway. γH2AX expression is an early cellular response to the detection of DNA DSBs and its detection has emerged as a highly sensitive molecular marker for monitoring DNA damage and repair. Western blot quantified changes in γH2AX expression levels in OSCC and HEK293 cells in response to cisplatin treatment over 8 hours and immediately after 1 hour of cisplatin withdrawal. The difference between cisplatin treatment times of 24 hours for MTT assays and 8 hours for western blots is because the MTT assays were used to determine lethal concentration of cisplatin. However, for lncRNA studies, the intension was to investigate early stages of DNA damage response. Therefore, treatment time was reduced to 8 hours as the intention was not to cause cell death. The 8 hours cisplatin treatment was selected because studies have shown that cisplatin treatment induce DNA damage and apoptosis 8 hours post treatment in different cell lines (Pabla *et al*., 2008; Kuashal *et al*., 2001; Lau, 1999).

Cisplatin treatment resulted in increased γH2AX expression in HEK293 cells in both cisplatin only and all the withdrawal time points in comparison to the untreated control (Figure 3.4). The γH2AX expression levels were upregulated by 131% (231± 118%), 268% (168 ± 178%), 424% (324 ± 231%) and 500% (400 ± 176%) in cisplatin only, 5, 30 and 60 minutes withdrawal respectively, relative to the untreated control (Figure 3.4). No statistical significance was observed in the cisplatin only and 5 minutes cisplatin withdrawals in comparison to the untreated control. However, a statistical significance for γH2AX expression was observed after 30 and 60 minutes cisplatin withdrawal compared to untreated control (Figure 3.4).

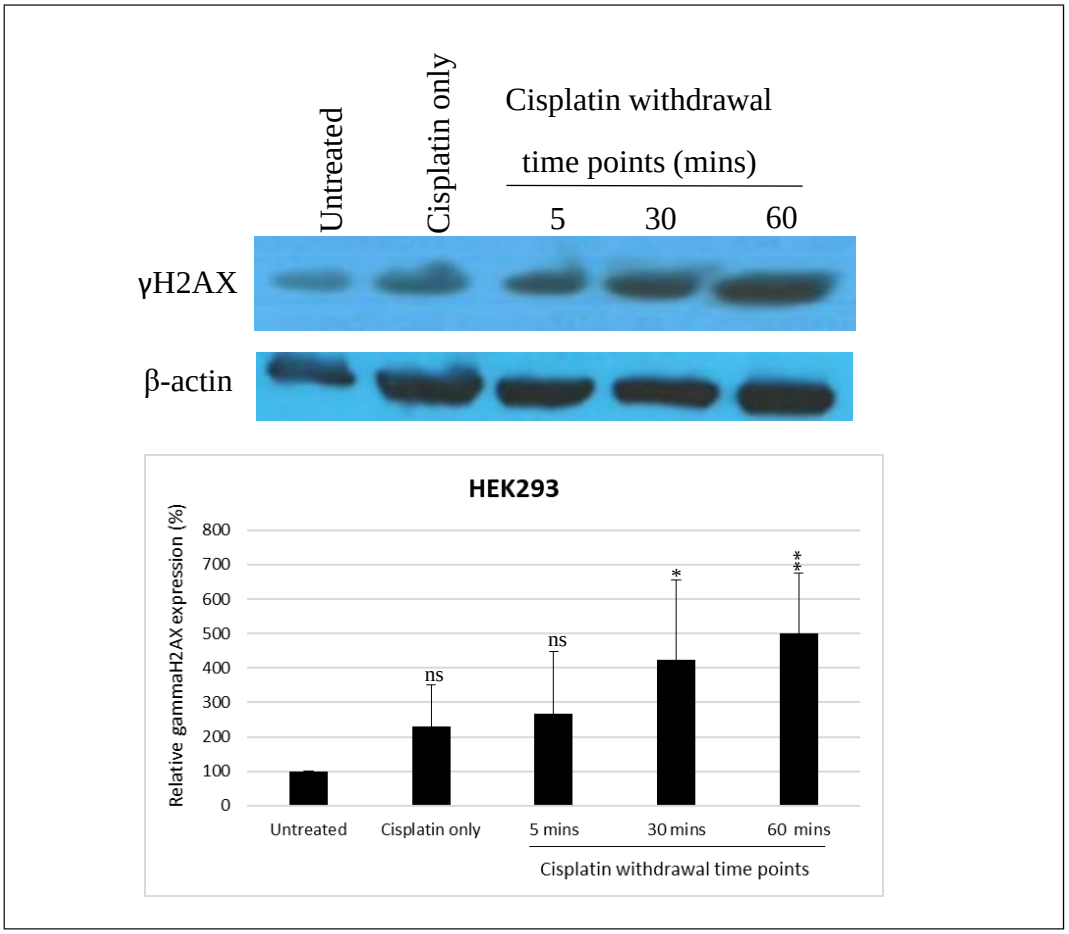

Figure 3.4: γH2AX expression in response to cisplatin in HEK293 cells. Immunoblot results indicated that γH2AX expression levels were elevated in response to cisplatin over 8 hours and after 1 hour cisplatin withdrawal in HEK293 cells. ImageStudio Lite software was used for band quantification as described in the methods section (n=3 ± SD), ns (not significant), **p<0.01, *p<0.05.

The WHCO1 cells also showed an increase in γH2AX expression levels in response to cisplatin treatment (Figure 3.5). However, this increase was not as consistent in different withdrawal time points, as observed in HEK293 cells. A 47% (147 ± 45%) and 72% (172 ± 164%) γH2AX increases were observed in cisplatin only and after 5 minutes cisplatin withdrawal in WHCO1 cells. These expression levels then lowered to 34% (134 ± 49%) after 30 minutes withdrawal. However, after one hour cisplatin withdrawal, γH2AX increased by 73% (173 ± 264%) in comparison to the untreated control (Figure 3.5). The WHCO1 cisplatin treated cells showed no statistical difference in γH2AX expression 8 hours post cisplatin treatment and for all the withdrawal time points in comparison to the untreated controls in WHCO1 cells (Figure 3.5).

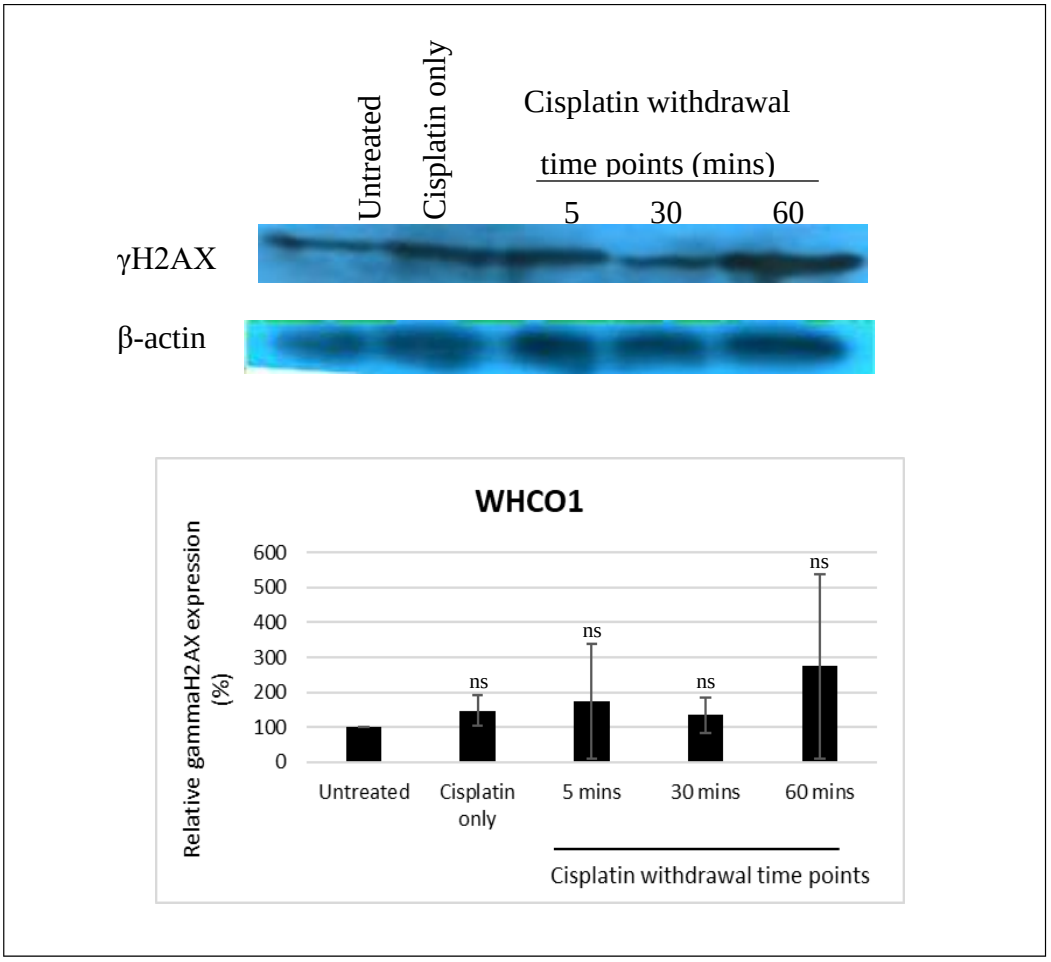

Figure 3.5: **γH2AX expression in response to cisplatin in WHCO1 cells.** WHCO1 immunoblot results indicated that γH2AX expression levels were fluctuated in response to cisplatin over 8 hours and after 1 hour cisplatin withdrawal. ImageStudio Lite software was used for band quantification as described in the methods section (n=3 ± SD), ns (not significant).

Only one western blot batch was done for WHCO5. Similar to WHCO1, γH2AX showed fluctuating expression levels in response to cisplatin (Figure 3.6). There was a 18%, 5% and 31% increase of γH2AX expression in cisplatin only, 5 minutes and 60 minutes withdrawal in comparison to the untreated control. Post 30 minutes cisplatin withdrawal, γH2AX levels showed a 6% decrease in response to cisplatin compared to the untreated control (Figure 3.6). However, the data remains vague as only one batch was achieved for this cell line.

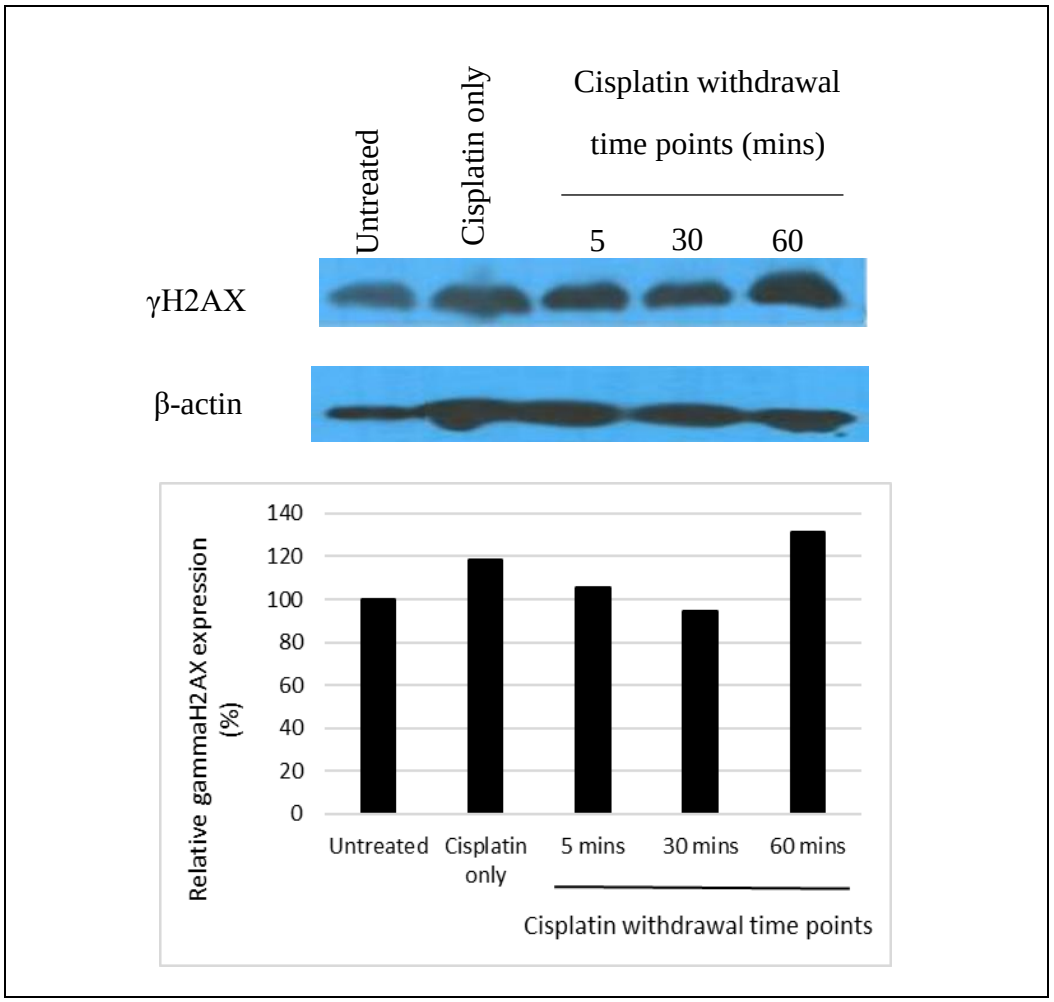

Figure 3.6: γH2AX expression in response to cisplatin in WHCO5 cells. Immunoblot results indicated that γH2AX expression levels were fluctuated in response to cisplatin over 8 hours and after 1 hour cisplatin withdrawal. ImageStudio software was used for band quantification as described in the methods section (n=1).

3.3.Evaluation of the quality of RNA extracted from HEK293 and WHCO1 cisplatin treated cells.

Based on the cell line, the EC_{50} concentrations in 3.1 were used for treating cells. After 8 hours cisplatin treatment, cells underwent different withdrawal times. Total RNA was extracted from HEK293 and OSCC cisplatin treated cell lines. The extracted RNA was separated on a 1% non-denaturing agarose gel to assess the integrity. Two distinct 28S and 18S ribosomal RNA bands of sizes ~1500 bp and ~750 bp respectively were observed (Figure 3.7). The 28S rRNA band was twice as intenseas the 18S rRNA band and this 2:1 (28S:18S) ratio indicates good quality

intact RNA. Good RNA quality entails both purity and integrity and the two are crucial for ensuring the relevance, accuracy and reproducibility of RNA-based downstream applications such as gene expression by RT-PCR. The RNA integrity gel showed that the RNA extracted from cisplatin treated HEK293 and OSCC cell lines was ofa good quality as the 28S and 18S bands appear quite distinct for all samples, withthe 28S band having double the intensity in comparison to the 18S band.

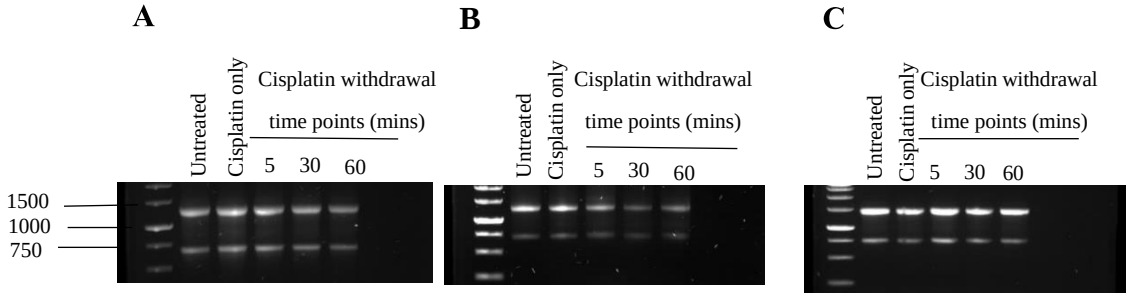

Figure 3.7: Electrophoresis of RNA extracted from cisplatin treated cells at different withdrawal times on 1% agarose gel, stained with ethidium bromide. The quality of total RNA extracted from **A.** HEK293, **B**. WHCO1 and **C.** WHCO5 cellsis indicated by 2 bands of 28S and 18S rRNA at ~1500 bp and ~750 bp respectively. 10 µl of diluted 200 ng/µl RNA was mixed with 2 µl of the 6X loading dye making a total of 12 µl loaded per well for each sample. (MW): GeneRulerTM 1 kb DNA ladder.

3.4.PANDA and ANRIL expressions in response to cisplatin treated HEK293 and OSCC cells.

The expression of lncRNAs ANRIL and PANDA were established by RT-PCR, with GADPDH used as the loading control. The RT-PCR data serve as preliminary results for qRT-PCR.

The consistent GAPDH expression levels observed in HEK293 cells supports successful cDNA synthesis from HEK293 extracted RNA (Figure 3.8A). The absence of bands in the no template control (NTC) and no RT control lanes indicate that PCR was not contaminated with foreign DNA (Figure 3.8). PANDA expression levels appeared to be upregulated in cisplatin treated HEK293 cells and 30 minutes after cisplatin withdrawal (Figure 3.8B). No changes in PANDA expression were observed after 5 minutes cisplatin withdrawal and a decrease in expression was observed

post 60 minutes cisplatin withdrawal, in comparison to the untreated control (Figure 3.8B). HEK293 control cell line showed an upregulated ANRIL expression when cells were treated with cisplatin and a slight increase during the 60 minutes post cisplatin withdrawal for all withdrawal time points (Figure 3.8C). The levels of ANRIL in all three withdrawal time points (5, 30 and 60) showed a slight increase in comparison to the untreated control (Figure 3.8C).

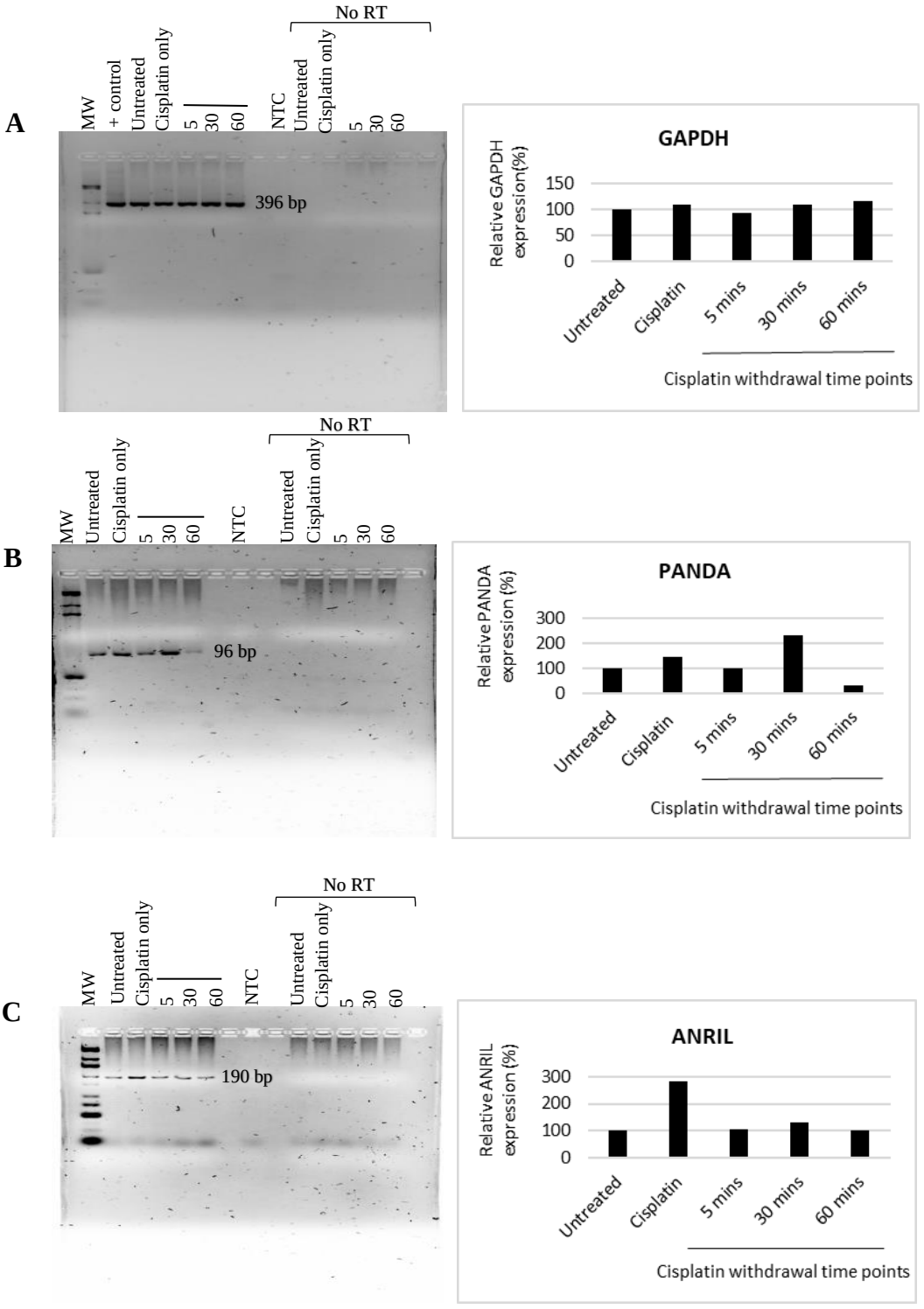

Figure 3.8: GAPDH control, PANDA and ANRIL lncRNAs expression in HEK293 cisplatin treated cells. The expression levels of A. GAPDH control, B. PANDA and C. ANRIL lncRNAs of sizes of 396, 96 and 190 bp respectively after 8 hours cisplatin treatment in HEK293 cells. No bands were observed for the NTC and no RT controls. ImageStudio Lite software and Excel 2019 were used for plotting graphs. (MW): TriDye Ultra-low range DNA ladder (10-700 bp) (ThermoFisher Scientific) (n=1).

Successful cDNA synthesis was also achieved from WHCO1 extracted RNA as GADPH control was successfully amplified in all experimental samples (Figure 3.9A). The absence of bands in the NTC and no RT controls showed that there was no DNA contamination during PCR (Figure 3.9). PANDA showed a slight upregulation in cisplatin treated WHCO1 and 1 hour post cisplatin withdrawal for all the time points (Figure3.9B). This minor increase of PANDA expression in cisplatin treated WHCO1 cells compared to untreated cells can only be confirmed by qRT-PCR (Figure 3.9B). ANRIL appeared upregulated in cisplatin treated WHCO1 and 60 minutes post cisplatin withdrawal in comparison to the untreated control (Figure 3.9). ANRIL expression levels appear to have been reduced following cisplatin withdrawal at 5 minutes and 30 minutes. However, expression levels returned to untreated levels at 60 minutes post withdrawal (Figure 3.9C).

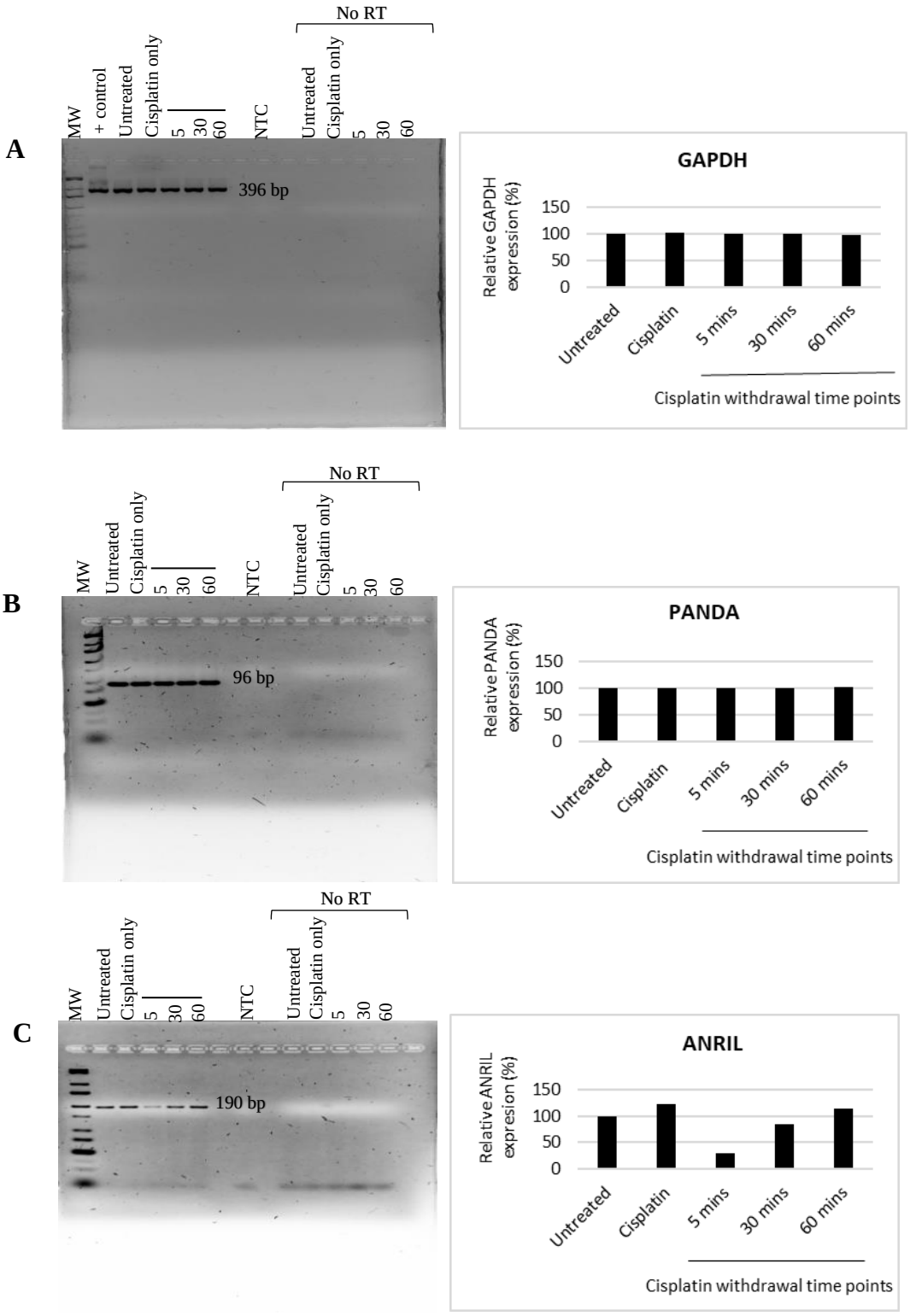

Figure 3.9: GAPDH control, PANDA and ANRIL lncRNAs in cisplatin treated WHCO1 cells. Expression of **A.** GAPDH control, **B**. PANDA and **C**. ANRIL lncRNAs of sizes of 396, 96 and 190 bp respectively post 8 hours cisplatin treatment in WHCO1 cells**.** No bands were observed for the NTC and no RT controls. ImageStudio Lite software and Excel 2019 were used for plotting graphs. (MW): TriDye Ultra-low range DNA ladder (10-700 bp) (ThermoFisher Scientific) (n=1).

Similar to HEK293 and WHCO1 cell lines, successful cDNA synthesis was observed in WHCO5 cells with GAPDH showing successful amplification in all three PCRs had no DNA contamination (Figure 3.10). PANDA showed an upregulated expression in cisplatin treated cells (Figure 3.10B). Similar to WHCO1 PANDA expression (Figure 3.9B), WHCO5 also showed a slight increase in PANDA expression in cisplatin treated and during cisplatin withdrawal times compared to the untreated control (Figure 3.10B). However, this can only be confirmed with RT- qPCR. WHCO5 cisplatin treated cells showed a slight upregulation in ANRIL expression in cisplatin treated cells and 60 minutes post cisplatin withdrawal (Figure 3.10C). However, post 5 minutes and 30 minutes cisplatin withdrawal, ANRIL levels were downregulated in cisplatin treated WHCO5 cells compared to the untreated control (Figure 3.10C).

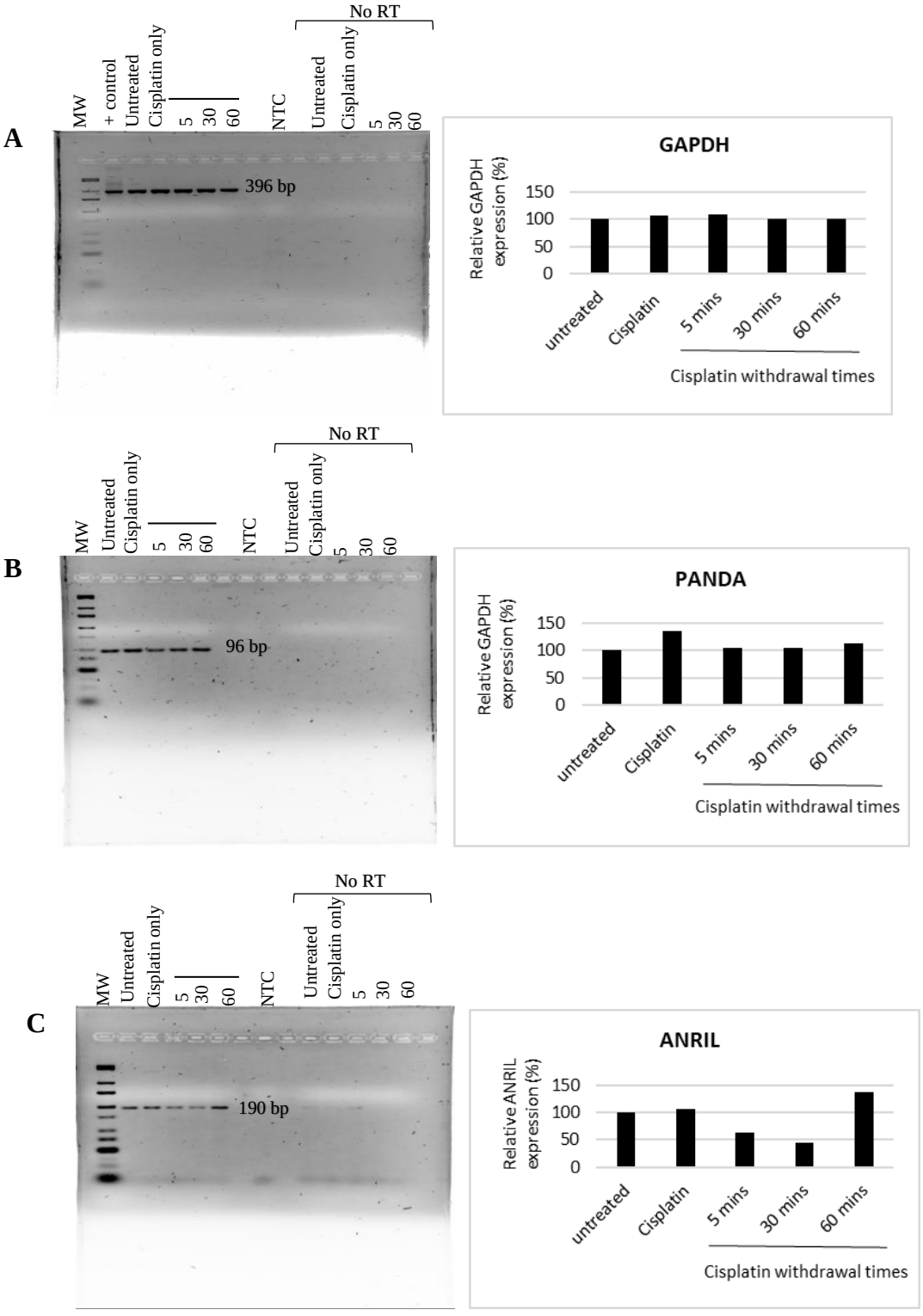

Figure 3.10: GAPDH control, PANDA and ANRIL lncRNAs in cisplatin treated WHCO5 cells. Expression of **A.** GAPDH control, **B**. PANDA and **C**. ANRIL lncRNAs of sizes of 396, 96 and 190 bp respectively post 8 hours cisplatin treatment in WHCO5 cells**.** No bands were observed for the NTC and no RT controls. (MW): ImageLite Studio software and Excel 2019 were used for plotting graphs. TriDye Ultra-low range DNA ladder (10-700 bp) (ThermoFisher Scientific) (n=1).

4. Discussion

OSCC prognosis remains poor in South Africa and other developing countries despite a variety of treatment options that are available (Sewram *et al*., 2014; Lipenga *et al*., 2021). Although cisplatin is widely used and effective, its intrinsic and acquired resistance observed in various cancer types limits its efficacy (Ando *et al*., 2012). Emerging evidence has highlighted the roles of lncRNAs in the development of cisplatin chemoresistance (Hu *et al*., 2018). LncRNAs involved in the repair of DSBs by DDR, ANRIL and PANDA expressions were studied in response to cisplatin treatment and immediately after cisplatin withdrawal in HEK293 and OSCC cell lines. The study aimed to provide potential lncRNA-targeted strategies for overcoming cisplatin resistance in cancer therapy, especially OSCC.

Cisplatin-induced DNA intra-strand crosslinks and ICLs disturb DNA replication and transcription processes resulting in the activation of replication stress and DDR, eventually causing cell cycle arrest and apoptosis (Kottemannand and Smogorzewska, 2013). The induction of γH2AX in response to cisplatin-induced DSBs has been used as a measure of cell exposure to chemotherapeutic drugs and as an indicator of repair after DNA damage in several studies (Banath and Olive, 2003; Huang *et al*., 2004). Studies have shown that the phosphorylation of histone H2AX to γH2AX happens immediately at the DSBs site reaching a peak 30 minutes after DSBs induction (Markova *et al*., 2007). γH2AX is not only crucial for sensing DSBs but also plays a role in chromatin remodelling processes involved in DNA repair.

To investigate whether cisplatin induces DNA DSBs and the DDR via γH2AX activation, cisplatin EC_{50} concentrations were determined by MTT assay in HEK293 and OSCC cell lines. The results obtained in this study were consistent with those observed in previous OSCC studies done at our laboratory. Low cisplatin EC_{50} concentrations of 18.6 µM in HEK293 cells compared to WHCO1 and WHCO5 with EC_{50} concentrations of 47.1 and 32.5 µM respectively means the HEK293 control cell line is in line with expectations of being more sensitive to cisplatin in comparison to the cancerous WHCO1 and WHCO5 OSCC cell lines. Studies by Halabian *et al*., 2015 and Sadeghi *et al*., 2018 also showed that low

cisplatin concentrations are sufficient to induce a maximum response and cytotoxicity in HEK293 cells.

The western blot data in this study revealed that cisplatin-induced DNA DSBs repair occurs in cisplatin treated HEK293 and OSCC cell lines. An increase in γH2AX expression was observed in cisplatin treated cells and 1 hour post cisplatin withdrawal. The consistent γH2AX increase in HEK293 cells after cisplatin treatment and during the first hour of cisplatin withdrawal for all withdrawal time points may suggest that HEK293 cells are regularly sensing the cisplatin-induced DSBs and triggering relocalisation of DDR proteins to the DNA damage site to activate DNA damage repair.

Both the WHCO5 and WHCO1 OSCC cell lines, showed fluctuating γH2AX expressions. This proved that similar to the HEK29 control, the OSCC cells are also sensing the cisplatin-induced DSBs and activating DDR machinery. The γH2AX decrease post 30 minutes cisplatin withdrawal in comparison to other withdrawal time points may suggest that, the OSCC cells might rapidly be repairing the cisplatin-induced DSBs or continuing with cell proliferation even in the presence of DSBs. The decrease in γH2AX expression after 30 minutes cisplatin withdrawal is consistent with the results from Mariotti *et al*., 2013 showing a decrease in the radiation induced γH2AX expression after 30 minutes peak followed by restored γH2AX response after 6 hours.

Our study was consistent with a study by Kalra and Bapat (2013) in ovarian cancer demonstrating an upregulated γH2AX expression levels post cisplatin treatment. Their study further demonstrated that cisplatin induces DSBs, increasing the γH2AX levels as well as DNA repair proteins XRCC5, RAD50 and NPM1 (Kalra and Bapat, 2013). RAD50 is one of the MRN complex proteins responsible for recruiting DNA repair proteins to the DNA damage site (Kim e*t al*., 2015). Another study by Cruet-Hennequart *et al*., 2009 showed elevated γH2AX expression 6 hours post cisplatin treatment which was consistent with the formation of DNA DSBs in polŋ-deficient cells.

Upon DNA damage, several lncRNAs such as ANRIL and PANDA are induced and have been proposed to play a role in DSBs repair (Thapar, 2018). Our PCR results showed that the expression of ANRIL lncRNA was increased during

cisplatin treatment and 60 minutes post cisplatin withdrawal and decreased 5- and 30-minutes post cisplatin withdrawal in cisplatin treated OSCC cell lines. Studies involving ANRIL regulation during DDR have proven that DSBs increase ANRIL expression through the activation of E2F1 in an ATM dependent manner (Wan *et al*., 2013). However, the low ANRIL levels observed 5 and 30 minutes after cisplatin withdrawal in both the cisplatin treated OSCC cell lines during DDR are not consistent with similar studies performed in other cell lines which showed upregulated ANRIL expression in response to cisplatin treatment during DDR (Chen *et al*. 2017; Wang e*t al*., 2017).

Furthermore, the low ANRIL expression levels observed 5 and 30 minutes post cisplatin withdrawal in our study pose a question as to whether there is an alternative mechanism regulating ANRIL during DDR. This ANRIL upregulation after cisplatin treatment and immediate downregulation after 5 and 30 minutes cisplatin withdrawal might suggest that cisplatin-induced DSBs activated the ATM kinase to induce ANRIL expression in an E2F1 dependent manner and underwent DDR during withdrawal time points, decreasing ANRIL expression. This might suggest that OSCC cell line immediately activates the DDR to repair the cisplatin-induced DSBs, decreasing ANRIL expression levels. However, an increase of ANRIL expression 60 minutes post cisplatin withdrawal is questionable and needs further investigations.

PCR results showed that elevated PANDA expression was observed in cisplatin treated OSCC cell lines during DDR compared to the untreated control. The upregulated PANDA expressions are consistent with a similar ovarian cancer study where cisplatin-induced DSBs are believed to activate the ATM protein kinase and activating p53 thus preventing apoptosis by blocking NF-YA and promoting cell cycle progression (Wang *et al*., 2018). This PANDA upregulation in ovarian cancer improved cell survival and tumour growth in response to cisplatin treatment and reduced PANDA expression was associated with reduced tumour growth (Wang *et al*., 2018). There are limited studies investigating the relationship between cisplatin and PANDA expression in cancer.

Multiple studies identified lncRNAs as a new mechanism in drug resistance or sensitivity (Majidina *et al*., 2016; Deng *et al*. 2016; Chen *et al*., 2017). About 22 lncRNAs have been reported to play acrucial role in cisplatin resistance through

different mechanisms in various cancer types (Liu *et al*., 2020). Cisplatin's mechanisms of resistance associated with lncRNAs that induce cisplatin chemoresistance include intracellular detoxification, cisplatin influx/efflux, apoptosis, DNA repair and cell cycle, signalling pathways, ceRNAs, autophagy and cancer stem cells (CSCs). According to the DNA repair and cell cycle mechanism of resistance, chemo-resistant cancer cells appear to be associated with efficient activation of the DDR mechanism and have a higher tolerance to genotoxic stress caused by chemotherapeutic drug than primary cancercells (Özeş *et al*., 2016).

Upregulated PANDA and ANRIL expression are associated with cisplatin chemoresistance in multiple cancer types. High ANRIL expression has been shown to be associated with cancer progression and cisplatin resistance in different cancer types (Miao *et al*., 2019; Wang *et al*., 2020; Li *et al*., 2019). PANDA reduces cisplatin sensitivity and promotes tumourigenesis in ovarian cancer (Wang *et al*., 2018). Our study showed upregulated PANDA expression and fluctuating ANRIL expression during DDR in cisplatin treated OSCC cell lines.

5. Conclusion and Future Prospects

OSCC prognosis remains poor despite various treatment options available because its therapeutic approaches result in treatment failure due to poor efficacy, chemo-toxicity and chemo-resistance. Therefore, there is a compelling need for new chemotherapeutic strategies for OSCC treatment. LncRNAs have shown tumour suppressive and oncogenic properties and participate in cancer progression and suppression and play a prominent role in DSBs repair and are aberrantly expressed in multiple cancer types.

Our study has shown that cisplatin induced DNA damage correlates with γH2AX expression in OSCC cell lines. Moreover, in response to cisplatin, ANRIL lncRNA appeared fluctuating whereas PANDA lncRNA appeared upregulated during the DDR in OSCC cell lines. In conclusion, PANDA and ANRIL lncRNAs may serve as potential cisplatin chemoresistance biomarkers in OSCC cell lines.

Future studies should aim to investigate ANRIL and PANDA expression in response to cisplatin treated OSCC cells by quantitative RT-PCR. LncRNA based-therapy can be investigated by using siRNA to knockdown PANDA and ANRIL lncRNAs in OSCC cells in combination with cisplatin treatment to ascertain their role during treatment. Furthermore, to detect if the PANDA and ANRIL lncRNA could serves as a cisplatin chemoresistance markers, flow cytometry could be used to measure cisplatin-induced apoptosis in OSCC cells with and without ANRIL or PANDA siRNA knockdown to determine the different apoptosis levels induced.

References

Abnet, C.C., Arnold, M. and Wei, W.Q. (2018). Epidemiology of esophageal squamous cell carcinoma. *Gastroenterology*, *154*(2), pp.360-373.

Agrawal, S. (1996). Antisense oligonucleotides: towards clinical trials. *Trends in Biotechnology*, *14*(10), pp.376-387.

Alborzinia, H., Can, S., Holenya, P., Scholl, C., Lederer, E., Kitanovic, I. and Wölfl, S. (2011). Real-time monitoring of cisplatin-induced cell death. *PloS One*, *6*(5), p.e19714.

Ando, N., Kato, H., Igaki, H., Shinoda, M., Ozawa, S., Shimizu, H., Nakamura, T., Yabusaki, H., Aoyama, N., Kurita, A. and Ikeda, K. (2012). A randomized trial comparing postoperative adjuvant chemotherapy with cisplatin and 5-fluorouracil versus preoperative chemotherapy for localized advanced squamous cell carcinoma of the thoracic esophagus (JCOG9907). *Annals of Surgical Oncology*, *19*(1), pp.68-74.

Arnold, M., Soerjomataram, I., Ferlay, J. and Forman, D. (2015). Global incidence of oesophageal cancer by histological subtype in 2012. *Gut*, *64*(3), pp.381-387.

Arun, G., Diermeier, S.D. and Spector, D.L. (2018). Therapeutic targeting of long non-coding RNAs in cancer. *Trends in Molecular Medicine*, *24*(3), pp.257-277.

Autrup, H., Harris, C.C., Wu, S.M., Bao, L.Y., Pei, X.F., Lu, S., Sun, T.T. and Hsia, C.C. (1984). Activation of chemical carcinogens by cultured human fetal liver, esophagus and stomach. *Chemico-Biological Interactions*, *50*(1), pp.15-25.

Ayers, D. (2013). Long non-coding RNAs: novel emergent biomarkers for cancer diagnostics. *Journal of Cancer Research Treatment*, *1*(2), pp.31-5.

Bai, L. and Zhu, W.G. (2006). P53: structure, function and therapeutic applications. *Journal of Molecular Cancer*, *2*(4), pp.141-153.

Banáth, J.P. and Olive, P.L. (2003). Expression of phosphorylated histone H2AX as a surrogate of cell killing by drugs that create DNA double-strand breaks. *Cancer Research*, *63*(15), pp.4347-4350.

Bassing, C.H. and Alt, F.W. (2004). The cellular response to general and programmed DNA double strand breaks. *DNA Repair*, *3*(8-9), pp.781-796.

Bernstein, C., Bernstein, H., Payne, C.M. and Garewal, H. (2002). DNA repair/pro-apoptotic dual-role proteins in five major DNA repair pathways: fail-safe protection against carcinogenesis. *Mutation Research/Reviews in Mutation Research*, *511*(2), pp.145-178.

Bernstein, E. and Allis, C.D. (2005). RNA meets chromatin. *Genes & Development*, *19*(14), pp.1635-1655.

Bramhall, S., Noack, N., Wu, M. and Loewenberg, J.R. (1969). A simple colorimetric method for determination of protein. *Analytical Biochemistry*, *31*, pp.146-148.

Branch, P., Masson, M., Aquilina, G., Bignami, M. and Karran, P. (2000). Spontaneous development of drug resistance: mismatch repair and p53 defects in resistance to cisplatin in human tumor cells. *Oncogene*, *19*(28), pp.3138-3145.

Bray, F., Ferlay, J., Soerjomataram, I., Siegel, R.L., Torre, L.A. and Jemal, A. (2018). Global cancer statistics 2018: GLOBOCAN estimates of incidence and mortality worldwide for 36 cancers in 185 countries. *CA: A Cancer Journal for Clinicians*, *68*(6), pp.394-424.

Broustas, C.G. and Lieberman, H.B. (2014). DNA damage response genes and the development of cancer metastasis. *Radiation Research*, *181*(2), pp.111-130.

Brown, L.M., Hoover, R.N., Greenberg, R.S., Schoenberg, J.B., Schwartz, A.G., Swanson, G.M., Liff, J.M., Silverman, D.T., Hayes, R.B. and Pottern, L.M. (1994). Are racial differences in squamous cell esophageal cancer explained by alcohol and tobacco use. *JNCI: Journal of the National Cancer Institute*, *86*(17), pp.1340-1345.

Brozovic, A. and Osmak, M. (2007). Activation of mitogen-activated protein kinases by cisplatin and their role in cisplatin-resistance. *Cancer Letters*, *251*(1), pp.1-16.

Burma, S., Chen, B.P., Murphy, M., Kurimasa, A. and Chen, D.J. (2001). ATM phosphorylates histone H2AX in response to DNA double-strand breaks. *Journal of Biological Chemistry*, *276*(45), pp.42462-42467.

Burnett, J.C., Rossi, J.J. and Tiemann, K. (2011). Current progress of siRNA/shRNA therapeutics in clinical trials. *Biotechnology Journal*, *6*(9), pp.1130-1146.

Carlevaro-Fita, J. and Johnson, R. (2019). Global positioning system: understanding long noncoding RNAs through subcellular localization. *Molecular Cell*, *73*(5), pp.869-883.

Carrieri, C., Cimatti, L., Biagioli, M., Beugnet, A., Zucchelli, S., Fedele, S., Pesce, E., Ferrer, I., Collavin, L., Santoro, C. and Forrest, A.R. (2012). Long non-coding antisense RNA controls Uchl1 translation through an embedded SINEB2 repeat. *Nature*, *491*(7424), pp.454-457.

Cao, T., Shen, J., Pan, W., Li, C. and Qiao, Z. (2018). Upregulation of long noncoding RNA ANRIL correlates with tumor progression and poor prognosis in esophageal squamous cell carcinoma. *Journal of Balkan Union of Oncology*, *23*(6), pp.1862-1866.

Chandawarkar, R.Y., Kakegawa, T., Fujita, H., Yamana, H. and Hayabuthi, N. (1996). Comparative analysis of imaging modalities in the preoperative assessment of nodal metastasis in esophageal cancer. *Journal of Surgical Oncology*, *61*(3), pp.214-217.

Chaudhary, R. and Lal, A. (2017). Long noncoding RNAs in the p53 network. *Wiley Interdisciplinary Reviews: RNA*, *8*(3), p.e1410.

Chen, H.H., Chen, W.C., Liang, Z.D., Tsai, W.B., Long, Y., Aiba, I., Fu, S., Broaddus, R., Liu, J., Feun, L.G. and Savaraj, N. (2015). Targeting drug transport mechanisms for improving platinum-based cancer chemotherapy. *Expert Opinion on Therapeutic Targets*, *19*(10), pp.1307-1317.

Chen, Q.N., Wei, C.C., Wang, Z.X. and Sun, M. (2017). Long non-coding RNAs in anti-cancer drug resistance. *Oncotarget*, *8*(1), p.1925.

Chen, S., Zhang, J.Q., Chen, J.Z., Chen, H.X., Qiu, F.N., Yan, M.L., Chen, Y.L., Peng, C.H., Tian, Y.F. and Wang, Y.D. (2017). The over expression of long non-coding RNA ANRIL promotes epithelial-mesenchymal transition by activating the ATM-E2F1 signaling pathway in pancreatic cancer: An in vivo and in vitrostudy. *International Journal of Biological Macromolecules*, *102*, pp.718-728.

Chen, D., Zhang, Z., Mao, C., Zhou, Y., Yu, L., Yin, Y., Wu, S., Mou, X. and Zhu, Y. (2014). ANRIL inhibits p15INK4b through the TGFβ1 signaling pathway in human esophageal squamous cell carcinoma. *Cellular Immunology*, *289*(1-2), pp.91-96.

Chu, C., Qu, K., Zhong, F.L., Artandi, S.E. and Chang, H.Y. (2011). Genomic maps of long noncoding RNA occupancy reveal principles of RNA-chromatin interactions. *Molecular Cell*, *44*(4), pp.667-678.

Chung, C.S., Lee, Y.C., Wang, C.P., Ko, J.Y., Wang, W.L., Wu, M.S. and Wang, H.P. (2010). Secondary prevention of esophageal squamous cell carcinoma in areas where smoking, alcohol, and betel quid chewing are prevalent. *Journal of the Formosan Medical Association*. *109*(6), pp.408–421.

Comings, D.E. (1972). The structure and function of chromatin. *Advances in Human Genetics*, pp.237-431.

Cong, L., Ran, F.A., Cox, D., Lin, S., Barretto, R., Habib, N., Hsu, P.D., Wu, X., Jiang, W., Marraffini, L.A. and Zhang, F. (2013). Multiplex genome engineering using CRISPR/Cas systems. *Science*, *339*(6121), pp.819-823.

Cross, T.G., Scheel-Toellner, D., Henriquez, N.V., Deacon, E., Salmon, M. and Lord, J.M. (2000). Serine/threonine protein kinases and apoptosis. *Experimental Cell Research*, *256*(1), pp.34-41.

Cruet-Hennequart, S., Villalan, S., Kaczmarczyk, A., O'Meara, E., Sokol, A.M. and Carty, M.P. (2009). Characterization of the effects of cisplatin and carboplatin on cell cycle progression and DNA damage response activation in DNA polymerase eta-deficient human cells. *Cell Cycle*, *8*(18), pp.3043-3054.

Dabholkar, M., Vionnet, J., Bostick-Bruton, F., Yu, J.J. and Reed, E. (1994). Messenger RNA levels of XPAC and ERCC1 in ovarian cancer tissue correlate with response to platinum-based chemotherapy. *The Journal of Clinical Investigation*, *94*(2), pp.703-708.

Damelin, L.H., Jivan, R., Veale, R.B., Rousseau, A.L. and Mavri-Damelin, D. (2014). Metformin induces an intracellular reductive state that protects oesophageal squamous cell carcinoma cells against cisplatin but not copper-bis (thiosemicarbazones). *British Medical Journal Cancer*, *14*(1), p.314.

Dasari, S. and Tchounwou, P.B. (2014). Cisplatin in cancer therapy: molecular mechanisms of action. *European Journal of Pharmacology*, *740*, pp.364-378.

Deans, A.J. and West, S.C. (2011). DNA interstrand crosslink repair and cancer. *Nature Reviews Cancer*, *11*(7), pp.467-480.

Delmastro, D.A., Li, J., Vaisman, A., Solle, M. and Chaney, S.G. (1996). DNA damage inducible-gene expression following platinum treatment in human ovarian carcinoma cell lines. *Cancer Chemotherapy and Pharmacology*, *39*(3), pp.245-253.

Deng, H., Zhang, J., Shi, J., Guo, Z., He, C., Ding, L., Tang, J.H. and Hou, Y. (2016). Role of long non-coding RNA in tumor drug resistance. *Tumor Biology*, *37*(9), pp.11623-11631.

Derrien, T., Johnson, R., Bussotti, G., Tanzer, A., Djebali, S., Tilgner, H., Guernec, G., Martin, D., Merkel, A., Knowles, D.G. and Lagarde, J. (2012). The GENCODE v7 catalog of human long noncoding RNAs: analysis of their gene structure, evolution, and expression. *Genome Research*, *22*(9), pp.1775-1789.

De Vries, G., Rosas-Plaza, X., van Vugt, M.A., Gietema, J.A. and de Jong, S. (2020). Testicular cancer: determinants of cisplatin sensitivity and noveltherapeutic opportunities. *Cancer Treatment Reviews*, *88*, p.102054.

Dong, X., Jin, Z., Chen, Y., Xu, H., Ma, C., Hong, X., Li, Y. and Zhao, G. (2017). Knockdown of long non-coding RNA ANRIL inhibits proliferation, migration, and invasion but promotes apoptosis of human glioma cells by upregulation of miR-34a. *Journal of Cellular Biochemistry*, *119*(3), pp.2708-2718.

Dorsett, Y. and Tuschl, T. (2004). siRNAs: applications in functional genomics and potential as therapeutics. *Nature Reviews Drug Discovery*, *3*(4), pp.318-329.

Drak Alsibai, K., Vacher, S., Meseure, D., Nicolas, A., Lae, M., Schnitzler, A., Chemlali, W., Cros, J., Longchampt, E., Cacheux, W. and Pignot, G. (2019). High positive correlations between ANRIL and p16-CDKN2A/p15-CDKN2B/p14-ARF gene cluster overexpression in multi-tumor types suggest deregulated activation of an ANRIL–ARF bidirectional promoter. *Non-coding RNA*, *5*(3), p.44.

Dutertre, M. and Vagner, S. (2017). DNA-damage response RNA-binding proteins (DDRBPs): perspectives from a new class of proteins and their RNA targets. *Journal of Molecular Biology*, *429*(21), pp.3139-3145.

Eastman, A. (1987). The formation, isolation and characterization of DNA adducts produced by anticancer platinum complexes. *Pharmacology & Therapeutics*, *34*(2), pp.155-166.

El-Khateeb, M., Appleton, T.G., Gahan, L.R., Charles, B.G., Berners-Price, S.J. and Bolton, A.M. (1999). Reactions of cisplatin hydrolytes with methionine, cysteine, and plasma ultrafiltrate studied by a combination of HPLC and NMR techniques. *Journal of Inorganic Biochemistry*, *77*(1-2), pp.13-21.

Engel, L.S., Chow, W.H., Vaughan, T.L., Gammon, M.D., Risch, H.A., Stanford, J.L., Schoenberg, J.B., Mayne, S.T., Dubrow, R., Rotterdam, H. and West, A.B. (2003). Population attributable risks of esophageal and gastric cancers. *Journal of the National Cancer Institute*, *95*(18), pp.1404-1413.

Ernst, E., Pittler, M.H., Wider, B. and Boddy, K. (2007). Complementary/alternative medicine for supportive cancer care: development of the evidence-base. *Supportive Care in Cancer*, *15*(5), pp.565-568.

Faghihi, M.A., Zhang, M., Huang, J., Modarresi, F., Van der Brug, M.P., Nalls, M.A., Cookson, M.R., St-Laurent, G. and Wahlestedt, C. (2010). Evidence for natural antisense transcript-mediated inhibition of microRNA function. *Genome Biology*, *11*(5), pp.1-13.

Fang, S., Zhang, L., Guo, J., Niu, Y., Wu, Y., Li, H., Zhao, L., Li, X., Teng, X., Sun, X. and Sun, L. (2018). NONCODEV5: a comprehensive annotation database for long non-coding RNAs. *Nucleic Acids Research*, *46*(D1), pp. D308-D314.

Fatima, R., Akhade, V.S., Pal, D. and Rao, S.M. (2015). Long noncoding RNAs in development and cancer: potential biomarkers and therapeutic targets. *Molecular and Cellular Therapies*, *3*(1), pp.1-19.

Fitzmaurice, C., Dicker, D., Pain, A., Hamavid, H., Moradi-Lakeh, M., MacIntyre, M.F., Allen, C., Hansen, G., Woodbrook, R., Wolfe, C. and Hamadeh, R.R. (2015). The global burden of cancer 2013. *JAMA Oncology*, *1*(14), pp.505–527.

Furuta, T., Ueda, T., Aune, G., Sarasin, A., Kraemer, K.H. and Pommier, Y. (2002). Transcription-coupled nucleotide excision repair as a determinant of cisplatin sensitivity of human cells. *Cancer Research*, *62*(17), pp.4899-4902.

Ghosh, S. (2019). Cisplatin: The first metal based anticancer drug. *Bioorganic Chemistry*, *88*, p.102925.

Gibb, E.A., Brown, C.J. and Lam, W.L. (2011). The functional role of long non-coding RNA in human carcinomas. *Molecular Cancer*, *10*(1), pp.1-17.

Gilbert, L.A., Larson, M.H., Morsut, L., Liu, Z., Brar, G.A., Torres, S.E., Stern-Ginossar, N., Brandman, O., Whitehead, E.H., Doudna, J.A. and Lim, W.A. (2013). CRISPR-mediated modular RNA-guided regulation of transcription in eukaryotes. *Cell*, *154*(2), pp.442-451.

Gillies, R.J., Didier, N. and Denton, M. (1986). Determination of cell number in monolayer cultures. *Analytical Biochemistry*, *159*(1), pp.109-113.

Goyal, A., Myacheva, K., Groß, M., Klingenberg, M., Duran Arqué, B. and Diederichs, S. (2017). Challenges of CRISPR/Cas9 applications for long non-coding RNA genes. *Nucleic Acids Research*, *45*(3), pp.e12-e12.

Greene, F.L., Balch, C.M., Fleming, I.D., Fritz, A., Haller, D.G., Morrow, M. and Page, D.L. (2002). *AJCC Cancer Staging Handbook: TNM Classification of Malignant Tumors*. Springer Science & Business Media.

Grillone, L.R. and Lanz, R. (2001). Fomivirsen. *Drugs of Today (Barcelona, Spain: 1998)*, *37*(4), pp.245-255.

Griesenbeck, J.S., Steck, M.D., Huber, J.C., Sharkey, J.R., Rene, A.A. and Brender, J.D. (2009). Development of estimates of dietary nitrates, nitrites, and nitrosamines for use with the Short Willet Food Frequency Questionnaire. *Nutrition Journal*, *8*(1), pp.1-9.

Gu, M., Li, S.Y., Huang, X.E., Lin, Y., Cheng, H.Y. and Liu, L. (2012). A phase II study on continuous infusional paclitaxel and 5-Fu as first-line chemotherapy for patients with advanced esophageal cancer. *Asian Pacific Journal of Cancer Prevention*, *13*(11), pp.5587-5591.

Gupta, R.A., Shah, N., Wang, K.C., Kim, J., Horlings, H.M., Wong, D.J., Tsai, M.C., Hung, T., Argani, P., Rinn, J.L. and Wang, Y. (2010). Long non-coding RNA HOTAIR reprograms chromatin state to promote cancer metastasis. *Nature*, *464*(7291), pp.1071-1076.

Guttman, M. and Rinn, J.L. (2012). Modular regulatory principles of large non-coding RNAs. *Nature*, *482*(7385), pp.339-346.

Gutschner, T. and Diederichs, S. (2012). The hallmarks of cancer: a long non-coding RNA point of view. *RNA Biology*, *9*(6), pp.703-719.

Halabian, R., Roudkenar, M.H., Jahanian-Najafabadi, A., Hosseini, K.M. and Tehrani, H.A. (2015). Co-culture of bone marrow-derived mesenchymal stem cells overexpressing lipocalin 2 with HK-2 and HEK293 cells protects the kidney cells against cisplatin-induced injury. *Cell Biology International*, *39*(2), pp.152-163.

Hanahan, D. and Weinberg, R.A. (2000). The hallmarks of cancer. *Cell*, *100*(1), pp.57-70.

Hannou, S.A., Wouters, K., Paumelle, R. and Staels, B. (2015). Functional genomics of the CDKN2A/B locus in cardiovascular and metabolic disease: what have we learned from GWASs?. *Trends in Endocrinology & Metabolism*, *26*(4), pp.176-184.

Hara, H., Tahara, M., Daiko, H., Kato, K., Igaki, H., Kadowaki, S., Tanaka, Y., Hamamoto, Y., Matsushita, H., Nagase, M. and Hosoya, Y. (2013). Phase II feasibility study of preoperative chemotherapy with docetaxel, cisplatin, and fluorouracil for esophageal squamous cell carcinoma. *Cancer Science*, *104*(11), pp.1455-1460.

Hassan, M., Watari, H., AbuAlmaaty, A., Ohba, Y. and Sakuragi, N. (2014). Apoptosis and molecular targeting therapy in cancer. *BioMed Research International*, *2014*.

He, L.J., Shan, H.B., Luo, G.Y., Li, Y., Zhang, R., Gao, X.Y., Wang, G.B., Lin,

S.Y., Xu, G.L. and Li, J.J. (2014). Endoscopic ultrasonography for staging of T1a and T1b esophageal squamous cell carcinoma. *World Journal of Gastroenterology: WJG*, *20*(5), p.1340.

Helbig, R. and Fackelmayer, F.O. (2003). Scaffold attachment factor A (SAF-A) is concentrated in inactive X chromosome territories through its RGGdomain. *Chromosoma*, *112*(4), pp.173-182.

Hengartner, M.O. (2000). The biochemistry of apoptosis. *Nature*, *407*(6805), pp.770-776.

Hezroni, H., Koppstein, D., Schwartz, M.G., Avrutin, A., Bartel, D.P. and Ulitsky,

I. (2015). Principles of long noncoding RNA evolution derived from direct comparison of transcriptomes in 17 species. *Cell Reports*, *11*(7), pp.1110-1122.

Holdt, L.M., Hoffmann, S., Sass, K., Langenberger, D., Scholz, M., Krohn, K., Finstermeier, K., Stahringer, A., Wilfert, W., Beutner, F. and Gielen, S. (2013). Alu elements in ANRIL non-coding RNA at chromosome 9p21 modulate atherogenic cell functions through trans-regulation of gene networks. *PLoS Genetics*, *9*(7), p.e1003588.

Holdt, L.M., Sass, K., Gäbel, G., Bergert, H., Thiery, J. and Teupser, D. (2011). Expression of Chr9p21 genes CDKN2B (p15INK4b), CDKN2A (p16INK4a, p14ARF) and MTAP in human atherosclerotic plaque. *Atherosclerosis*, *214*(2), pp.264-270.

Holdt, L.M., Stahringer, A., Sass, K., Pichler, G., Kulak, N.A., Wilfert, W., Kohlmaier, A., Herbst, A., Northoff, B.H., Nicolaou, A. and Gäbel, G. (2016). Circular non-coding RNA ANRIL modulates ribosomal RNA maturation and atherosclerosis in humans. *Nature Communications*, *7*(1), pp.1-14.

Holzer, A.K., Manorek, G.H. and Howell, S.B. (2006). Contribution of the major copper influx transporter CTR1 to the cellular accumulation of cisplatin, carboplatin, and oxaliplatin. *Molecular Pharmacology, 70*(4), pp.1390-1394.

Hrdlickova, B., de Almeida, R.C., Borek, Z. and Withoff, S. (2014). Genetic variation in the non-coding genome: Involvement of micro-RNAs and long non-coding RNAs in disease. *Biochimica et Biophysica Acta (BBA)-Molecular Basis of Disease*, *1842*(10), pp.1910-1922.

https://www.cansa.org.za/files/2020/02/Fact-Sheet-on-Oesophageal-Cancer-NCR-2014-web-February-2020.pd

https://www.who.int/news-room/fact-sheets/detail/cancer

Huang, X., Okafuji, M., Traganos, F., Luther, E., Holden, E. and Darzynkiewicz,

Z. (2004). Assessment of histone H2AX phosphorylation induced by DNA topoisomerase I and II inhibitors topotecan and mitoxantrone and by the DNA cross-linking agent cisplatin. *Cytometry Part A: The Journal of the International Society for Analytical Cytology*, *58*(2), pp.99-110.

Huarte, M., Guttman, M., Feldser, D., Garber, M., Koziol, M.J., Kenzelmann-Broz, D., Khalil, A.M., Zuk, O., Amit, I., Rabani, M. and Attardi, L.D. (2010). A large intergenic noncoding RNA induced by p53 mediates global gene repression in the p53 response. *Cell*, *142*(3), pp.409-419.

Hung, T., Wang, Y., Lin, M.F., Koegel, A.K., Kotake, Y., Grant, G.D., Horlings, H.M., Shah, N., Umbricht, C., Wang, P. and Wang, Y. (2011). Extensive and coordinated transcription of noncoding RNAs within cell-cycle promoters. *Nature Genetics*, *43*(7), pp.621-629.

International Agency for Research on Cancer. (2012). Personal habits and indoor combustions: Volume 100 E. *Lyon: International Agency for Research on Cancer and World Health Organization*.

Ishida, S., Lee, J., Thiele, D.J. and Herskowitz, I. (2002). Uptake of the anticancer drug cisplatin mediated by the copper transporter Ctr1 in yeast and mammals. *Proceedings of the National Academy of Sciences*, *99*(22), pp.14298- 14302.

Jaegerstad, M. and Skog, K. (2005). Genotoxicity of heat-processed foods. *Mutation Research/Fundamental and Molecular Mechanisms of Mutagenesis, 574*(1-2), pp.156-172.

Jansen, B.A., Brouwer, J. and Reedijk, J. (2002). Glutathione induces cellular resistance against cationic dinuclear platinum anticancer drugs. *Journal of Inorganic Biochemistry*, *89*(3-4), pp.197-202.

Jarinova, O., Stewart, A.F., Roberts, R., Wells, G., Lau, P., Naing, T., Buerki, C., McLean, B.W., Cook, R.C., Parker, J.S. and McPherson, R. (2009). Functional analysis of the chromosome 9p21. 3 coronary artery disease risk locus. *Arteriosclerosis, Thrombosis, and Vascular Biology*, *29*(10), pp.1671-1677.

Kaushal, G.P., Kaushal, V., Hong, X. and Shah, S.V. (2001). Role and regulation of activation of caspases in cisplatin-induced injury to renal tubular epithelial cells. *Kidney International*, *60*(5), pp.1726-1736.

Kalra, R.S. and Bapat, S.A. (2013). Enhanced levels of double-strand DNA break repair proteins protect ovarian cancer cells against genotoxic stress-induced apoptosis. *Journal of Ovarian Research*, *6*(1), pp.1-10.

Kartalou, M. and Essigmann, J.M. (2001). Mechanisms of resistance tocisplatin. *Mutation Research/Fundamental and Molecular Mechanisms of Mutagenesis*, *478*(1-2), pp.23-43.

Krasna, M.J., Reed, C.E., Nedzwiecki, D., Hollis, D.R., Luketich, J.D., DeCamp, M.M., Mayer, R.J. and Sugarbaker, D.J. (2001). CALGB 9380: a prospective trial of the feasibility of thoracoscopy/laparoscopy in staging esophageal cancer. *The Annals of Thoracic Surgery*, *71*(4), pp.1073-1079.

Kelland, L.R. (1993). New platinum antitumor complexes. *Critical Reviews in Oncology/Hematology*, *15*(3), pp.191-219.

Kelland, L.R. (2000). Preclinical perspectives on platinum resistance. *Drugs*, *59*(4), pp.1-8.

Khochbin, S.A.A.D.I., Brocard, M.P., Grunwald, D.I.D.I.E.R. and Lawrence, J.J. (1992). Antisense RNA and p53 regulation in induced murine cell differentiation. *Annals of the New York Academy of Sciences*, *660*, pp.77-87.

Kies, M.S., Rosen, S.T., Tsang, T.K., Shetty, R., Schneider, P.A., Wallemark, C.B. and Shields, T.W. (1987). Cisplatin and 5-fluorouracil in the primary management of squamous esophageal cancer. *Cancer*, *60*(9), pp.2156-2160.

Kigawa, J., Sato, S., Shimada, M., Kanamori, Y., Itamochi, H. and Terakawa, N. (2002). Effect of p53 gene transfer and cisplatin in a peritonitis carcinomatosa model with p53-deficient ovarian cancer cells. *Gynecologic Oncology*, *84*(2), pp.210-215.

Kim, Y.J., Kim, T.W., Park, S.R., Kim, H.T., Ryu, S.Y. and Jung, J.Y. (2015).

Expression of the Mre11–Rad50–Nbs1 complex in cisplatinnephrotoxicity. *Environmental Toxicology and Pharmacology*, *40*(1), pp.12-17.

Köberle, B., Tomicic, M.T., Usanova, S. and Kaina, B. (2010). Cisplatin resistance: preclinical findings and clinical implications. *Biochimica et Biophysica Acta (BBA)-Reviews on Cancer*, *1806*(2), pp.172-182.

Kong, Y., Hsieh, C.H. and Alonso, L.C. (2018). ANRIL: a lncRNA at the CDKN2A/B locus with roles in cancer and metabolic disease. *Frontiers in Endocrinology*, *9*, p.405.

Kong, Y., Sharma, R.B., Nwosu, B.U. and Alonso, L.C. (2016). Islet biology, the CDKN2A/B locus and type 2 diabetes risk. *Diabetologia*, *59*(8), pp.1579-1593.

Kotake, Y., Goto, T., Naemura, M., Inoue, Y., Okamoto, H. and Tahara, K. (2017). Long noncoding RNA PANDA positively regulates proliferation of osteosarcoma cells. *Anticancer Research*, *37*(1), pp.81-85.

Kottemann, M.C. and Smogorzewska, A. (2013). Fanconi anaemia and the repair of Watson and Crick DNA crosslinks. *Nature*, *493*(7432), pp.356-363.

Kumari, R. and Jat, P. (2021). Mechanisms of cellular senescence: cell cycle arrest and senescence associated secretory phenotype. *Frontiers in Cell and Developmental Biology*, *9*, p.485.

Kung, J.T., Colognori, D. and Lee, J.T. (2013). Long noncoding RNAs: past, present, and future. *Genetics*, *193*(3), pp.651-669.

Kuo, L.J. and Yang, L.X. (2008). γ-H2AX-a novel biomarker for DNA double-strand breaks. *In ivo*, *22*(3), pp.305-309.

Kurokawa, R., Rosenfeld, M.G. and Glass, C.K. (2009). Transcriptional regulation through noncoding RNAs and epigenetic modifications. *RNA Biology*, *6*(3), pp.233-236.

Kuwano, H., Nishimura, Y., Oyama, T., Kato, H., Kitagawa, Y., Kusano, M., Shimada, H., Takiuchi, H., Toh, Y., Doki, Y. and Naomoto, Y. (2015). Guidelines for diagnosis and treatment of carcinoma of the esophagus April 2012 edited by the Japan Esophageal Society. *Esophagus*, *12*(1), pp.1-30.

Lambert, R. and Hainaut, P. (2007). Epidemiology of oesophagogastric cancer. *Best Practice & Research Clinical Gastroenterology*, *21*(6), pp.921-945.

Lander, E.S. (2001). Initial sequencing and analysis of the human genome. International Human Genome Sequencing Consortium. *Nature*, *409*, pp.860-921.

Lau, A.H. (1999). Apoptosis induced by cisplatin nephrotoxic injury. *Kidney International*, *56*(4), pp.1295-1298.

Le Bras, G.F., Farooq, M.H., Falk, G.W. and Andl, C.D. (2016). Esophageal cancer: The latest on chemoprevention and state of the art therapies. *Pharmacological Research*, *113*, pp.236-244.

Levard, H., Pouliquen, X., Hay, J.M., Fingerhut, A., Langlois-Zantain, O., Huguier, M., Lozach, P. and Testart, J. (1998). 5-Fluorouracil and cisplatin as palliative treatment of advanced oesophageal squamous cell carcinoma: A multicentre randomised controlled trial. *European Journal of Surgery*, *164*(11), pp.849-857.

Levine, M.S., Chu, P., Furth, E.E., Rubesin, S.E., Laufer, I. and Herlinger, H. (1997). Carcinoma of the esophagus and esophagogastric junction: sensitivity of radiographic diagnosis. *AJR. American Journal of Roentgenology*, *168*(6), pp.1423-1426.

Li, Y., Wang, Z., Shi, H., Li, H., Li, L., Fang, R., Cai, X., Liu, B., Zhang, X. and Ye, L. (2016). HBXIP and LSD1 scaffolded by lncRNA hotair mediate transcriptional activation by c-Myc. *Cancer Research*, *76*(2), pp.293-304.

Li, F., Zhang, Z., Wang, P., Wen, P., Xu, Q., Wang, Y., Pan, P. and Ma, L. (2019). ALC1 knockdown enhances cisplatin cytotoxicity of esophageal squamous cell carcinoma cells by inhibition of glycolysis through PI3K/Akt pathway. *Life Sciences*, *232*, p.116679.

Li, G. and Zhu, Y. (2019). Effect of lncRNA ANRIL knockdown on proliferation and cisplatin chemoresistance of osteosarcoma cells in vitro. *Pathology-Research and Practice*, *215*(5), pp.931-938.

Li, G. and Zhu, Y. (2019). Effect of lncRNA ANRIL knockdown on proliferation and cisplatin chemoresistance of osteosarcoma cells in vitro. *Pathology-Research and Practice*, *215*(5), pp.931-938.

Li, J., Li, Z., Zheng, W., Li, X., Wang, Z., Cui, Y. and Jiang, X. (2017). PANDAR:

a pivotal cancer-related long non-coding RNA in human cancers. *Molecular BioSystems*, *13*(11), pp.2195-2201.

Lipenga, T., Matumba, L., Vidal, A., Herceg, Z., McCormack, V., De Saeger, S. and De Boevre, M. (2021). A concise review towards defining the exposome of oesophageal cancer in sub-Saharan Africa. *Environment International*, *157*, p.106880.

Loh, S.Y., Mistry, P., Kelland, L.R., Abel, G. and Harrap, K.R. (1992). Reduced drug accumulation as a major mechanism of acquired resistance to cisplatin in a human ovarian carcinoma cell line: circumvention studies using novel platinum (II) and (IV) ammine/amine complexes. *British Journal of Cancer*, *66*(6), pp.1109-1115.

Longley, D.B. and Johnston, P.G. (2005). Molecular mechanisms of drug resistance. *The Journal of Pathology: A Journal of the Pathological Society of Great Britain and Ireland*, *205*(2), pp.275-292.

Lord, R.V., Brabender, J., Gandara, D., Alberola, V., Camps, C., Domine, M., Cardenal, F., Sánchez, J.M., Gumerlock, P.H., Tarón, M. and Sánchez, J.J. (2002). Low ERCC1 expression correlates with prolonged survival after cisplatin plus gemcitabine chemotherapy in non-small cell lung cancer. *Clinical Cancer Research*, *8*(7), pp.2286-2291.

Losko, M., Kotlinowski, J. and Jura, J. (2016). Long noncoding RNAs in metabolic syndrome related disorders. *Mediators of inflammation*, *2016*.

Lou, N., Liu, G. and Pan, Y. (2020). Long noncoding RNA ANRIL as a novel biomarker in human cancer. *Future Oncology*, *16*(35), pp.2981-2995.

Luo, J., Xu, L., Jiang, Y., Zhuo, D., Zhang, S., Wu, L., Xu, H. and Huang, Y. (2016). Expression profile of long non-coding RNAs in colorectal cancer: A microarray analysis. *Oncology Reports*, *35*(4), pp.2035-2044.

Ma, P., Xu, T., Huang, M. and Shu, Y. (2016). Increased expression of LncRNA PANDAR predicts a poor prognosis in gastric cancer. *Biomedicine & Pharmacotherapy*, *78*, pp.172-176.

Mamenta, E.L., Poma, E.E., Kaufmann, W.K., Delmastro, D.A., Grady, H.L. and Chaney, S.G. (1994). Enhanced replicative bypass of platinum-DNA adducts in cisplatin-resistant human ovarian carcinoma cell lines. *Cancer Research*, *54*(13), pp.3500-3505.

Mannironi, C., Bonner, W.M. and Hatch, C.L. (1989). H2A. X. a histone isoprotein with a conserved C-terminal sequence, is encoded by a novel mRNA with both DNA replication type and polyA 3′ processing signals. *Nucleic Acids Research*, *17*(22), pp.9113-9126.

Mantovani, R. (1998). A survey of 178 NF-Y binding CCAAT boxes. *Nucleic Acids Research*, *26*(5), pp.1135-1143.

Mao, C., Zeng, X., Zhang, C., Yang, Y., Xiao, X., Luan, S., Zhang, Y. and Yuan, Y. (2021). Mechanisms of pharmaceutical therapy and drug resistance in esophageal cancer. *Frontiers in Cell and Developmental Biology*, *9*, p.612451.

Markova, E., Schultz, N. and Belyaev, I.Y. (2007). Kinetics and dose-response of residual 53BP1/γ-H2AX foci: Co-localization, relationship with DSB repair and clonogenic survival. *International Journal of Radiation Biology*, *83*(5), pp.319-329.

Mariotti, L.G., Pirovano, G., Savage, K.I., Ghita, M., Ottolenghi, A., Prise, K.M. and Schettino, G. (2013). Use of the γ-H2AX assay to investigate DNA repair dynamics following multiple radiation exposures. *PloS One*, *8*(11), p.e79541.

Meijer, C., Mulder, N.H., Timmer-Bosscha, H., Sluiter, W.J., Meersma, G.J. and de Vries, E.G. (1992). Relationship of cellular glutathione to the cytotoxicity and resistance of seven platinum compounds. *Cancer Research*, *52*(24), pp.6885-6889.

Mellish, K.J., Kelland, L.R. and Harrap, K.R. (1993). In vitro platinum drug chemosensitivity of human cervical squamous cell carcinoma cell lines with intrinsic and acquired resistance to cisplatin. *British Journal of Cancer*, *68*(2), pp.240-250.

Melton, D.W., Ketchen, A.M., Núñez, F., Bonatti-Abbondandolo, S., Abbondandolo, A., Squires, S. and Johnson, R.T. (1998). Cells from ERCC1-deficient mice show increased genome instability and a reduced frequency of S-phase-dependent illegitimate chromosome exchange but a normal frequency of homologous recombination. *Journal of Cell Science*, *111*(3), pp.395-404.

Mercer, T.R., Dinger, M.E. and Mattick, J.S. (2009). Long non-coding RNAs: insights into functions. *Nature Reviews Genetics*, *10*(3), pp.155-159.

Miller, B.J., Billedeau, S.M. and Miller, D.W. (1989). Formation of N-nitrosamines in microwaved versus skillet-fried bacon containing nitrite. *Food and Chemical Toxicology*, *27*(5), pp.295-299.

Modarresi, F., Faghihi, M.A., Lopez-Toledano, M.A., Fatemi, R.P., Magistri, M., Brothers, S.P., Van Der Brug, M.P. and Wahlestedt, C. (2012). Inhibition of natural antisense transcripts in vivo results in gene-specific transcriptional upregulation. *Nature Biotechnology*, *30*(5), pp.453-459.

Morgan, E., Soerjomataram, I., Rumgay, H., Coleman, H.G., Thrift, A.P., Vignat, J., Laversanne, M., Ferlay, J. and Arnold, M. (2022). The global landscape of esophageal squamous cell carcinoma and esophageal adenocarcinoma incidence and mortality in 2020 and projections to 2040: New estimates from GLOBOCAN 2020. *Gastroenterology*.

Morita, M., Kumashiro, R., Kubo, N., Nakashima, Y., Yoshida, R., Yoshinaga, K., Saeki, H., Emi, Y., Kakeji, Y., Sakaguchi, Y. and Toh, Y. (2010). Alcohol drinking, cigarette smoking, and the development of squamous cell carcinoma of the esophagus: epidemiology, clinical findings, and prevention. *International Journal of Clinical Oncology*, *15*(2), pp.126-134.

Mosmann, T. (1983). Rapid colorimetric assay for cellular growth and survival: application to proliferation and cytotoxicity assays. *Journal of Immunological Methods*, *65*(1-2), pp.55-63.

Muggia, F.M., Bonetti, A., Hoeschele, J.D., Rozencweig, M. and Howell, S.B. (2015). Platinum antitumor complexes: 50 years since Barnett Rosenberg's discovery. *Journal of Clinical Oncology*, *33*(35), pp.4219-4226.

Mynhardt, C., Damelin, L.H., Jivan, R., Peres, J., Prince, S., Veale, R.B. and Mavri-Damelin, D. (2018). Metformin-induced alterations in nucleotide metabolism cause 5-fluorouracil resistance but gemcitabine susceptibility in oesophageal squamous cell carcinoma. *Journal of Cellular Biochemistry*, *119*(1), pp.1193-1203.

NCR, N.H.L.S. (2011). Summary Statistics of Cancer Diagnosed Histologically in 2011. 1–43. Available: *http://www.cansa.org.za/south-african-cancer-statistics/*

Ormerod, M. G., O'Neill, C., Robertson, D., Kelland, L. R. and Harrap, K. R. (1996). *Cancer Chemotherapy. Pharmacology,* 37, pp.463–471.

Özeş, A.R., Miller, D.F., Özeş, O.N., Fang, F., Liu, Y., Matei, D., Huang, T. and Nephew, K.P. (2016). NF-κB-HOTAIR axis links DNA damage response, chemoresistance and cellular senescence in ovarian cancer. *Oncogene*, *35*(41), pp.5350-5361.

Pabla, N., Huang, S., Mi, Q.S., Daniel, R. and Dong, Z. (2008). ATR-Chk2 signaling in p53 activation and DNA damage response during cisplatin-induced apoptosis. *Journal of Biological Chemistry*, *283*(10), pp.6572-6583.

Palazzo, A.F. and Lee, E.S. (2015). Non-coding RNA: what is functional and what is junk?. *Frontiers in Genetics*, *6*, p.2.

Pasmant, E., Laurendeau, I., Héron, D., Vidaud, M., Vidaud, D. and Bieche, I. (2007). Characterization of a germ-line deletion, including the entire INK4/ARF locus, in a melanoma-neural system tumor family: identification of ANRIL, an antisense noncoding RNA whose expression coclusters with ARF. *Cancer Research*, *67*(8), pp.3963-3969.

Pavet, V., Portal, M.M., Moulin, J.C., Herbrecht, R. and Gronemeyer, H. (2011). Towards novel paradigms for cancer therapy. *Oncogene*, *30*(1), pp.1-20.

Pennathur, A., Gibson, M.K., Jobe, B.A. and Luketich, J.D. (2013). Oesophageal carcinoma. *The Lancet*, *381*(9864), pp.400-412.

Peng, C., Hu, W., Weng, X., Tong, R., Cheng, S., Ding, C., Xiao, H., Lv, Z., Xie, H., Zhou, L. and Wu, J. (2017). Over expression of long non-coding RNA PANDA promotes hepatocellular carcinoma by inhibiting senescence associated inflammatory factor IL8. *Scientific Reports*, *7*(1), pp.1-11.

Peng, W. and Fan, H. (2015). Long non-coding RNA PANDAR correlates with poor prognosis and promotes tumorigenesis in hepatocellular carcinoma. *Biomedicine & Pharmacotherapy*, *72*, pp.113-118.

Perez-Pinera, P., Kocak, D.D., Vockley, C.M., Adler, A.F., Kabadi, A.M., Polstein, L.R., Thakore, P.I., Glass, K.A., Ousterout, D.G., Leong, K.W. and Guilak, F. (2013). RNA-guided gene activation by CRISPR-Cas9–based transcriptionfactors. *Nature Methods*, *10*(10), pp.973-976.

Persons, D.L., Yazlovitskaya, E.M. and Pelling, J.C. (2000). Effect of extracellular signal-regulated kinase on p53 accumulation in response to cisplatin. *Journal of Biological Chemistry*, *275*(46), pp.35778-35785.

Peschansky, V.J. and Wahlestedt, C. (2014). Non-coding RNAs as direct and indirect modulators of epigenetic regulation. *Epigenetics*, *9*(1), pp.3-12.

Poliseno, L., Salmena, L., Zhang, J., Carver, B., Haveman, W.J. and Pandolfi, P.P. (2010). A coding-independent function of gene and pseudogene mRNAs regulates tumour biology. *Nature*, *465*(7301), pp.1033-1038.

Ponting, C.P., Oliver, P.L. and Reik, W. (2009). Evolution and functions of long noncoding RNAs. *Cell*, *136*(4), pp.629-641.

Pullirsch, D., Härtel, R., Kishimoto, H., Leeb, M., Steiner, G. and Wutz, A. (2010). The Trithorax group protein Ash2l and Saf-A are recruited to the inactive X chromosome at the onset of stable X inactivation. *Development*, *137*(6), pp.935-943.

Puvvula, P.K., Desetty, R.D., Pineau, P., Marchio, A., Moon, A., Dejean, A. and Bischof, O. (2014). Long noncoding RNA PANDA and scaffold-attachment-factor SAFA control senescence entry and exit. *Nature Communications*, *5*(1), pp.1-16.

Qiu, J.J., Wang, Y., Liu, Y.L., Zhang, Y., Ding, J.X. and Hua, K.Q. (2016). The long non-coding RNA ANRIL promotes proliferation and cell cycle progression and inhibits apoptosis and senescence in epithelial ovarian cancer. *Oncotarget*, *7*(22), p.32478.

Rabik, C.A. and Dolan, M.E. (2007). Molecular mechanisms of resistance and toxicity associated with platinating agents. *Cancer Treatment Reviews*, *33*(1), pp.9-23.

Ran, F.A., Hsu, P.D., Wright, J., Agarwala, V., Scott, D.A. and Zhang, F. (2013). Genome engineering using the CRISPR-Cas9 system. *Nature Protocols*, *8*(11), pp.2281-2308.

Rao, S.S., Huntley, M.H., Durand, N.C., Stamenova, E.K., Bochkov, I.D., Robinson, J.T., Sanborn, A.L., Machol, I., Omer, A.D., Lander, E.S. and Aiden, E.L. (2014). A 3D map of the human genome at kilobase resolution reveals principles of chromatin looping. *Cell*, *159*(7), pp.1665-1680.

Reardon, J.T., Vaisman, A., Chaney, S.G. and Sancar, A. (1999). Efficient nucleotide excision repair of cisplatin, oxaliplatin, and bis-aceto-ammine-dichloro-cyclohexylamine-platinum (IV)(JM216) platinum Intrastrand DNA diadducts. *Cancer Research*, *59*(16), pp.3968-3971.

Reed, E. (1998). Platinum-DNA adduct, nucleotide excision repair and platinum based anti-cancer chemotherapy. *Cancer Treatment Reviews*, *24*(5), pp.331-344.

Rice, T.W., Ishwaran, H., Ferguson, M.K., Blackstone, E.H. and Goldstraw, P. (2017). Cancer of the esophagus and esophagogastric junction: an eighth edition staging primer. *Journal of Thoracic Oncology*, *12*(1), pp.36-42.

Roberts, T.C., Morris, K.V. and Weinberg, M.S. (2014). Perspectives on the mechanism of transcriptional regulation by long non-codingRNAs. *Epigenetics*, *9*(1), pp.13-20.

Rocha, C.R.R., Silva, M.M., Quinet, A., Cabral-Neto, J.B. and Menck, C.F.M. (2018). DNA repair pathways and cisplatin resistance: an intimate relationship. *Clinics*, *73*.

Roehr, B. (1998). Fomivirsen approved for CMV retinitis. *Journal of the International Association of Physicians in AIDS Care*, *4*(10), pp.14-16.

Rogakou, E.P., Pilch, D.R., Orr, A.H., Ivanova, V.S. and Bonner, W.M. (1998). DNA double-stranded breaks induce histone H2AX phosphorylation on serine 139. *Journal of Biological Chemistry*, *273*(10), pp.5858-5868.

Rosenberg, B., Vancamp, L., Trosko, J.E. and Mansour, V.H. (1969). Platinum compounds: a new class of potent antitumour agents. *Nature*, *222*(5191), pp.385-386.

Rustgi, A.K. and El-Serag, H.B. (2014). Esophageal carcinoma. *New England Journal of Medicine*, *371*(26), pp.2499-2509.

Sadeghi, F., Etebari, M., Roudkenar, M.H. and Jahanian-Najafabadi, A. (2018). Lipocalin2 protects human embryonic kidney cells against cisplatin–induced genotoxicity. *Iranian Journal of Pharmaceutical Research: IJPR*, *17*(1), p.147.

Sale, J.E. (2012). Competition, collaboration and coordination–determining how cells bypass DNA damage. *Journal of Cell Science*, *125*(7), pp.1633-1643.

Sager, R. (1997). Expression genetics in cancer: shifting the focus from DNA to RNA. *Proceedings of the National Academy of Sciences*, *94*(3), pp.952-955.

Sang, Y., Tang, J., Li, S., Li, L., Tang, X., Cheng, C., Luo, Y., Qian, X., Deng, L.M., Liu, L. and Lv, X.B. (2016). LncRNA PANDAR regulates the G1/S transition of breast cancer cells by suppressing p16 INK4A expression. *Scientific Reports*, *6*(1), pp.1-10.

Sato, K., Nakagawa, H., Tajima, A., Yoshida, K. and Inoue, I. (2010). ANRIL is implicated in the regulation of nucleus and potential transcriptional target ofE2F1. *Oncology Reports*, *24*(3), pp.701-707.

Sewram, V., Sitas, F., O'Connell, D. and Myers, J. (2014). Diet and esophageal cancer risk in the Eastern Cape Province of South Africa. *Nutrition and Cancer*, *66*(5), pp.791-799.

Shen, W.J., Zhang, F., Zhao, X. and Xu, J. (2016). LncRNAs and esophageal squamous cell carcinoma-implications for pathogenesis and drug development. *Journal of Cancer*, *7*(10), p.1258.

Shieh, S.Y., Ahn, J., Tamai, K., Taya, Y. and Prives, C. (2000). The human homologs of checkpoint kinases Chk1 and Cds1 (Chk2) phosphorylate p53 at multiple DNA damage-inducible sites. *Genes & Development*, *14*(3), pp.289-300.

Shi, W., Wang, Q., Bian, Y., Fan, Y., Zhou, Y., Feng, T., Li, Z. and Cao, X. (2019). Long noncoding RNA PANDA promotes esophageal squamous carcinoma cell progress by dissociating from NF-YA but interact with SAFA. *Pathology-Research and Practice*, *215*(10), p.152604.

Siddik, Z.H. (2003). Cisplatin: mode of cytotoxic action and molecular basis of resistance. *Oncogene*, *22*(47), pp.7265-7279.

Siewert, J.R. and Ott, K. (2007). Are squamous and adenocarcinomas of the esophagus the same disease? *Seminars in Radiation Oncology*, *17, (1),* pp. 38-44).

Shi, W., Wang, Q., Bian, Y., Fan, Y., Zhou, Y., Feng, T., Li, Z. and Cao, X. (2019). Long noncoding RNA PANDA promotes esophageal squamous carcinoma cell progress by dissociating from NF-YA but interact with SAFA. *Pathology-Research and Practice*, *215*(10), p.152604.

Song, K., Cowan, K.H. and Sinha, B.K. (1999). In vivo studies of adenovirus-mediated p53 gene therapy for cis-platinum-resistant human ovarian tumor xenografts. *Oncology Research Featuring Preclinical and Clinical Cancer Therapeutics*, *11*(3), pp.153-159.

Song, I.S., Savaraj, N., Siddik, Z.H., Liu, P., Wei, Y., Wu, C.J. and Kuo, M.T. (2004). Role of human copper transporter Ctr1 in the transport of platinum-based antitumor agents in cisplatin-sensitive and cisplatin-resistant cells. *Molecular Cancer Therapeutics*, *3*(12), pp.1543-1549.

Spierings, D.C.J., De Vries, E.G.E., Vellenga, E. and De Jong, S. (2003). Loss of drug-induced activation of the CD95 apoptotic pathway in a cisplatin-resistant testicular germ cell tumor cell line. *Cell Death & Differentiation*, *10*(7), pp.808-822.

Statello, L., Guo, C.J., Chen, L.L. and Huarte, M. (2021). Gene regulation by long non-coding RNAs and its biological functions. *Nature Reviews Molecular Cell Biology*, *22*(2), pp.96-118.

Stucki, M. and Jackson, S.P. (2006). γH2AX and MDC1: anchoring the DNA-damage-response machinery to broken chromosomes. *DNA Repair*, *5*(5), pp.534-543.

Su, M., Wang, H., Wang, W., Wang, Y., Ouyang, L., Pan, C., Xia, L., Cao, D. and Liao, Q. (2018). LncRNAs in DNA damage response and repair in cancer cells. *Acta Biochimica et Biophysica Sinica*, *50*(5), pp.433-439.

Subasinghe, D. and Samarasekera, D.N. (2010). A study comparing endoscopic ultrasound (EUS) and computed tomography (CT) in staging oesophageal cancer and their role in clinical decision making. *Journal of Gastrointestinal Cancer*, *41*(1), pp.38-42.

Sundaram, G.M. and Veera Bramhachari, P. (2017). Molecular interplay of pro-inflammatory transcription factors and non-coding RNAs in esophageal squamous cell carcinoma. *Tumor Biology*, *39*(6), p.1010428317705760.

Syrigos, K.N., Zalonis, A., Kotteas, E. and Saif, M.W. (2008). Targeted therapy for oesophageal cancer: an overview. *Cancer and Metastasis Reviews*, *27*(2), pp.273-288.

Tam, S.Y., Wu, V.W. and Law, H.K. (2020). JNK pathway mediates low oxygen level induced epithelial–mesenchymal transition and stemness maintenance in colorectal cancer cells. *Cancers*, *12*(1), p.224.

Tehrani, S.S., Karimian, A., Parsian, H., Majidinia, M. and Yousefi, B. (2018). Multiple functions of long non-coding RNAs in oxidative stress, DNA damage response and cancer progression. *Journal of Cellular Biochemistry*, *119*(1), pp.223-236.

Thapar, R. (2018). Regulation of DNA double-strand break repair by non-coding RNAs. *Molecules*, *23*(11), p.2789.

Then, E.O., Michell Lopez, S.S., Gayam, V., Sunkara, T., Culliford, A. and Gaduputi, V. (2020). Esophageal cancer: an updated surveillance epidemiology and end results database analysis. *World Journal of Oncology*, *11*(2), p.55.

Towbin, H., Staehelin, T. and Gordon, J. (1979). Electrophoretic transfer of proteins from polyacrylamide gels to nitrocellulose sheets: procedure and some applications. *Proceedings of the National Academy of Sciences*, *76*(9), pp.4350- 4354.

Tripathi, V., Ellis, J.D., Shen, Z., Song, D.Y., Pan, Q., Watt, A.T., Freier, S.M., Bennett, C.F., Sharma, A., Bubulya, P.A. and Blencowe, B.J. (2010). The nuclear-retained noncoding RNA MALAT1 regulates alternative splicing by modulating SR splicing factor phosphorylation. *Molecular Cell*, *39*(6), pp.925-938.

Uszczynska-Ratajczak, B., Lagarde, J., Frankish, A., Guigó, R. and Johnson, R. (2018). Towards a complete map of the human long non-coding RNA transcriptome. *Nature Reviews Genetics*, *19*(9), pp.535-548.

Vandersickel, V., Depuydt, J., Van Bockstaele, B., Perletti, G., Philippe, J., Thierens, H. and Vral, A. (2010). Early increase of radiation-induced γH2AX foci in a human Ku70/80 knockdown cell line characterized by an enhanced radiosensitivity. *Journal of Radiation Research*, *51*(6), pp.633-641.

Van der Kogel, A.J. and Joiner, M.C. (2009). The dose-rate effect. *Basic Clinical Radiobiology*, *4*, pp.158-168.

Vare, D., Groth, P., Carlsson, R., Johansson, F., Erixon, K. and Jenssen, D. (2012). DNA interstrand crosslinks induce a potent replication block followed by formation and repair of double strand breaks in intact mammalian cells. *DNA Repair*, *11*(12), pp.976-985.

Veedu, R.N. and Wengel, J. (2010). Locked nucleic acids: promising nucleic acid analogs for therapeutic applications. *Chemistry & Biodiversity*, *7*(3), pp.536-542.

Wan, G., Mathur, R., Hu, X., Liu, Y., Zhang, X., Peng, G. and Lu, X. (2013). Long non-coding RNA ANRIL (CDKN2B-AS) is induced by the ATM-E2F1 signaling pathway. *Cellular Signalling*, *25*(5), pp.1086-1095.

Wang, K.C. and Chang, H.Y. (2011). Molecular mechanisms of long noncoding RNAs. *Molecular Cell*, *43*(6), pp.904-914.

Wang, Y., Cheng, N. and Luo, J. (2017). Downregulation of lncRNA ANRIL represses tumorigenicity and enhances cisplatin-induced cytotoxicity via regulating microRNA let-7a in nasopharyngeal carcinoma. *Journal of Biochemical and Molecular Toxicology*, *31*(7), p.e21904.

Wang, H., Fang, L., Jiang, J., Kuang, Y., Wang, B., Shang, X., Han, P., Li, Y., Liu, M., Zhang, Z. and Li, P. (2018). The cisplatin-induced lncRNA PANDAR dictates the chemoresistance of ovarian cancer via regulating SFRS2-mediated p53 phosphorylation. *Cell Death & Disease*, *9*(11), pp.1-15.

Wang, Y., Xu, Z., Jiang, J., Xu, C., Kang, J., Xiao, L., Wu, M., Xiong, J., Guo, X. and Liu, H. (2013). Endogenous miRNA sponge lincRNA-RoR regulates Oct4, Nanog, and Sox2 in human embryonic stem cell self-renewal. *Developmental Cell*, *25*(1), pp.69-80.

Wetzel, C.C. and Berberich, S.J. (2001). p53 binds to cisplatin-damaged DNA. *Biochimica et Biophysica Acta (BBA)-Gene Structure and Expression*, *1517*(3), pp.392-397.

Winkle, M., El-Daly, S.M., Fabbri, M. and Calin, G.A. (2021). Noncoding RNA therapeutics—Challenges and potential solutions. *Nature Reviews Drug Discovery*, *20*(8), pp.629-651.

Whitehead, J., Pandey, G.K. and Kanduri, C. (2009). Regulation of the mammalian epigenome by long noncoding RNAs. *Biochimica et Biophysica Acta (BBA)-General Subjects*, *1790*(9), pp.936-947.

Wilusz, J.E., Sunwoo, H. and Spector, D.L. (2009). Long noncoding RNAs: functional surprises from the RNA world. *Genes & Development*, *23*(13), pp.1494-1504.

Wong, E. and Goldberg, T. (2014). Mipomersen (kynamro): a novel antisense oligonucleotide inhibitor for the management of homozygous familial hypercholesterolemia. *Pharmacy and Therapeutics*, *39*(2), p.119.

Wong, M.C., Hamilton, W., Whiteman, D.C., Jiang, J.Y., Qiao, Y., Fung, F.D., Wang, H.H., Chiu, P.W., Ng, E.K., Wu, J.C. and Yu, J. (2018). Global incidence and mortality of oesophageal cancer and their correlation with socioeconomic indicators temporal patterns and trends in 41 countries. *Scientific Reports*, *8*(1), pp.1-13.

Xu, G.W., Mymryk, J.S. and Cairncross, J.G. (2005). Inactivation of p53 sensitizes astrocytic glioma cells to BCNU and temozolomide, but not cisplatin. *Journal of Neuro-oncology*, *74*(2), pp.141-149.

Yamasaki, M., Miyata, H., Tanaka, K., Shiraishi, O., Motoori, M., Peng, Y.F., Yasuda, T., Yano, M., Shiozaki, H., Mori, M. and Doki, Y. (2011). Multicenter phase I/II study of docetaxel, cisplatin and fluorouracil combination chemotherapy in patients with advanced or recurrent squamous cell carcinoma of the esophagus. *Oncology*, *80*(5-6), pp.307-313.

Yang, C.X., Wang, H.Y., Wang, Z.M., Du, H.Z., Tao, D.M., Mu, X.Y., Chen, H.G., Lei, Y., Matsuo, K. and Tajima, K. (2005). Risk factors for esophageal cancer: a case-control study in South-western China. *Asian Pacific Journal of Cancer Prevention*, *6*(1), pp.48- 53.

Yap, K.L., Li, S., Muñoz-Cabello, A.M., Raguz, S., Zeng, L., Mujtaba, S., Gil, J., Walsh, M.J. and Zhou, M.M. (2010). Molecular interplay of the noncoding RNA ANRIL and methylated histone H3 lysine 27 by polycomb CBX7 in transcriptional silencing of INK4a. *Molecular Cell*, *38*(5), pp.662-674.

Yoon, J.H., Abdelmohsen, K., Srikantan, S., Yang, X., Martindale, J.L., De, S., Huarte, M., Zhan, M., Becker, K.G. and Gorospe, M. (2012). LincRNA-p21 suppresses target mRNA translation. *Molecular Cell*, *47*(4), pp.648-655.

Yoshizawa, K., Nozaki, S., Kitahara, H., Ohara, T., Kato, K., Kawashiri, S. and Yamamoto, E. (2007). Copper efflux transporter (ATP7B) contributes to the acquisition of cisplatin-resistance in human oral squamous cell lines. *Oncology Reports*, *18*(4), pp.987-991.

Youn, C.K., Kim, M.H., Cho, H.J., Kim, H.B., Chang, I.Y., Chung, M.H. and You, H.J. (2004). Oncogenic H-Ras up-regulates expression of ERCC1 to protect cells from platinum-based anticancer agents. *Cancer Research*, *64*(14), pp.4849-4857.

Zhang, E.B., Kong, R., Yin, D.D., You, L.H., Sun, M., Han, L., Xu, T.P., Xia, R., Yang, J.S., De, W. and fei Chen, J. (2014). Long noncoding RNA ANRIL indicates a poor prognosis of gastric cancer and promotes tumor growth by epigenetically silencing of miR-99a/miR-449a. *Oncotarget*, *5*(8), p.2276.

Zhang, C. and Peng, G. (2015). Non-coding RNAs: an emerging player in DNA damage response. *Mutation Research/Reviews in Mutation Research*, *763*, pp.202-211.

Zhang, J.J., Wang, D.D., Du, C.X. and Wang, Y. (2018). Long noncoding RNA ANRIL promotes cervical cancer development by acting as a sponge of miR-186. *Oncology Research*, *26*(3), p.345.

Zhang, X., Wang, W., Zhu, W., Dong, J., Cheng, Y., Yin, Z. and Shen, F. (2019). Mechanisms and functions of long non-coding RNAs at multiple regulatory levels. *International Journal of Molecular Sciences*, *20*(22), p.5573.

Zhang, P., Wu, W., Chen, Q. and Chen, M. (2019). Non-coding RNAs and their integrated networks. *Journal of Integrative Bioinformatics*, *16*(3).

Zhao, B., Lu, Y.L., Yang, Y., Hu, L.B., Bai, Y., Li, R.Q., Zhang, G.Y., Li, J., Bi, C.W., Yang, L.B. and Hu, C. (2018). Overexpression of lncRNA ANRIL promoted the proliferation and migration of prostate cancer cells via regulating let-7a/TGF-β1/Smad signaling pathway. *Cancer Biomarkers*, *21*(3), pp.613-620.

Zhao, H.U.I. and Piwnica-Worms, H. (2001). ATR-mediated checkpoint pathways regulate phosphorylation and activation of human Chk1. *Molecular and Cellular Biology*, *21*(13), pp.4129-4139.

Zhivotovsky, B. and Kroemer, G. (2004). Apoptosis and genomic instability. *Nature reviews Molecular Cell Biology*, *5*(9), pp.752-762.

Appendix A

Solution	Recipe
1XPBS	2.7 Mm KCl,137 Mm NaCl, 8.1 Mm Na2HPO4•12H2O, 1.8 Mm KH2PO4, pH 7.2, autoclaved
1XRIPA	1% Triton X-100, 0.1% SDS, 0.5% sodium deoxycholate, 150 mMNaCl, 50 Mm Tris-HCl Ph 8.0, 1 Mm PMSF, 10 Mm leupeptin
1XTAE	0.11% (v/v) glacial acetic acid, 1 Mm EDTA Ph 8.0, 40 Mm Tris-HCl Ph 8,
Trypan Blue	0.2% (w/v) Trypan blue in 1X PBS, filter sterilised
1xTBS/T	0.1%(v/v) Tween-2020 mM Tris-HCl pH 7.6, 137 mM NaCl,
Coomassie blue dye	3 mM Coomassie Brilliant Blue G-250, 10% (v/v) glacial acetic acid, 50% (v/v) methanol
Destain solution	12% (v/v) Acetic acid, 10% (v/v) methanol
Elution buffer	66% (v/v) Methanol, 1% (v/v) 25% ammonia
10% SDS	10% (w/v) SDS
10% APS	10% (w/v) APS
SDS-PAGE running buffer	3.5 mM SDS, 192 mM glycine, 25 mM Tris, pH 8.8
Transfer buffer	20% (v/v) methanol, 192 mM Glycine, 25 mM Tris
Blocking buffer	5% (w/v) BSA, 1XTBS/T
Developer	0.6 M Sodium sulphite, 6.4 M metol, 34 mM potassium bromine, 80 mM hydroquinone, 45 mM sodium carbonate
Fixer	0.2 M Sodium meta-sulphite, 0.8 M sodium thiosulphate
4X protein loading buffer	0.04% (w/v) Bromophenol blue, 5% (v/v) β-mercaptoethanol, 8% (w/v) SDS, 40% (v/v) glycerol, 240 mM Tris-HCl pH 6.8

Appendix B

SDS-PAGE recipes:

Reagents	Resolving gel (15%) (ml)	Stacking gel (7%) (ml)
dH_2O	2.3	3.095
29:1 Acrylamide/Bisacrylamide	5	1.17
1.5M Tris pH 8.8	2.5	-
1M Tris pH 6.8	-	0.63
10% SDS	0.1	0.05
10% ammonium persulfate (APS)	0.1	0.05
Tetramethylethylenediamine (TEMED)	0.004	0.005

Appendix C

RNA quantitation is necessary for RNA analysis methods. The absorbance of RNA sample is measured suing a UV spectrophotometer at both 260 nm and 280 nm wavelengths. These wavelengths are used for the calculation of RNA concentrations using Beer-Lambert law which predicts change in absorbance with concentration. The standard acceptable measurements for RNA quality are the A260/A280 of 1.8-2.0 and A260/A230 of 2 or above.

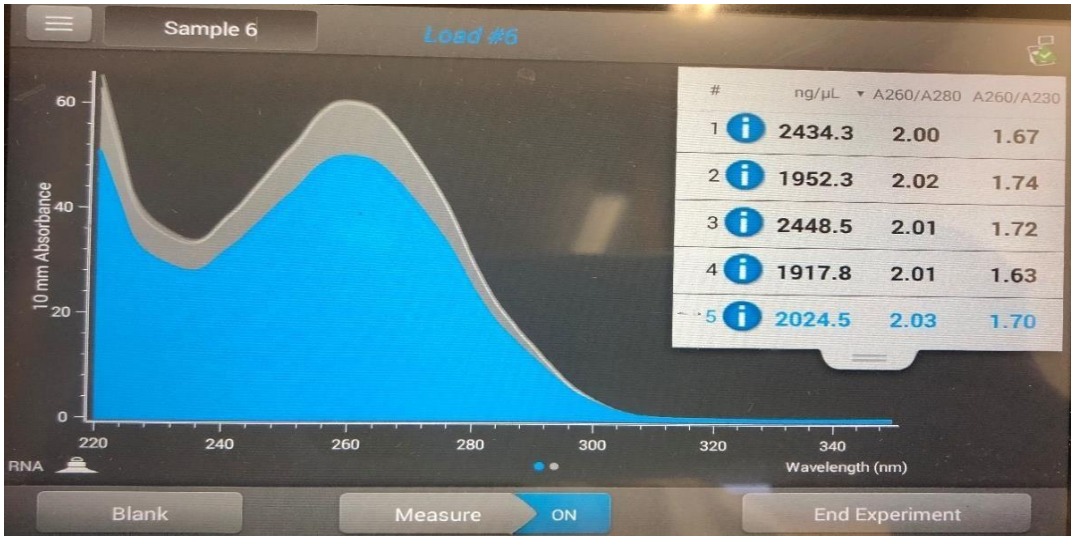

Figure C1: Nanodrop results showing HEK293 RNA concentrations and absorbance ratios. Five different samples were quantified and these include (1) untreated, (2) 0 minutes, (3) 5 minutes, (4) 30 minutes and (5) 1 hour withdrawal times.

Figure C2: Nanodrop results showing WHCO1 RNA concentrations and absorbance ratios. Five different samples were quantified and these include (1) untreated, (2) 0 minutes, (3) 5 minutes, (4) 30 minutes and (5) 1 hour withdrawal times.

Figure C3: Nanodrop results showing WHCO5 RNA concentrations and absorbance ratios. Five different samples were quantified and these include (1) untreated, (2) 0 minutes, (3) 5 minutes, (4) 30 minutes and (5) 1 hour withdrawal times.